Ductile fracture of shells: effective algorithms for non-smooth problems

P. Areias* (Phys. Dept. U. Evora/ICIST) &
T. Rabczuk (Bauhaus-University Weimar)

Key Concepts & Requirements:

- -Element agnostic (i.e. triangles & quads)
- -Trial-tested foundations
- -Newton-Raphson heuristics (control & step size)
- -Ductile and quasi-brittle fracture
- -Alternative crack path criteria
- -Multiple surface plasticity
- -Remaining difficulties

Related papers:

- Areias and co-workers CM (from 2009 to 2012)
- Areias and co-workers IJNME 2008 (and before)
- Areias and co-workers FEAD 2012
- Van Goethem and Areias IJF 2012

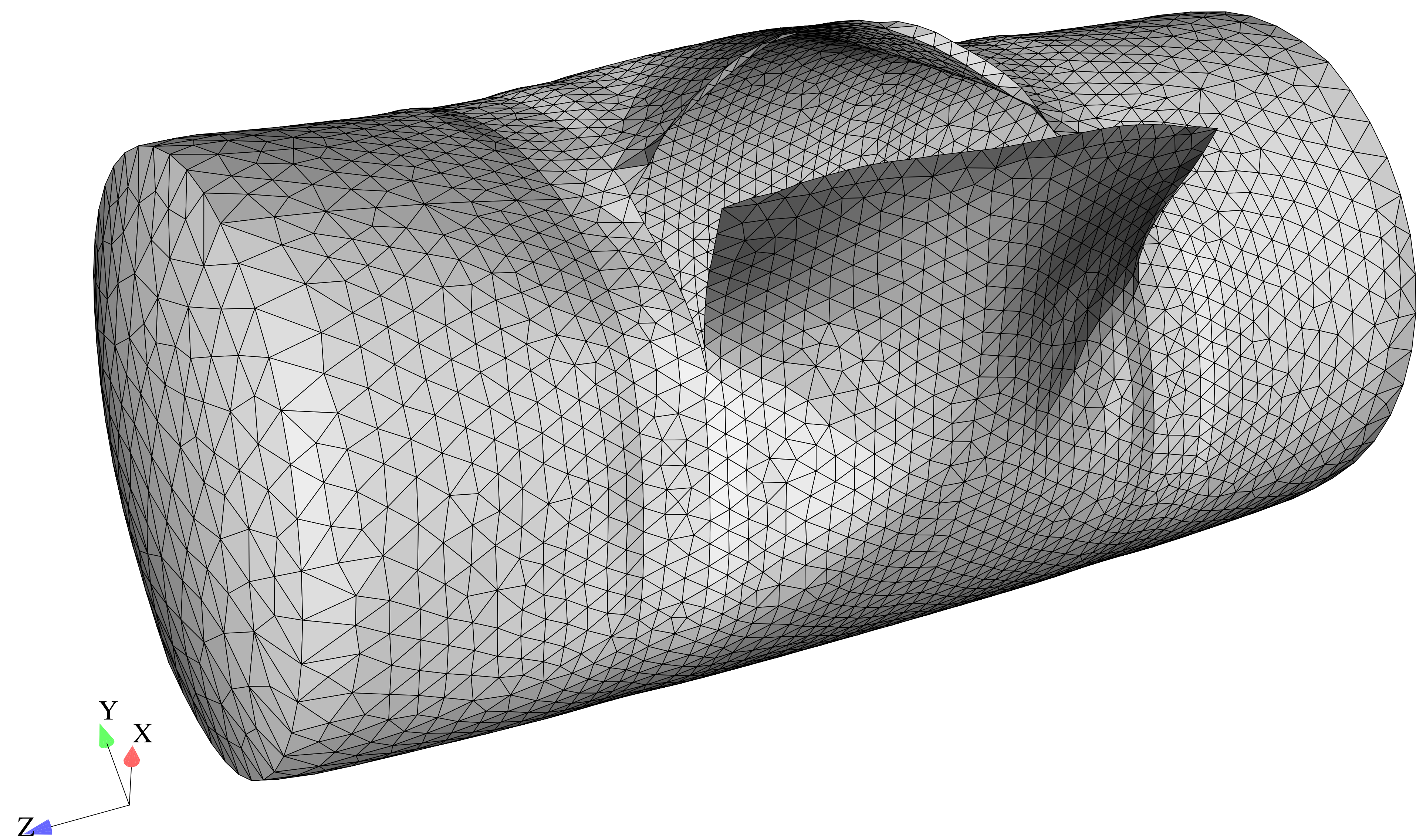

pmaa@uevora.pt
pareias@civil.ist.utl.pt

Power & virtual power
with cracks

$$\int_\Omega \boldsymbol{\sigma} : \dot{\boldsymbol{\varepsilon}} \mathrm{d}\Omega = \int_\Omega Q\boldsymbol{b}_\star \cdot \dot{\boldsymbol{u}} \mathrm{d}\Omega + \int_{\Gamma_t} Q\boldsymbol{t}_\star \cdot \dot{\boldsymbol{u}} \mathrm{d}\Gamma_t + \int_{\Gamma_u} \dot{q}\boldsymbol{t} \cdot \boldsymbol{u}_\star \mathrm{d}\Gamma_u + \int_{\Gamma_c} \boldsymbol{t}\left([[\boldsymbol{u}]]\right) \cdot [[\dot{\boldsymbol{u}}]] \mathrm{d}\Gamma_c$$

''Cohesive''

$$\underbrace{\int_\Omega \boldsymbol{\sigma} : \dot{\boldsymbol{\varepsilon}} \mathrm{d}\Omega}_{\dot{W}} = \underbrace{\int_\Omega Q\boldsymbol{b}_\star \cdot \dot{\boldsymbol{u}} \mathrm{d}\Omega + \int_{\Gamma_t} Q\boldsymbol{t}_\star \cdot \dot{\boldsymbol{u}} \mathrm{d}\Gamma_t + \int_{\Gamma_u} \dot{q}\boldsymbol{t} \cdot \boldsymbol{u}_\star \mathrm{d}\Gamma_u}_{\dot{F}} + \underbrace{\int_{\Gamma_c} \left(\boldsymbol{t}_\lambda \cdot [[\dot{\boldsymbol{u}}]] + \dot{\boldsymbol{t}}_\lambda \cdot [[\boldsymbol{u}]]\right) \mathrm{d}\Gamma_c}_{\dot{S}}$$

''Brittle''

$$W = \int_0^T \dot{W} \mathrm{d}t$$

''Strain work''

$$\frac{\mathrm{d}S}{\mathrm{d}s} = \frac{\mathrm{d}W}{\mathrm{d}s} - \frac{\mathrm{d}F}{\mathrm{d}s}$$

''Differentiation''

$$J = -\frac{\mathrm{d}S}{\mathrm{d}s} = \frac{\mathrm{d}\left(F - W\right)}{\mathrm{d}s}$$

''Energy release rate''

$$J = J_R - W_p \Rightarrow \text{crack growth}$$

''Crack growth criterion''

$$W_p = \int_0^T \boldsymbol{\sigma} : \boldsymbol{d}_p \mathrm{d}t$$

''Plastic work''

Initiation & propagation *pragmatic* technique

Finds best edge and releases the nodes

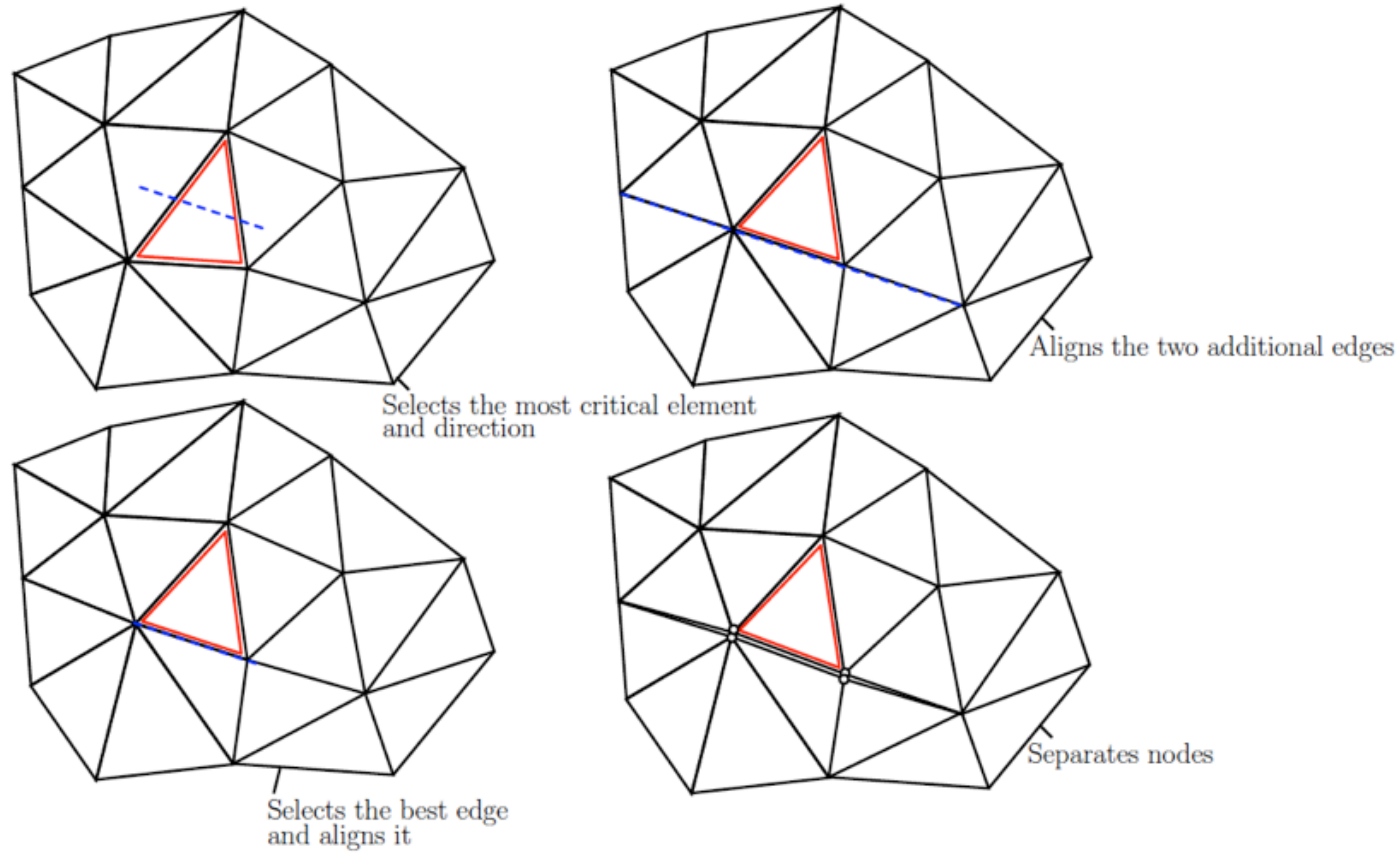

Finds best edge and releases the node

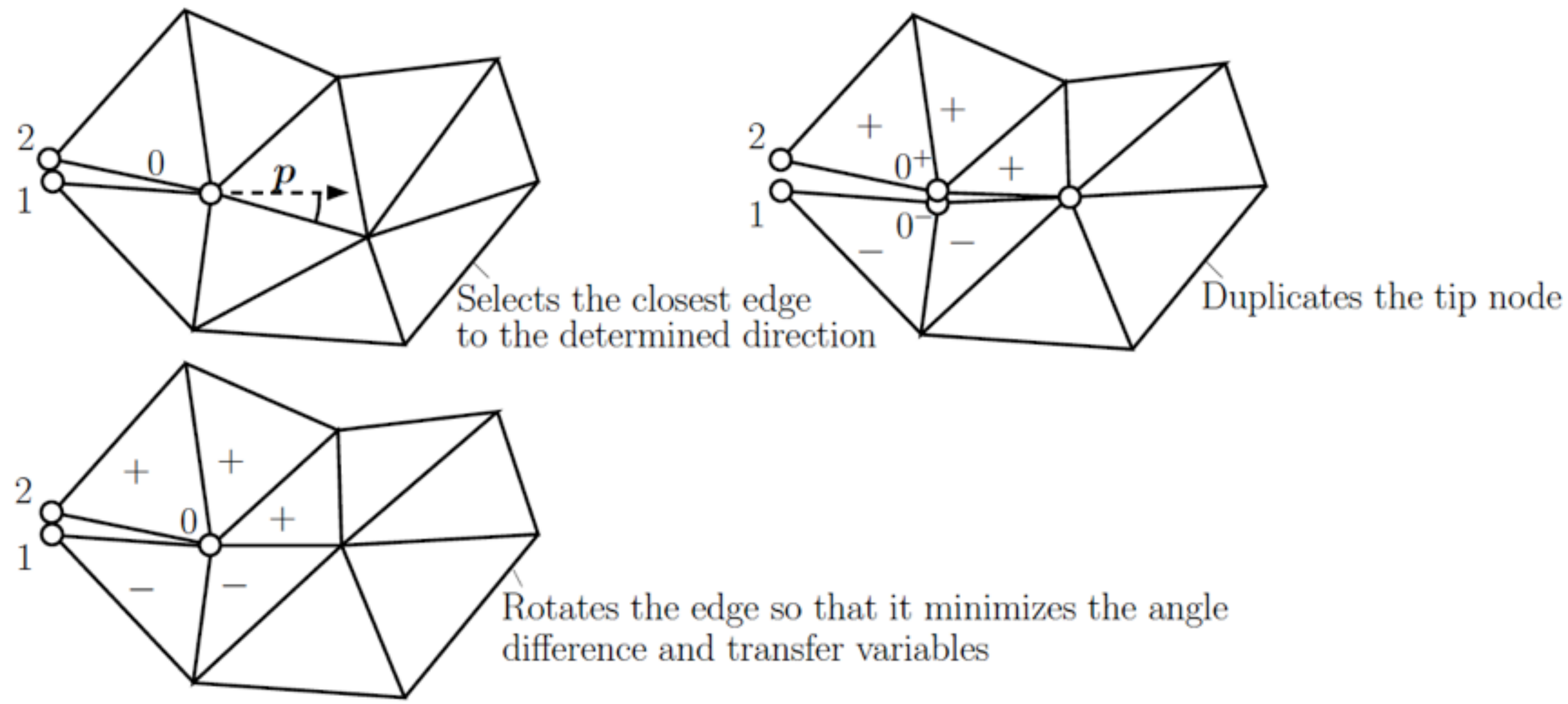

$$\Delta l = \|\boldsymbol{x}_2 - \boldsymbol{x}_1\|_2$$
$$\Delta s = h \Delta l$$

Cohesive discretization & forces (applicable to shells)

$$\boldsymbol{t} = \left\{ \begin{array}{c} \sigma \\ \tau_1 \\ \tau_2 \end{array} \right\} = (1-d)\exp(1)\frac{f_t}{\kappa_0}\left\{ \begin{array}{c} aw_n + \kappa_0 \\ \beta w_{t1} \\ \beta w_{t2} \end{array} \right\}$$

Cohesive stress

$$d = 1 - R^{-1}\left(1 + \alpha R - \alpha\right)e^{\alpha(1-R)-1}$$

Damage *internal* variable

$$R = \frac{\kappa + \kappa_0}{\kappa_0}$$

$$\kappa_0 = 2\mathrm{tol}\frac{J_R}{f_t}$$

Initial shift

$$\alpha = \frac{2 f_t \kappa_0}{J_R}$$

Regularization parameter

$$\begin{array}{ccc} \dot{d} & \geq & 0 \\ \dot{d}\phi & = & 0 \\ \phi & \leq & 0 \end{array}$$

Complementarity conditions

$$\phi = < w_n > + \beta w_t - \kappa$$

with the Loading function

However: bending requires set-valued traction separation laws

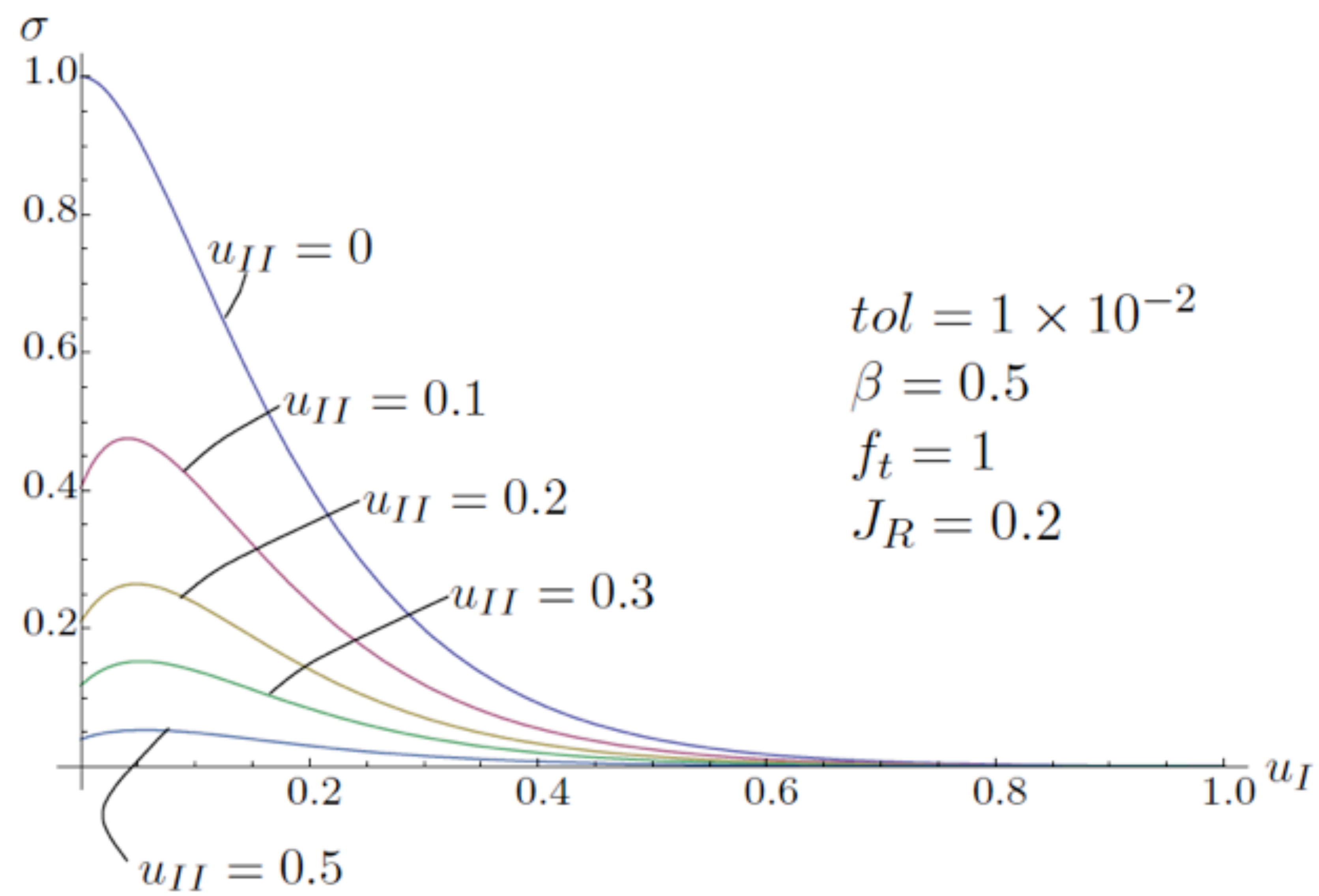

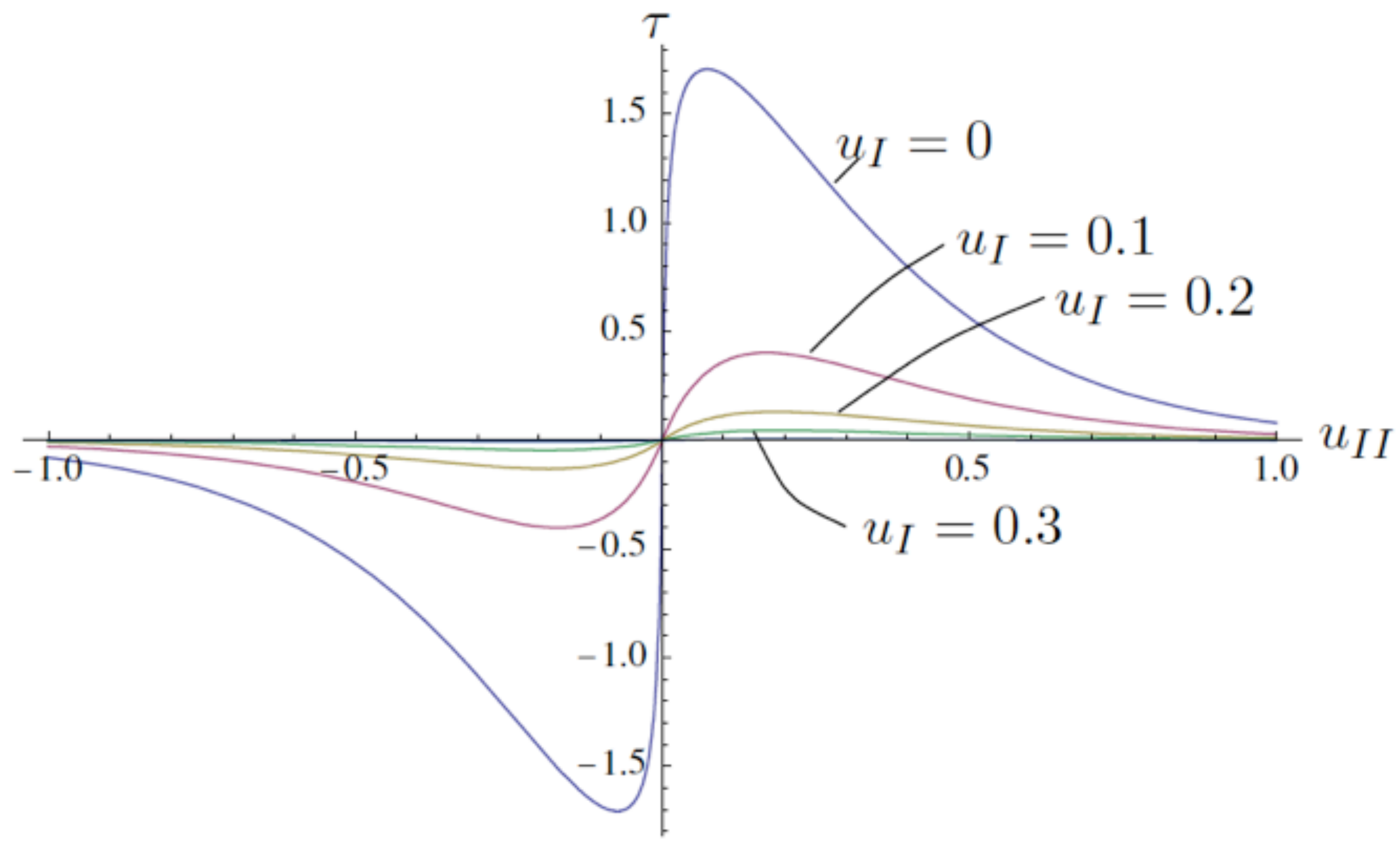

Cohesive discretization by a node-to-node element

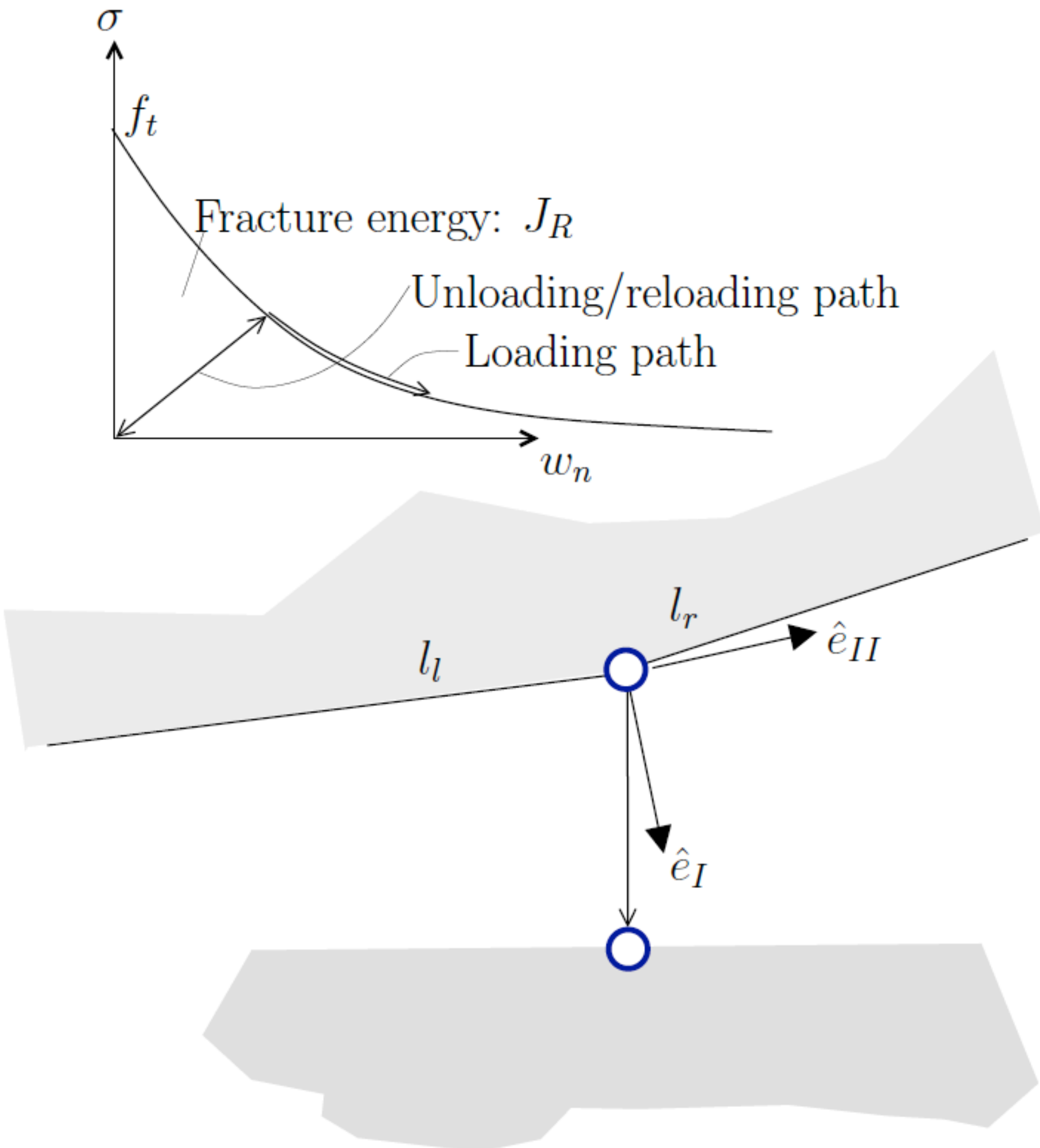

<u>Properly</u> implemented

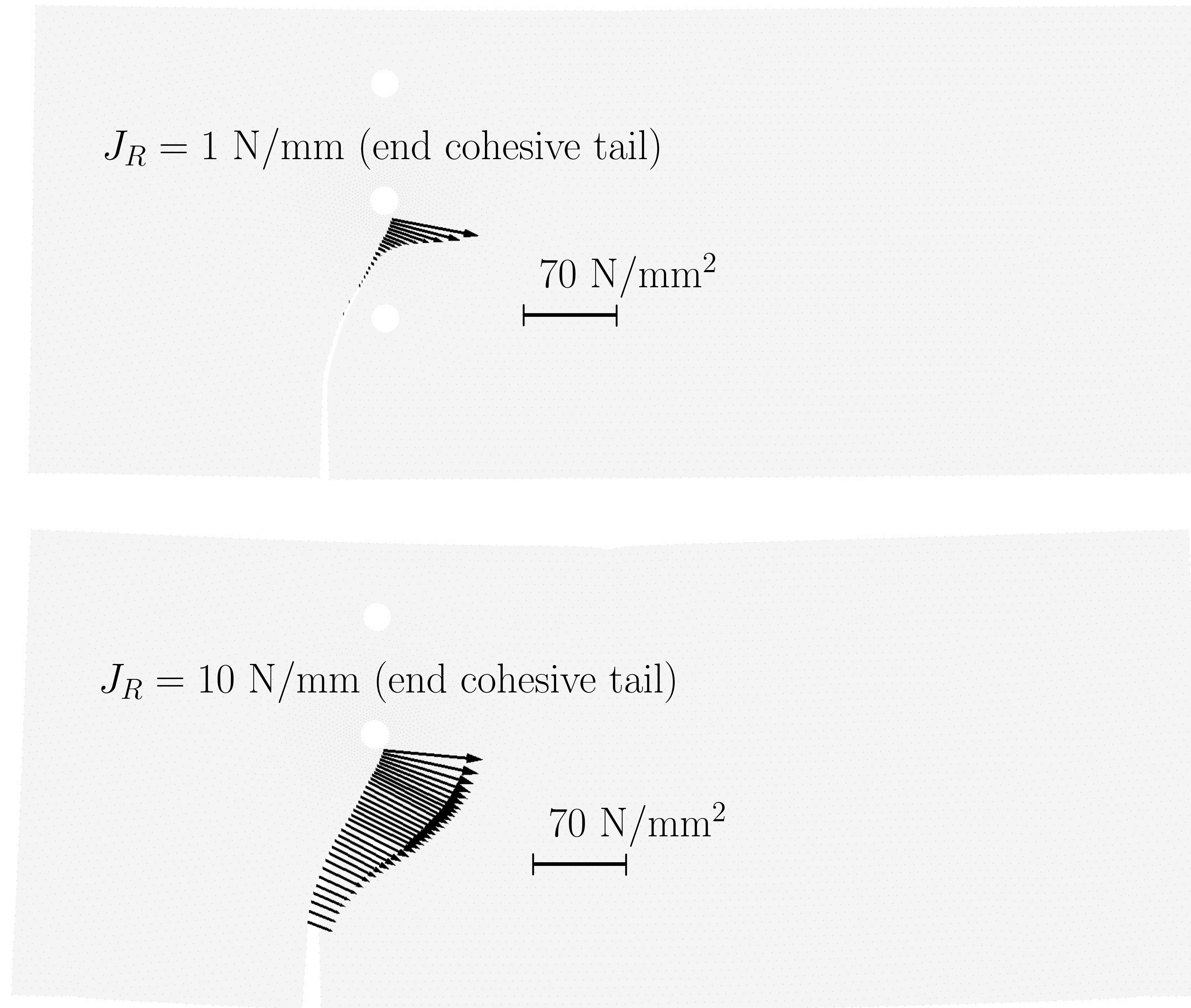

Configurational forces and moments for the <u>direction</u>

$$\boldsymbol{\Sigma} = \psi \boldsymbol{I} - \boldsymbol{F}^T J \boldsymbol{\sigma} \boldsymbol{F}^{-T}$$ <u>Eshelby stress relation (Gurtin)</u>

$$\int_{\Gamma_0} \boldsymbol{\Sigma} \cdot \boldsymbol{N} \mathrm{d}\Gamma_0 + \int_{\Omega_0} \boldsymbol{B}_0 \mathrm{d}\Omega_0 = \boldsymbol{0}$$ <u>Configurational form of equilibrium</u>

$$\underbrace{\int_{\Gamma_0} \delta \boldsymbol{U} \cdot \boldsymbol{\Sigma} \cdot \boldsymbol{N} \mathrm{d}\Gamma_0}_{\delta W_{\mathrm{sup}}} = \underbrace{\int_{\Omega_0} \nabla_0 \delta \boldsymbol{U} : \boldsymbol{\Sigma} \mathrm{d}\Omega_0}_{\delta W_{\mathrm{int}}} - \underbrace{\int_{\Omega_0} \delta \boldsymbol{U} \cdot \boldsymbol{B}_0 \mathrm{d}\Omega_0}_{\delta W_{\mathrm{vol}}} \quad \forall \delta \boldsymbol{U}$$ <u>Weak form</u>

$$\delta W_{\mathrm{int}} = \int_{\Omega_0} \Sigma_{ij} \left[N_{0Kj} \left(\delta U_{Ki} + H \frac{\xi_3}{2} \delta U^\star_{Ki} \right) + N_K H \frac{\partial \xi_3}{\partial X_j} \delta U^\star_{Ki} \right] \mathrm{d}\Omega_0$$ <u>Discretized form</u>

<u>Configurational forces and moments</u>

$$\overline{F}_{Ki} = \int_{\Omega_0} \Sigma_{ij} N_{0Kj} \mathrm{d}\Omega_0$$

$$\overline{M}_{Ki} = \int_{\Omega_0} \Sigma_{ij} \frac{H}{2} \left(\xi_3 N_{Okj} + N_K \frac{\partial \xi_3}{\partial X_j} \right) \mathrm{d}\Omega_0$$

How to combine $\overline{\boldsymbol{F}}$ and $\overline{\boldsymbol{M}}$?

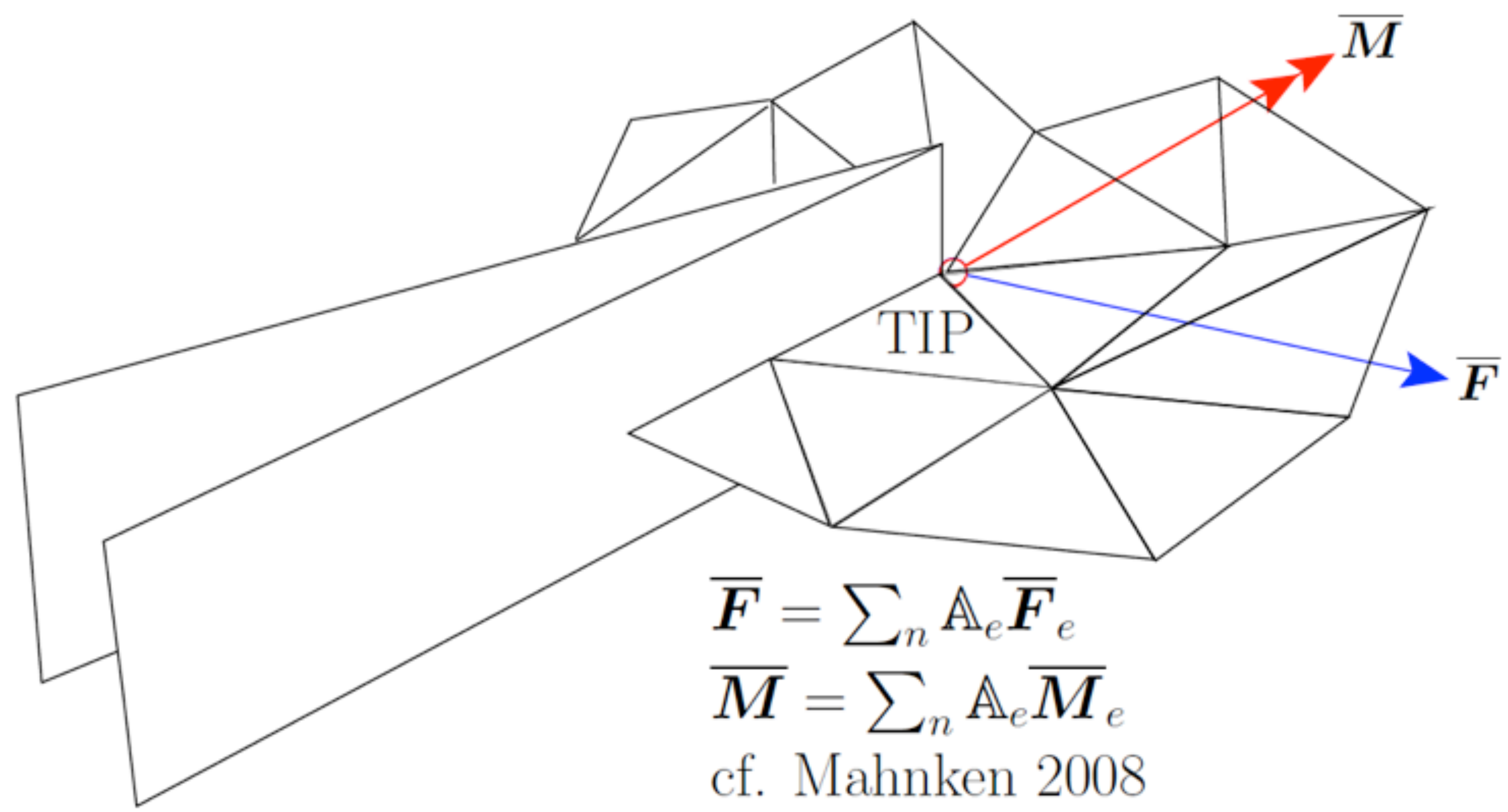

$$\overline{\boldsymbol{F}} = \sum_n \mathbb{A}_e \overline{\boldsymbol{F}}_e$$

$$\overline{\boldsymbol{M}} = \sum_n \mathbb{A}_e \overline{\boldsymbol{M}}_e$$

cf. Mahnken 2008

Analysis/Initiation/Propagation algorithm

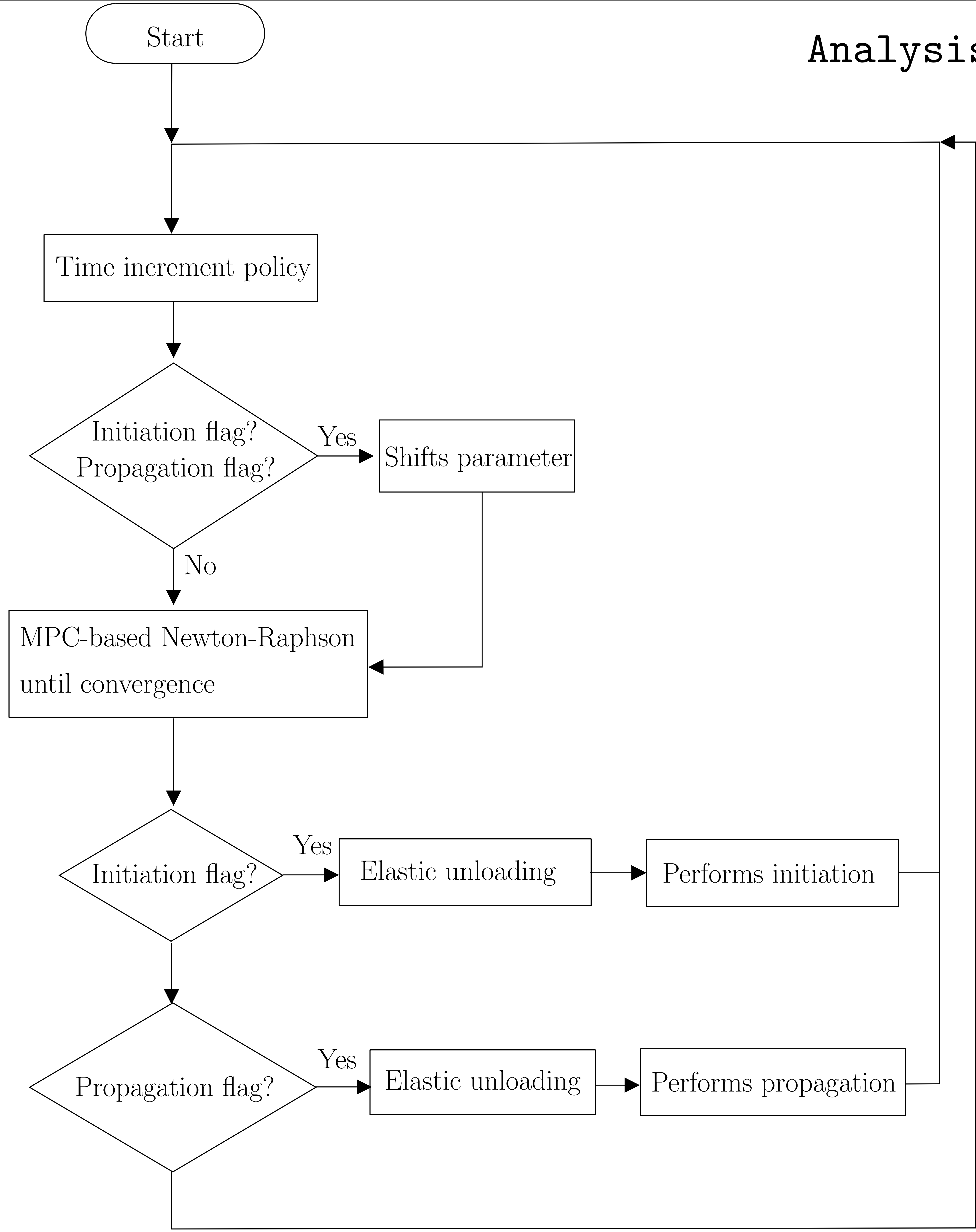

Key points to retain:

Unloading necessary for “hard” elasto-plastic problems

Careful step size adjustment

MPC discussed in FEAD paper

Trial-tested routines

Element technology

Triangle based on polar-decomposition

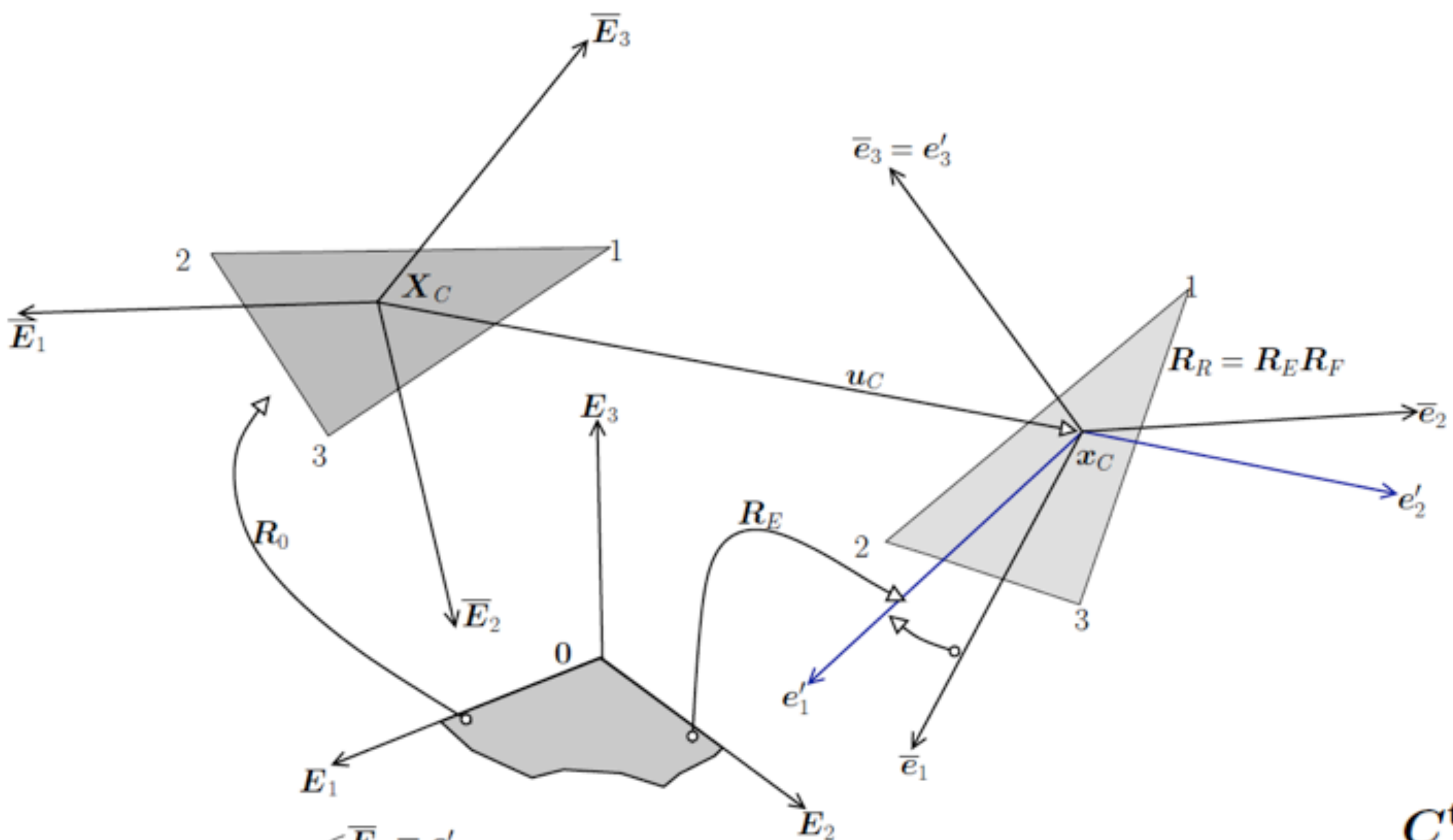

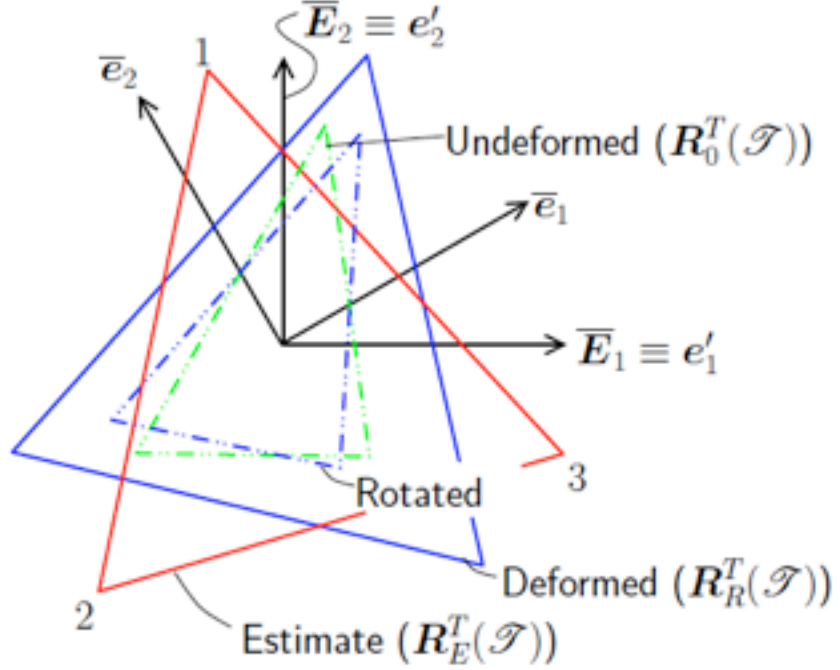

Experimentally observed elasto-plastic flange buckling

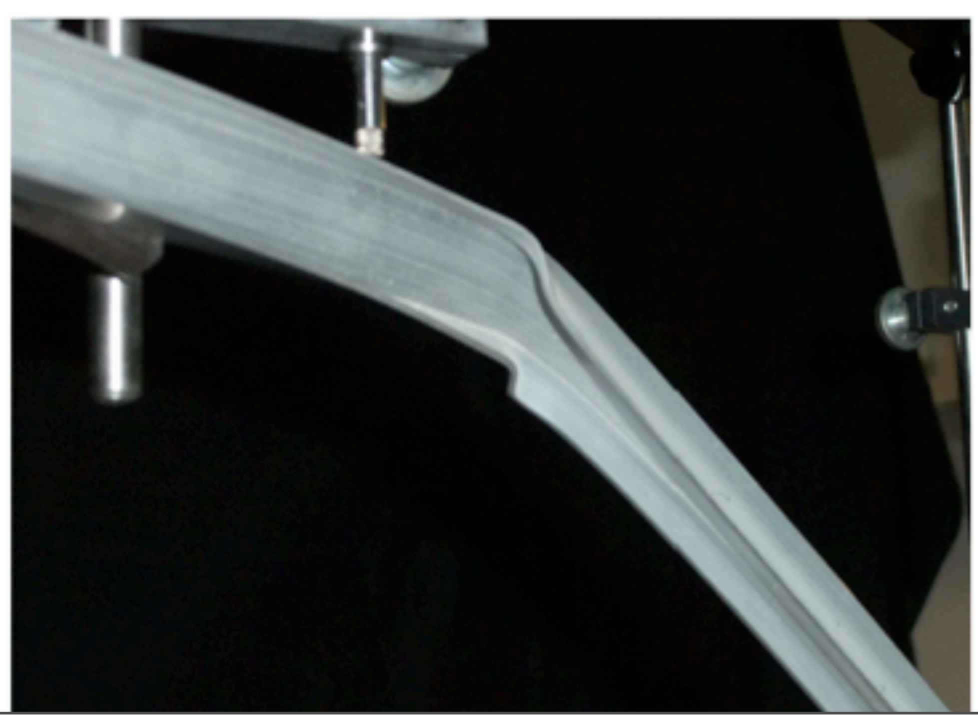

Numerically obtained elasto-plastic flange buckling
(thickness extrusion was performed)

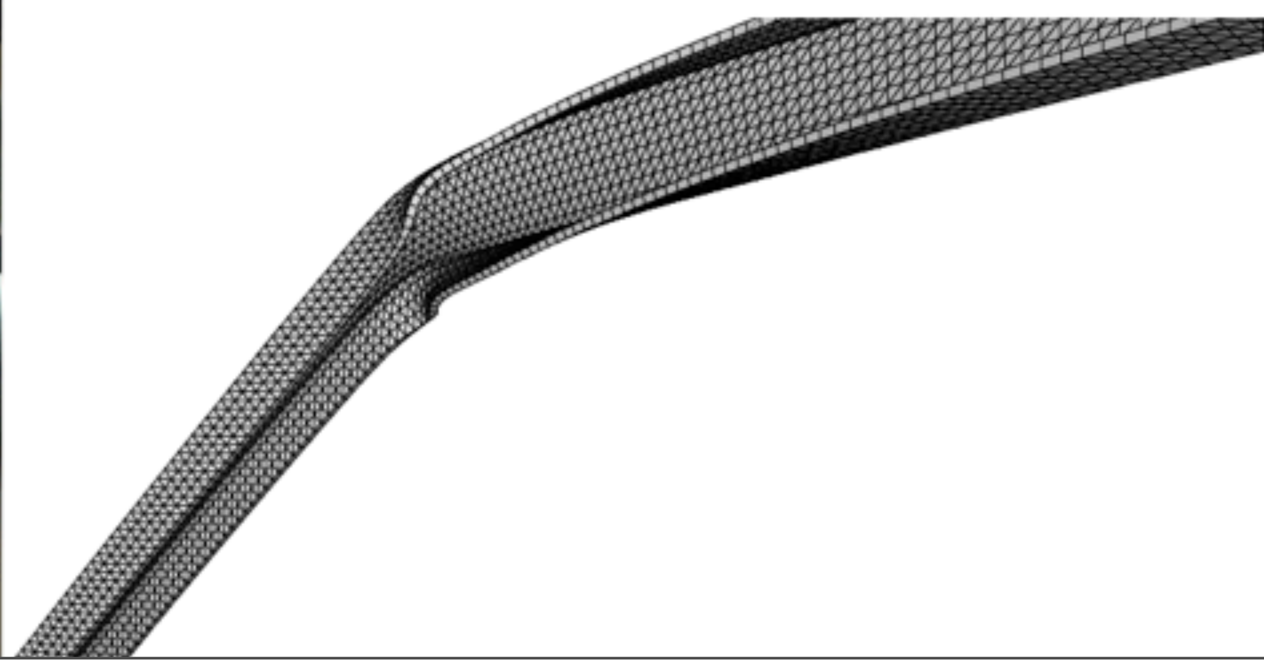

Quadrilateral based on Petrov-Galerkin approach (Areias CM, CMES)

$$C_{ab}^{\text{trial}} = \boldsymbol{y}_b^T \begin{bmatrix} m_{11} + \theta^1\gamma_1 & m_{12} + \theta^1\gamma_3 + \theta^2\gamma_4 & N_A m_{13A} + N_B m_{13B} \\ m_{21} + \theta^1\gamma_3 + \theta^2\gamma_4 & m_{21} + \theta^2\gamma_2 & N_C m_{23C} + N_D m_{23D} \\ N_A m_{13A} + N_B m_{13B} & N_C m_{23C} + N_D m_{23D} & m_{33} \end{bmatrix} \boldsymbol{y}_b$$

$$C_{ab}^{\text{test}} = \boldsymbol{y}_b^T \begin{bmatrix} m_{11} & m_{12} & 0 \\ m_{21} & m_{21} & 0 \\ 0 & 0 & m_{33} \end{bmatrix} \boldsymbol{y}_b + \overline{\boldsymbol{y}}_b^T \begin{bmatrix} 0 & 0 & N_A m_{13A} + N_B m_{13B} \\ 0 & 0 & N_C m_{23C} + N_D m_{23D} \\ N_A m_{13A} + N_B m_{13B} & N_C m_{23C} + N_D m_{23D} & 0 \end{bmatrix} \overline{\boldsymbol{y}}_b + \sqrt{\frac{\det[\overline{\boldsymbol{m}}_{bb}]}{\det[\boldsymbol{m}_{bb}]}} \overline{\boldsymbol{y}}_b^T \begin{bmatrix} \theta^1\gamma_1 & \theta^1\gamma_3 + \theta^2\gamma_4 & 0 \\ \theta^1\gamma_3 + \theta^2\gamma_4 & \theta^2\gamma_2 & 0 \\ 0 & 0 & 0 \end{bmatrix} \overline{\boldsymbol{y}}_b$$

2D benchmark exercises

1) Bittencourt, Ingraffea, Wawrzynek and Sousa EFM 1996

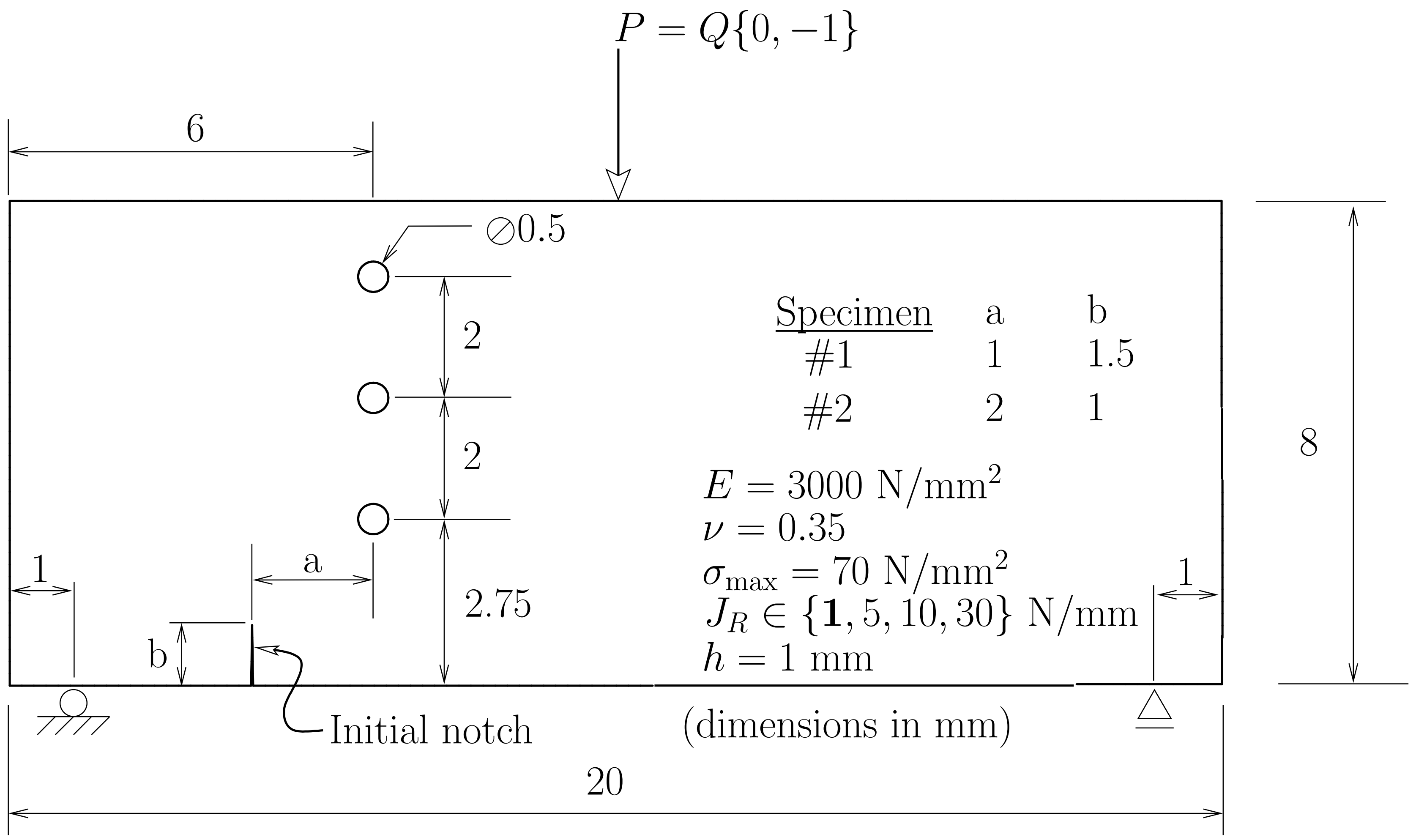

(a) Relevant data for Bittencourt's drilled plate.

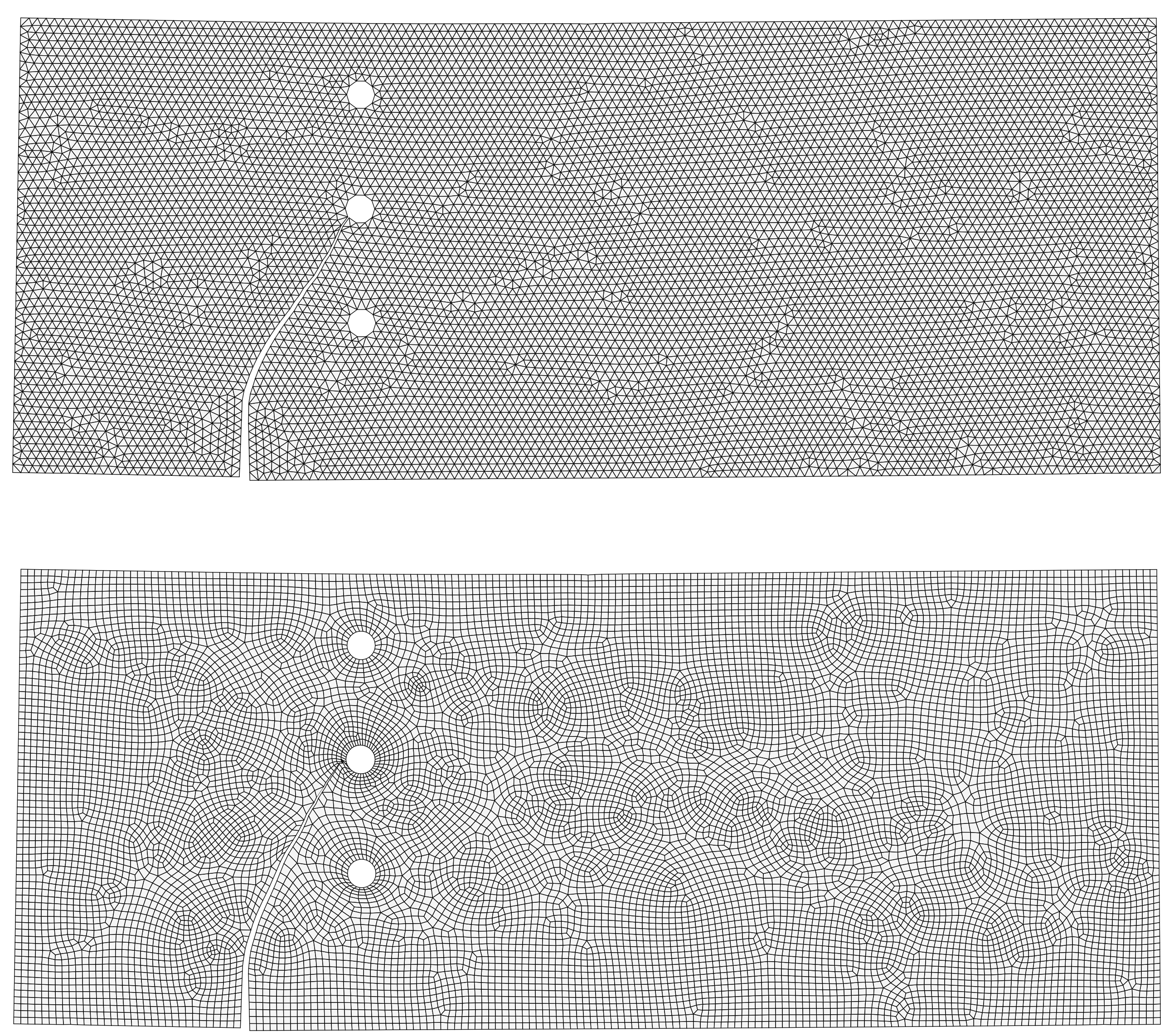

Figure 11: Bittencourt's drilled plate. Results shown for specimen #2. Triangular mesh contains 16082 elements and 8248 nodes. The quadrilateral mesh contains 12565 elements and 12850 nodes.

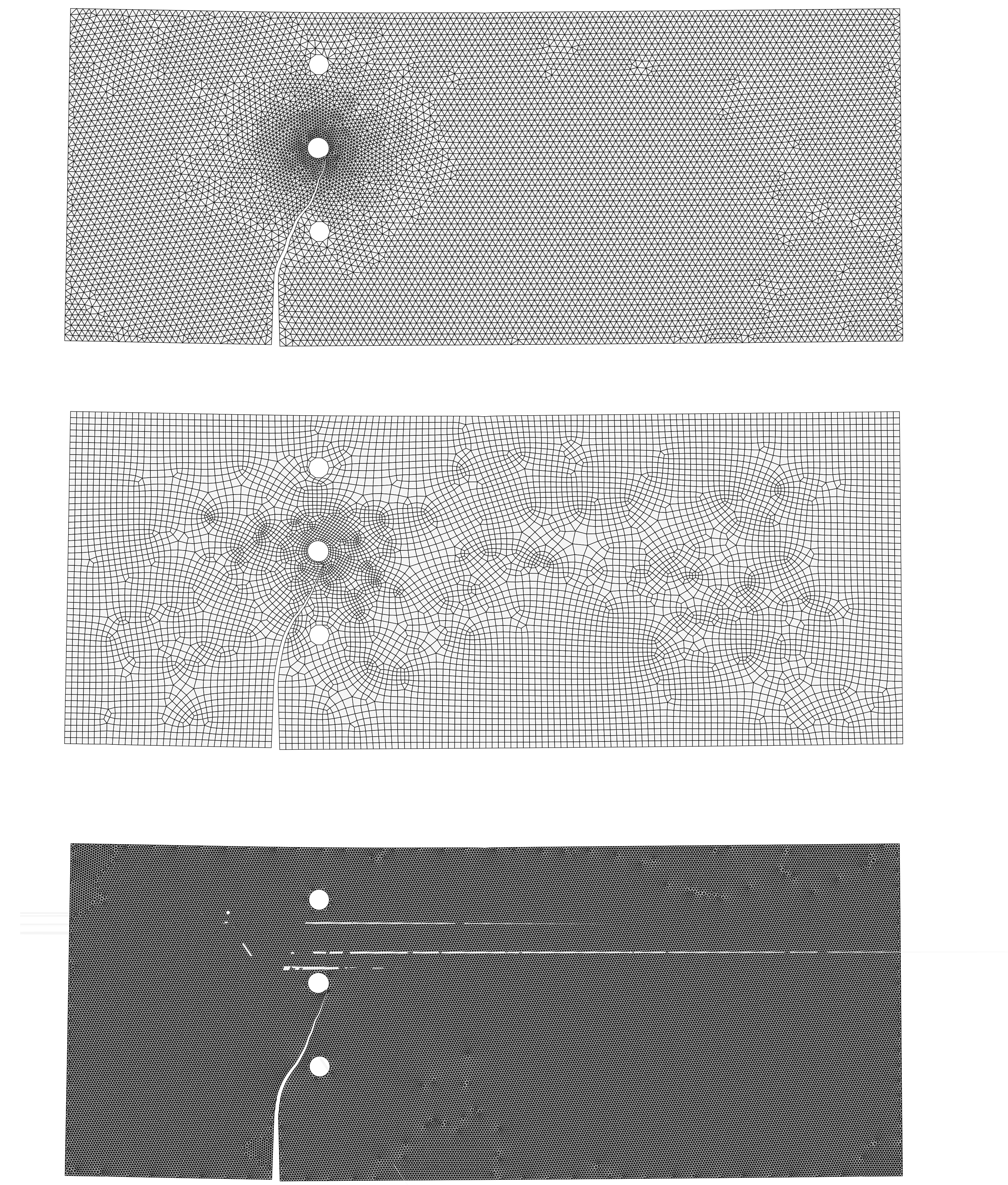

(b) Specimen #1 deformed mesh (triangles and quadrilaterals) with local refinement. Coarse triangular mesh contains 9126 nodes and 17812 elements and the coarse quadrilateral mesh contains 9062 nodes and 8841 elements. The uniform triangular mesh is also shown (51299 nodes and 101541 elements).

Load / CMOD

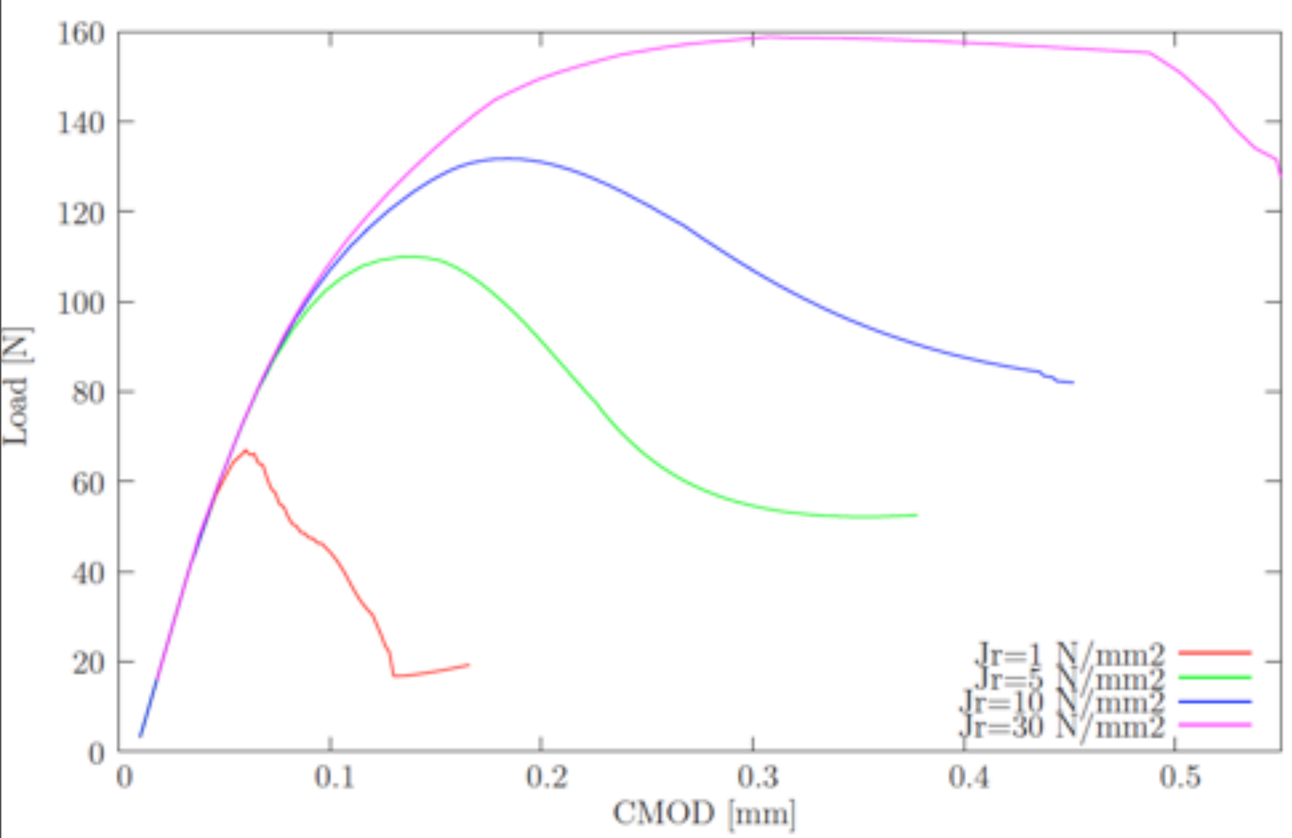

(a) Specimen #1

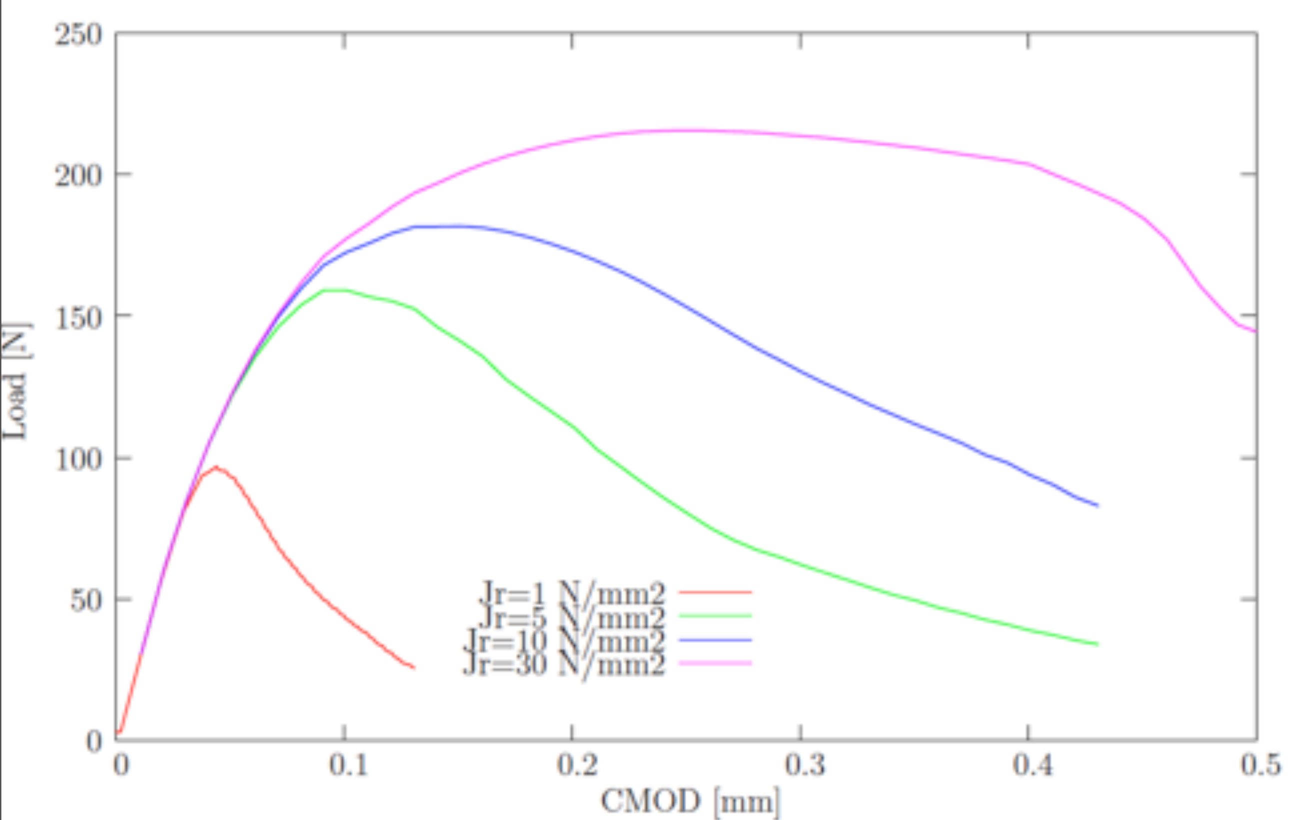

(b) Specimen #2

Load / Displacement

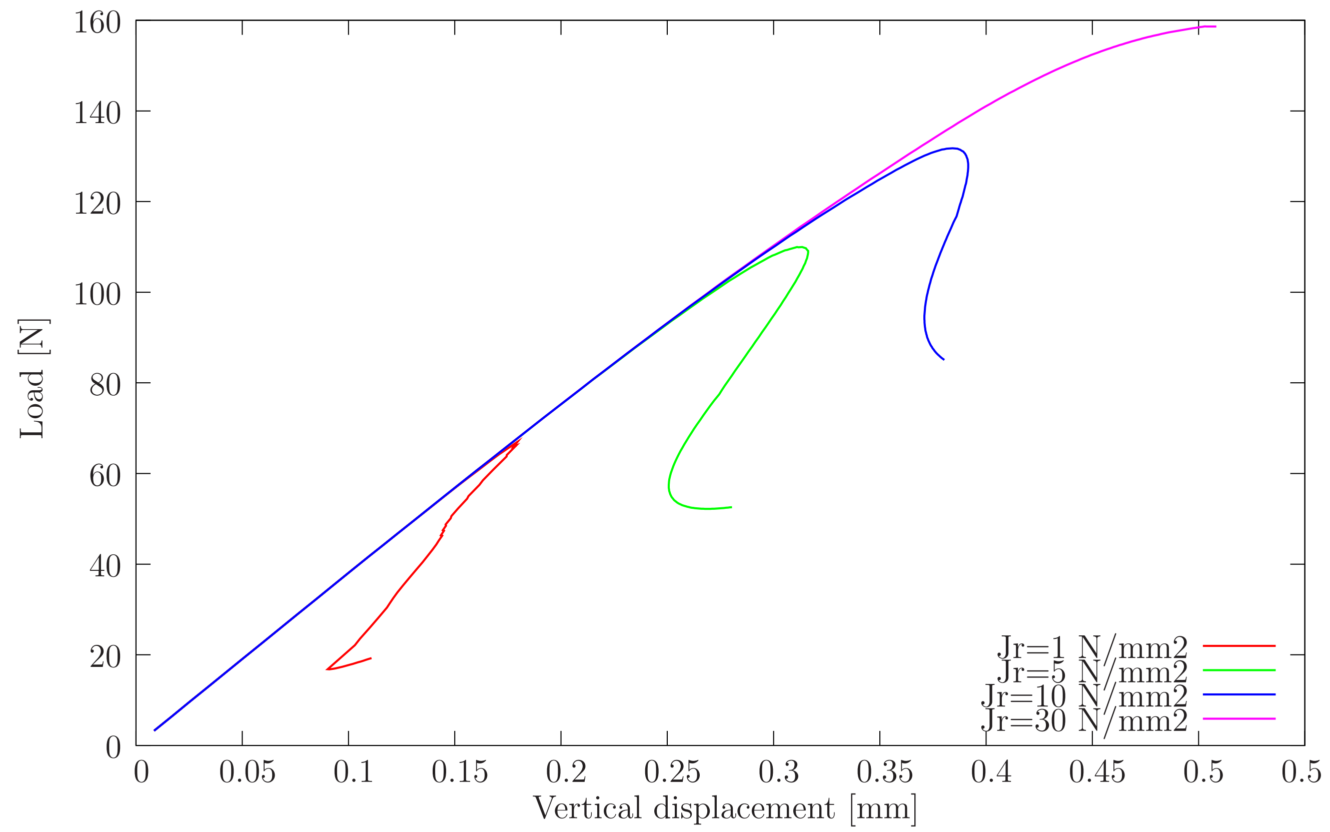

(a) Specimen #1

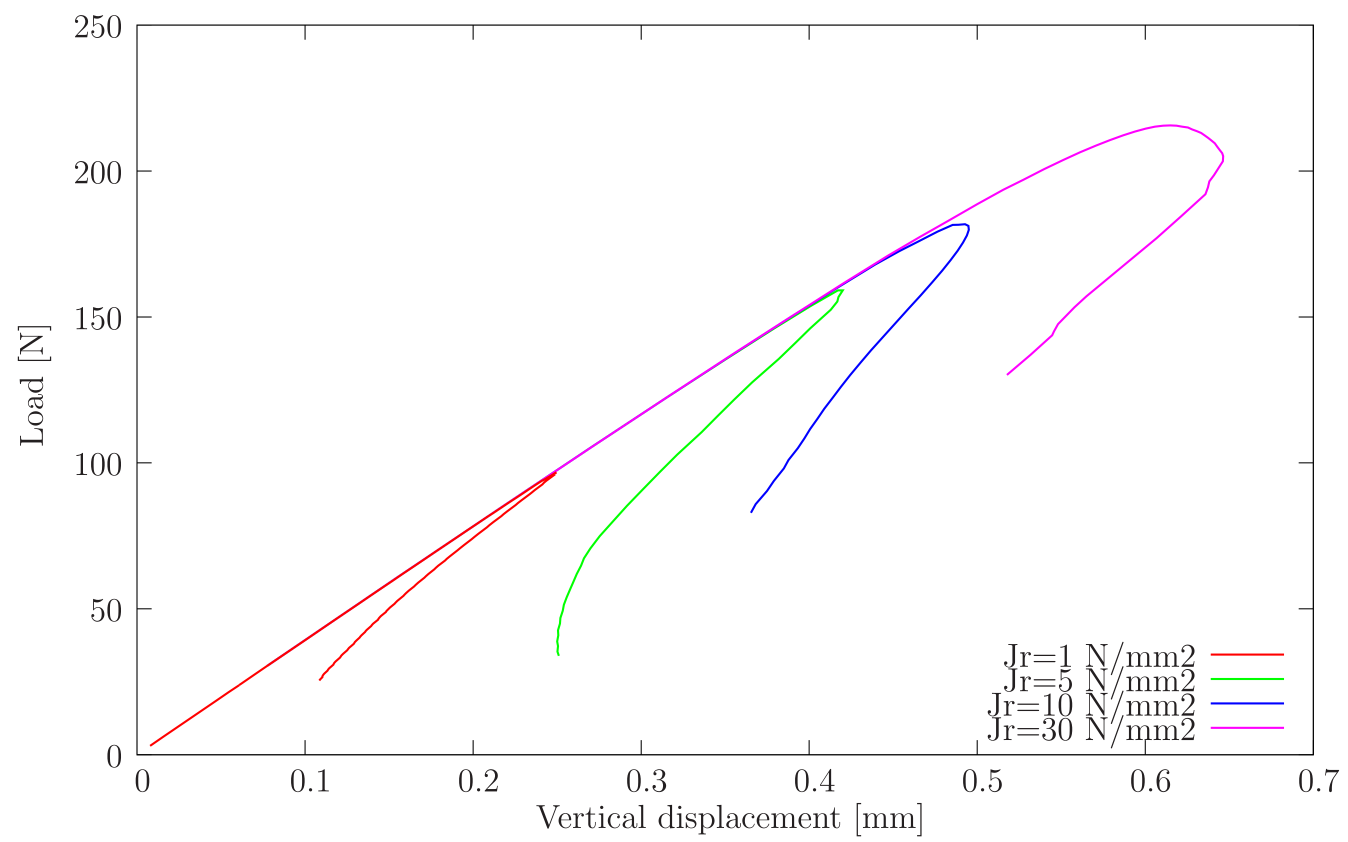

(b) Specimen #2

Cohesive tails

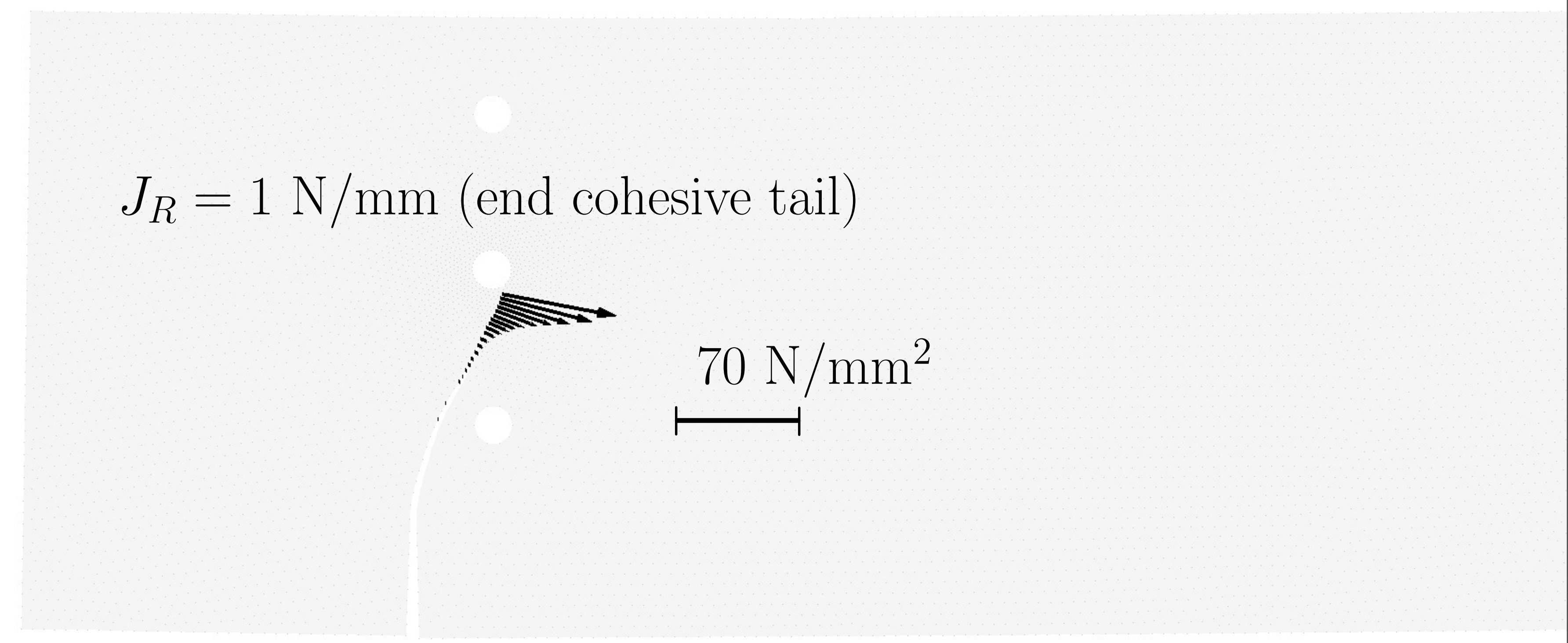

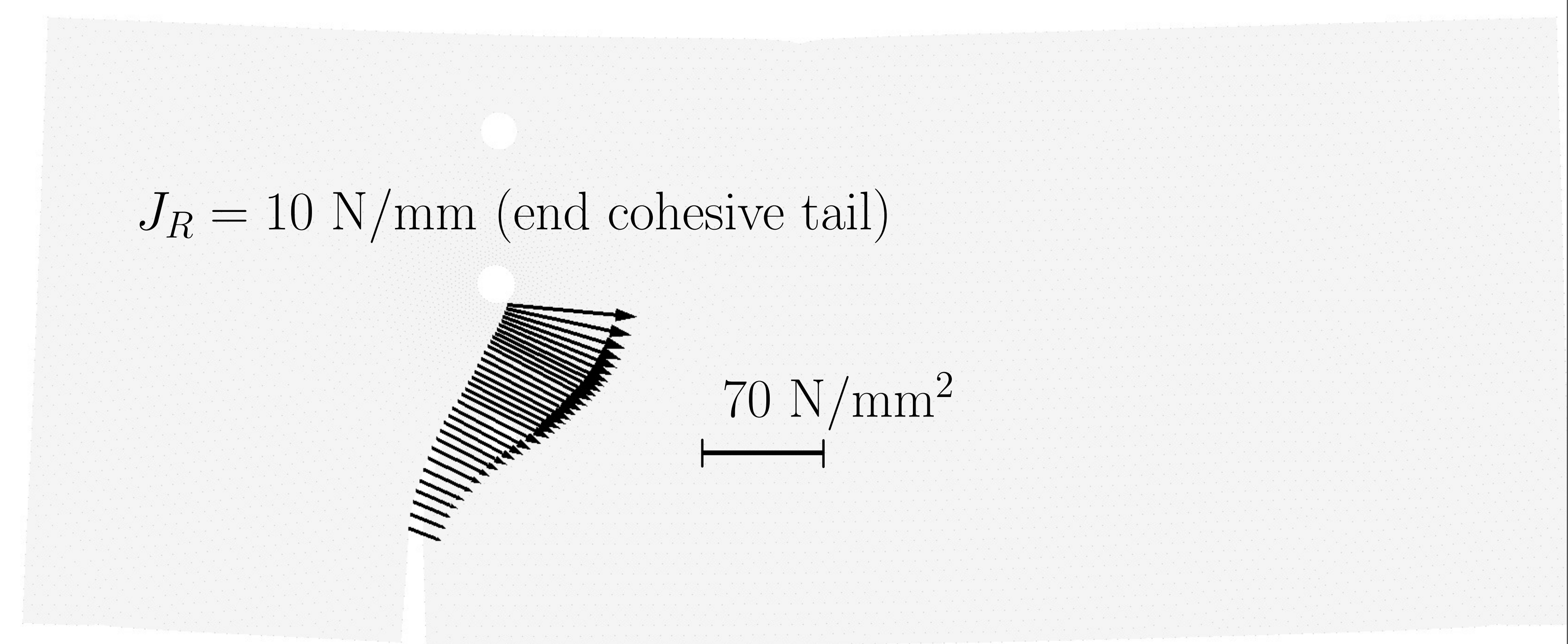

Movie specimens #1 and #2

3)Four point bending test (Bocca, Carpintieri and Valente IJSS 1991)

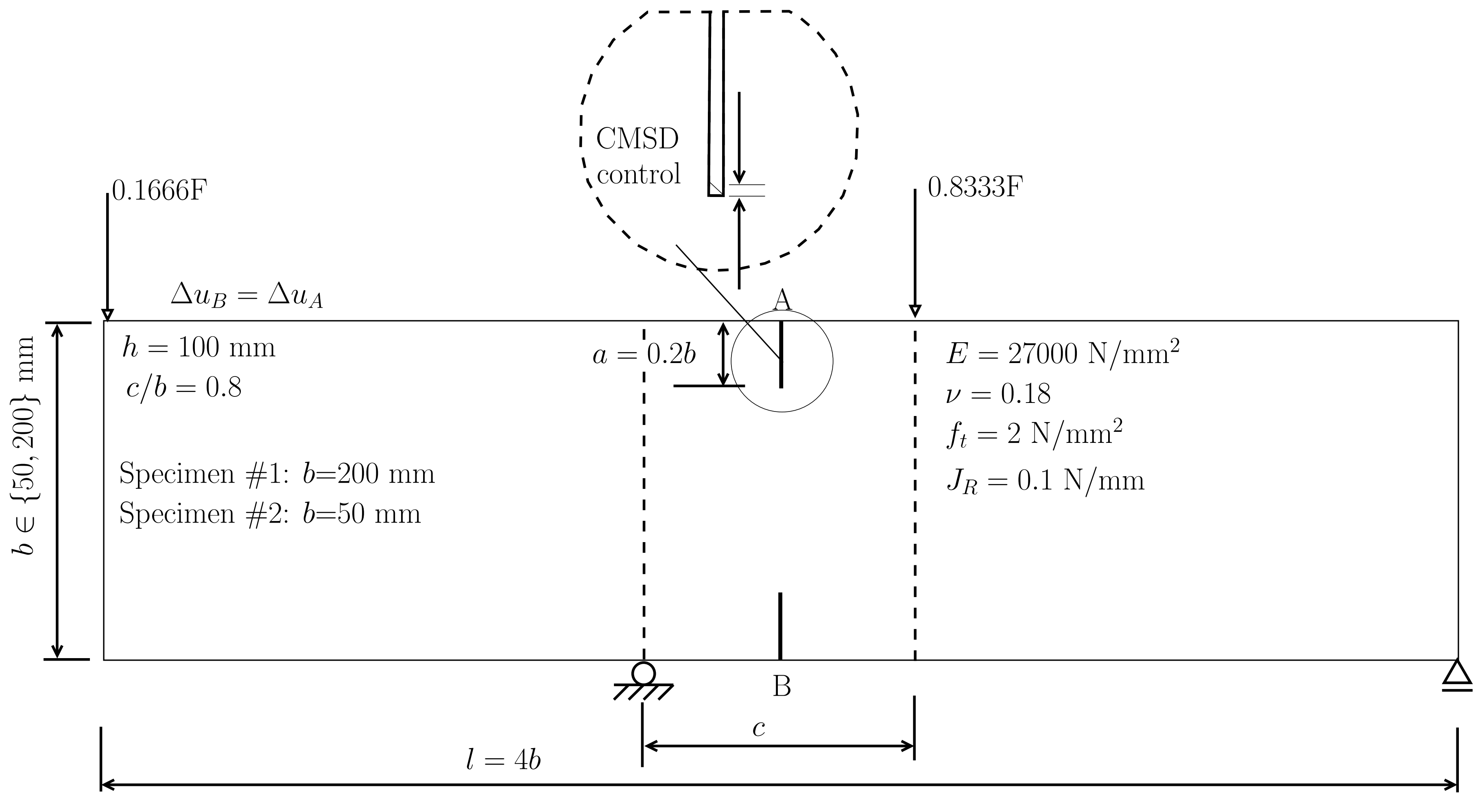

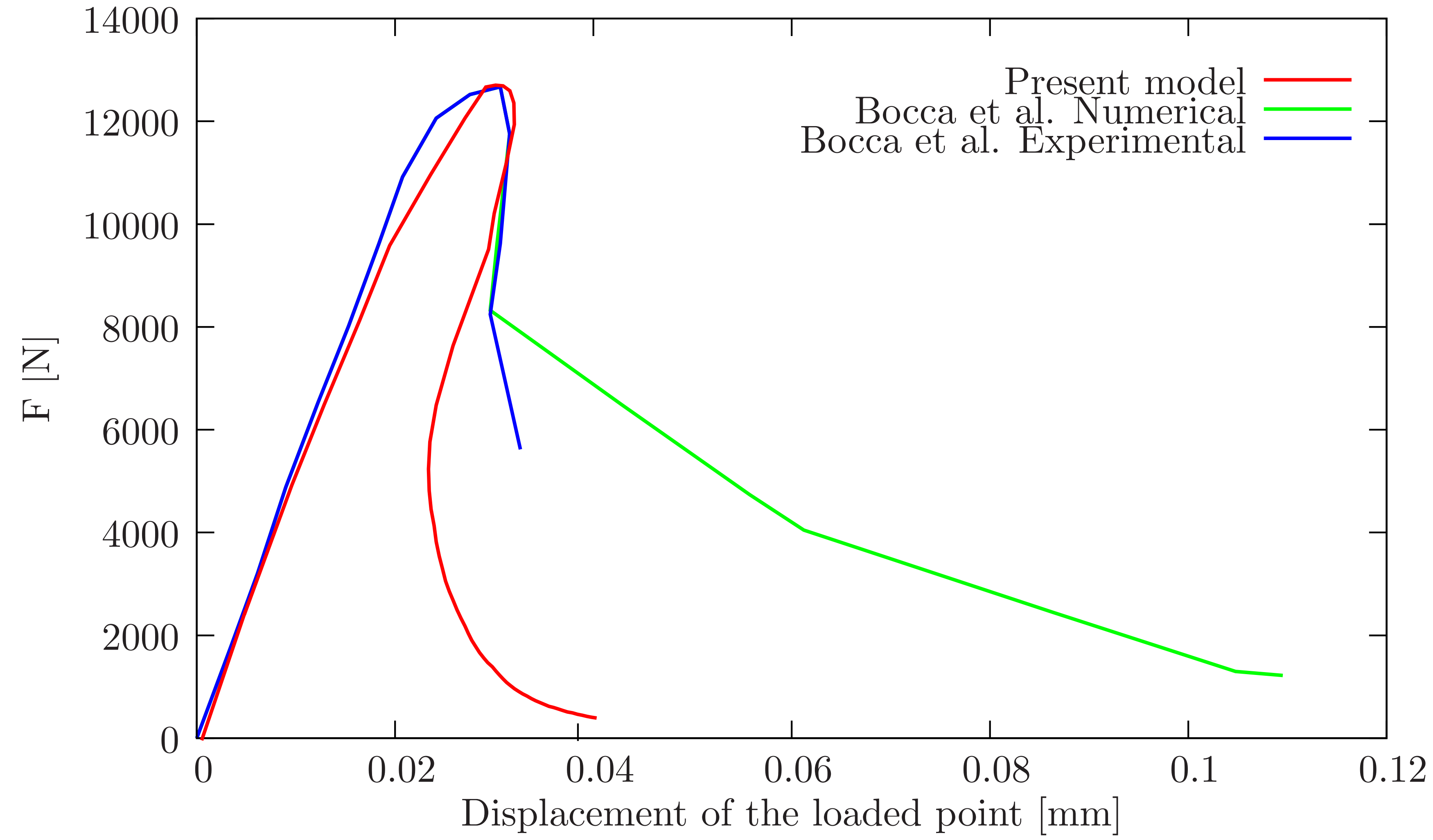

(a) $b = 50$ mm

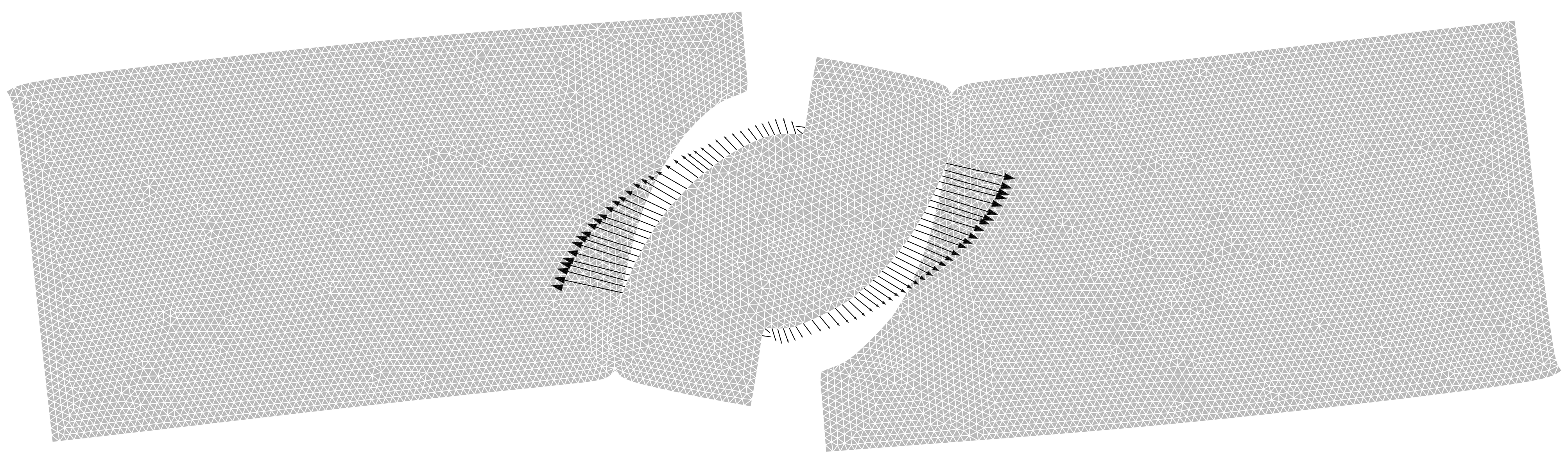

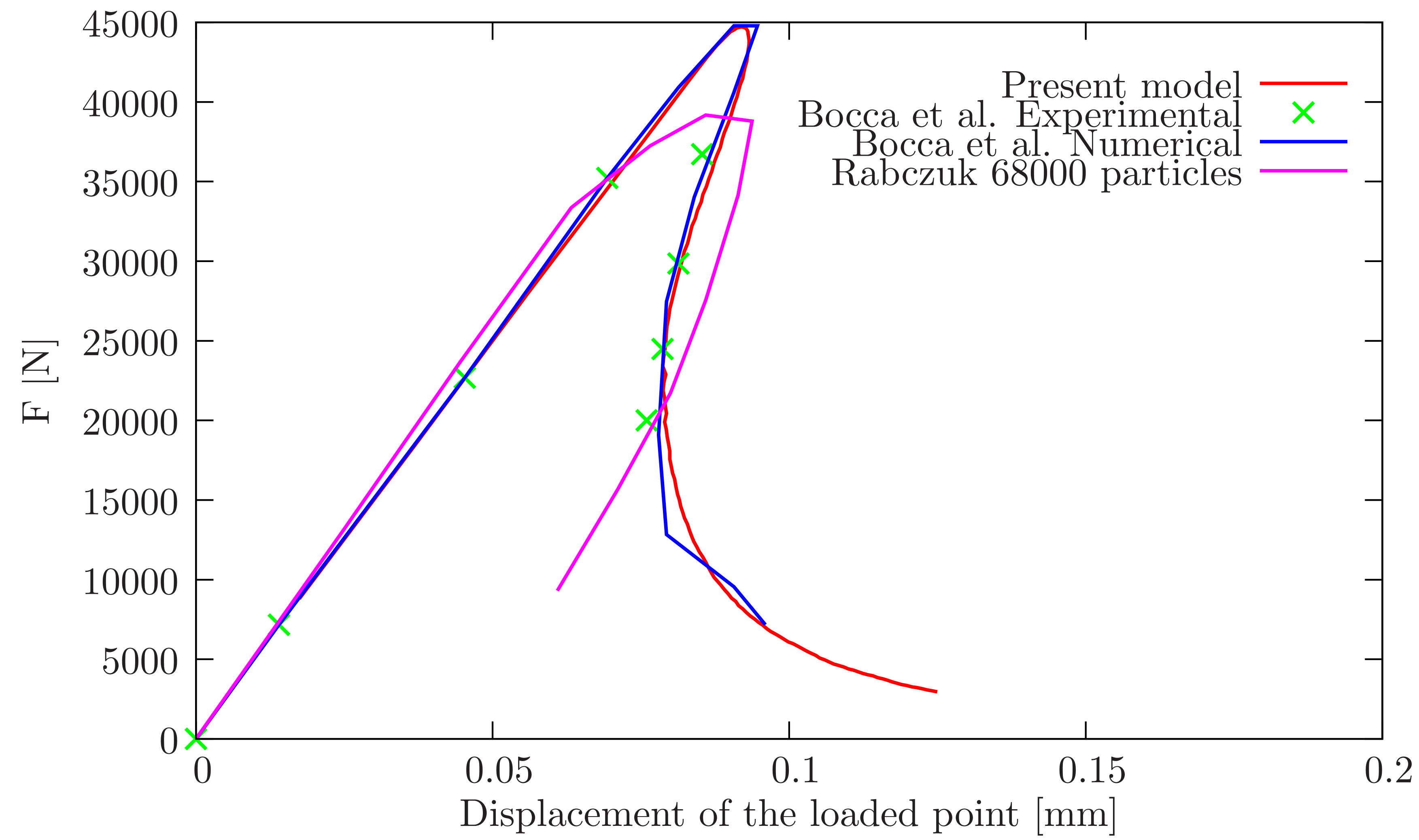

(b) $b = 200$ mm

4) Schlangen Ph.D. 1993

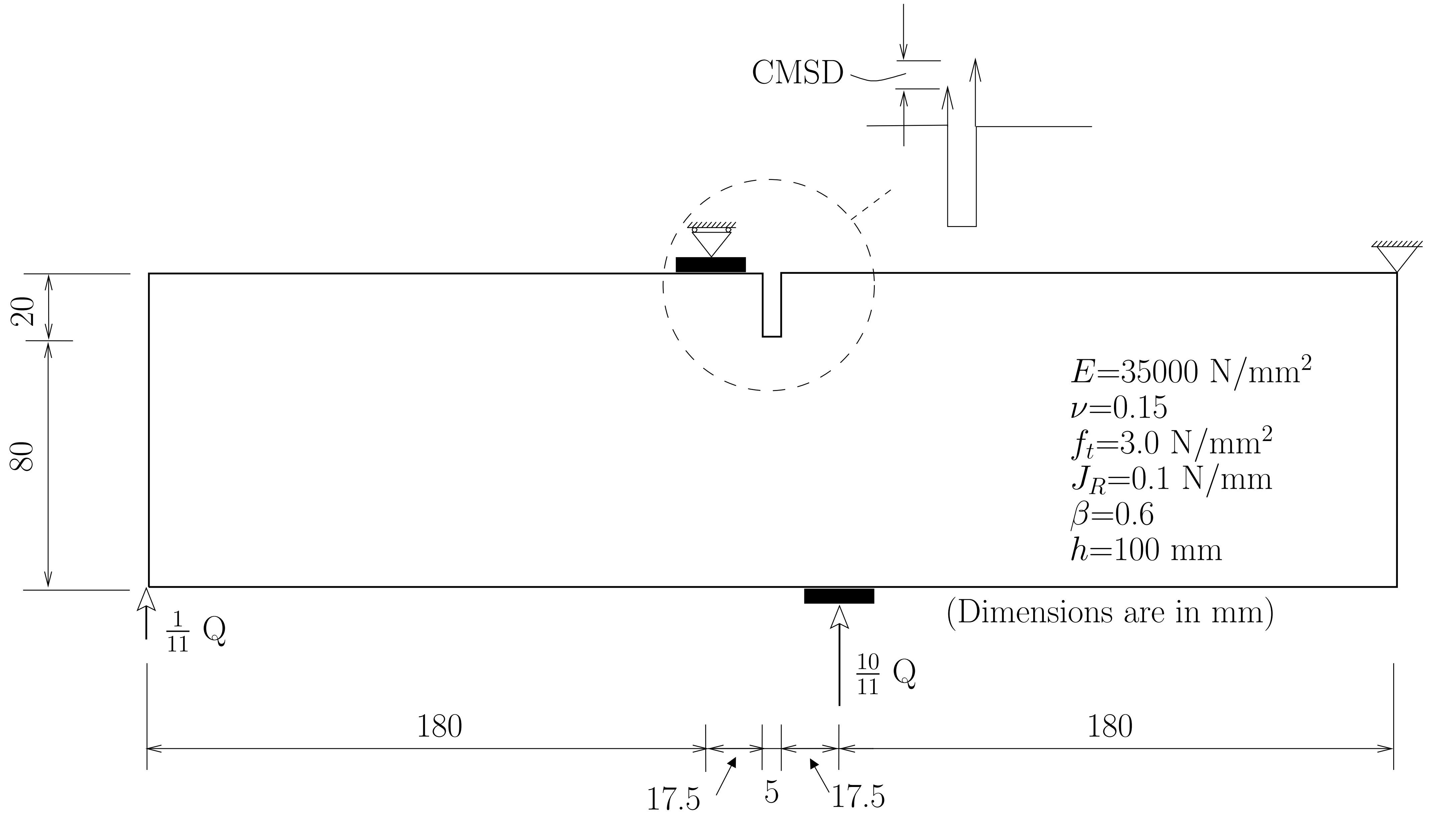

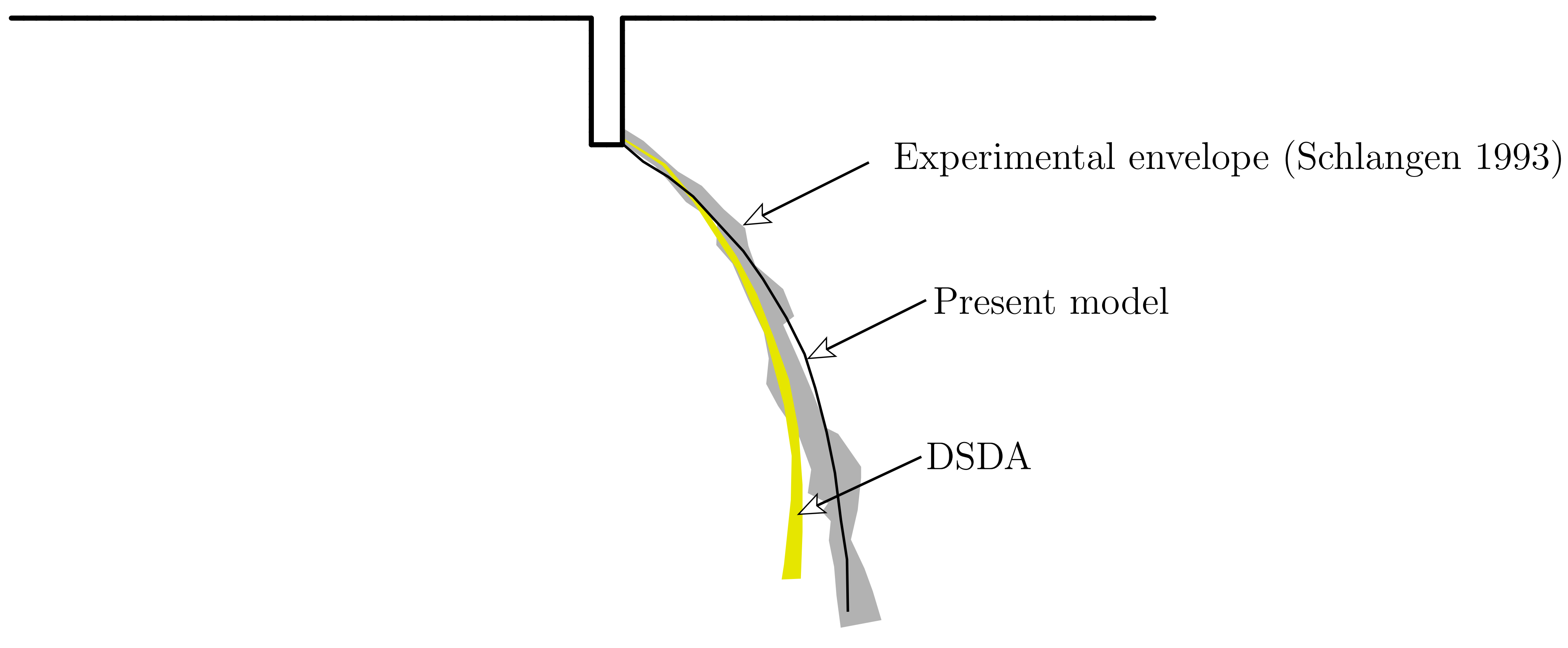

(d) Crack path comparison

Movie cohesive

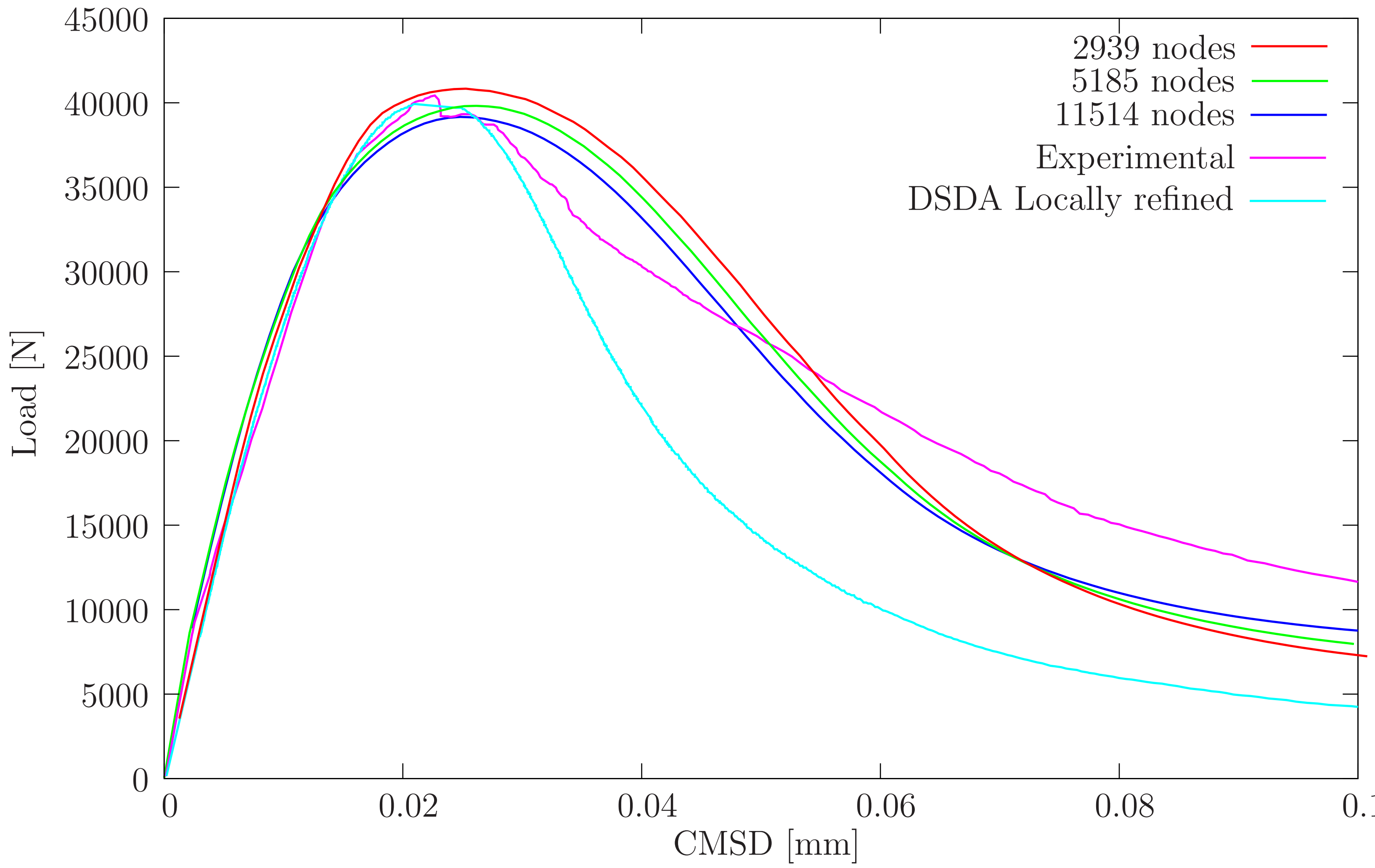

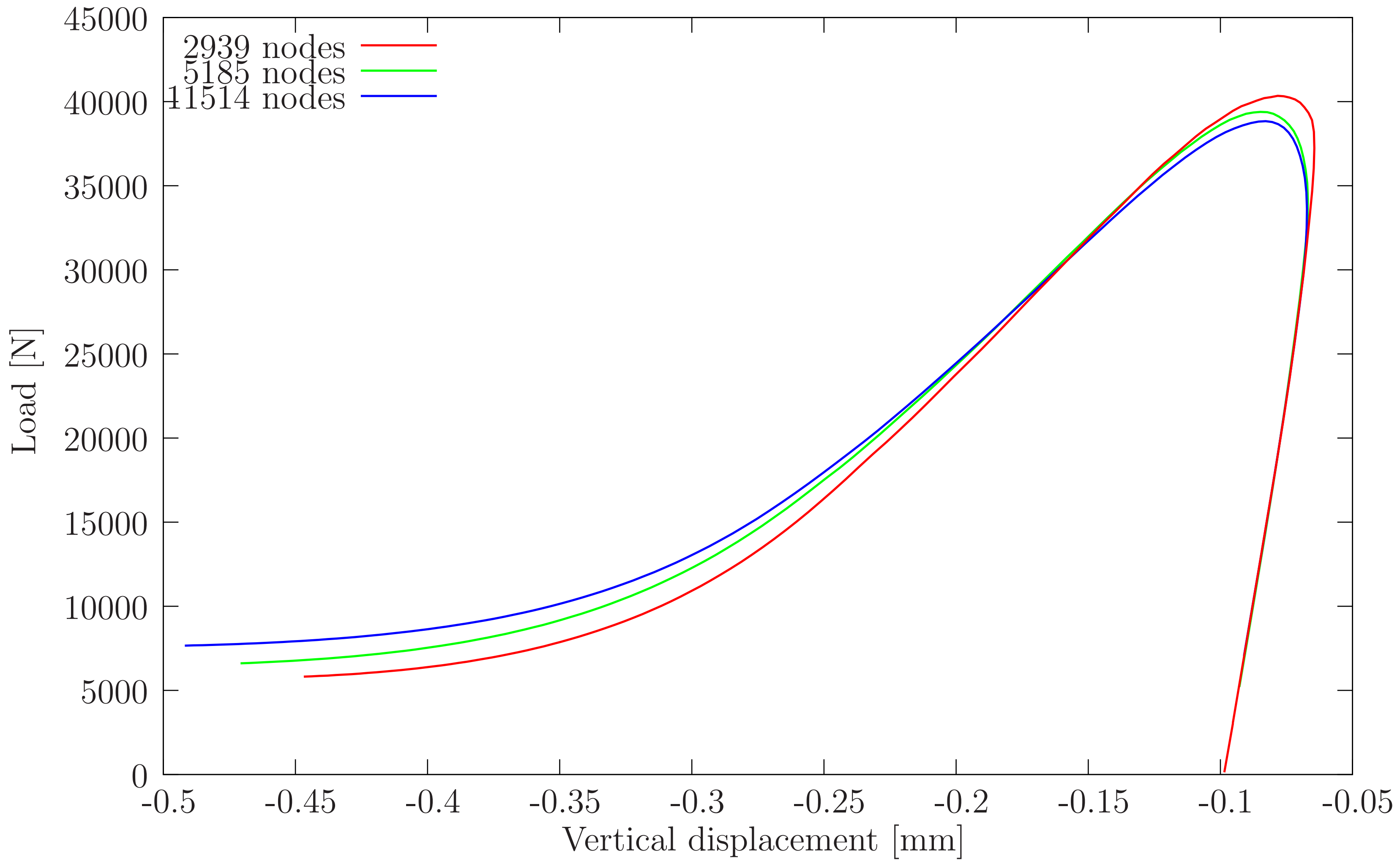

5) Gravity dam (Barpi and Valente ASCE JEM 2000)

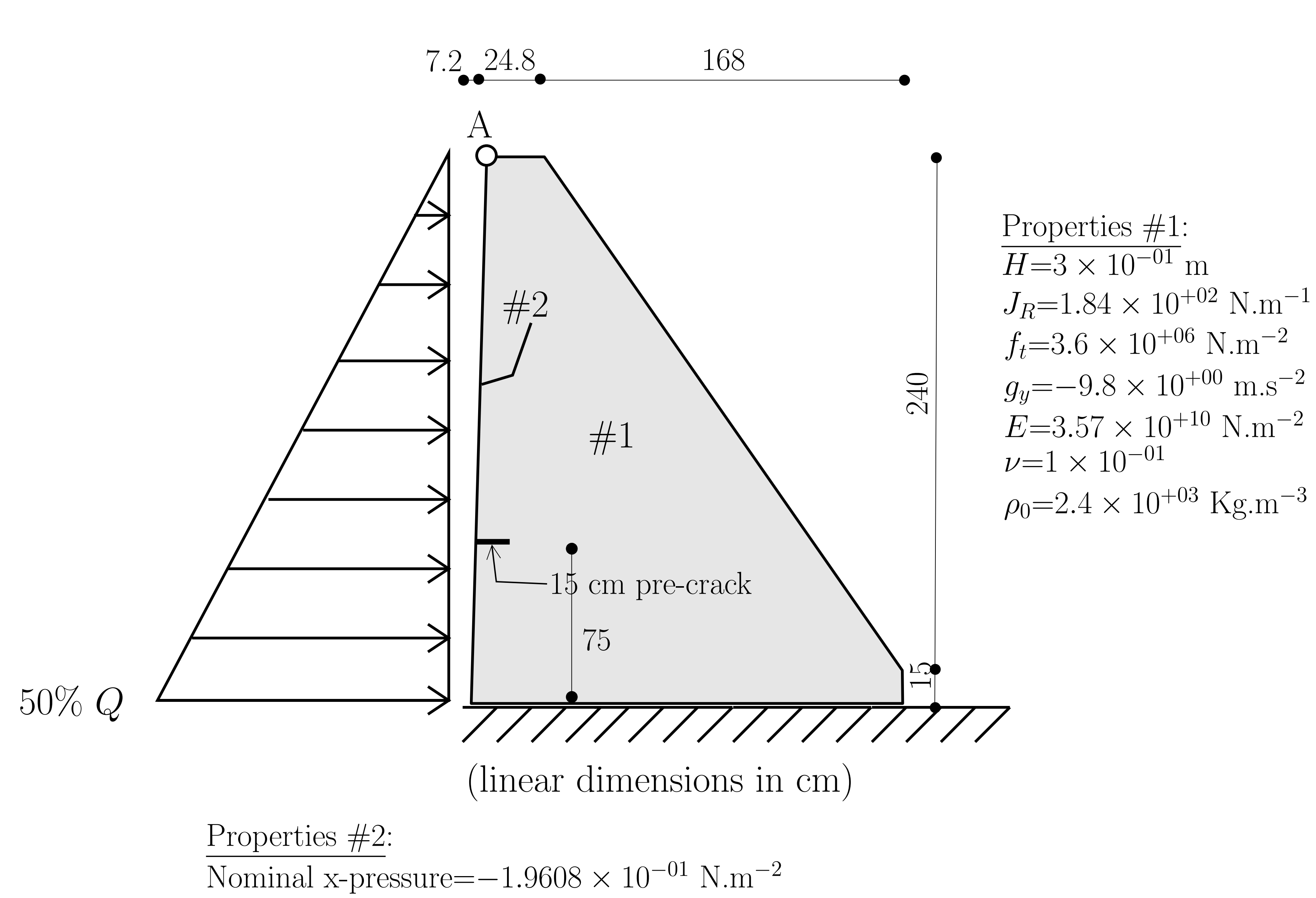

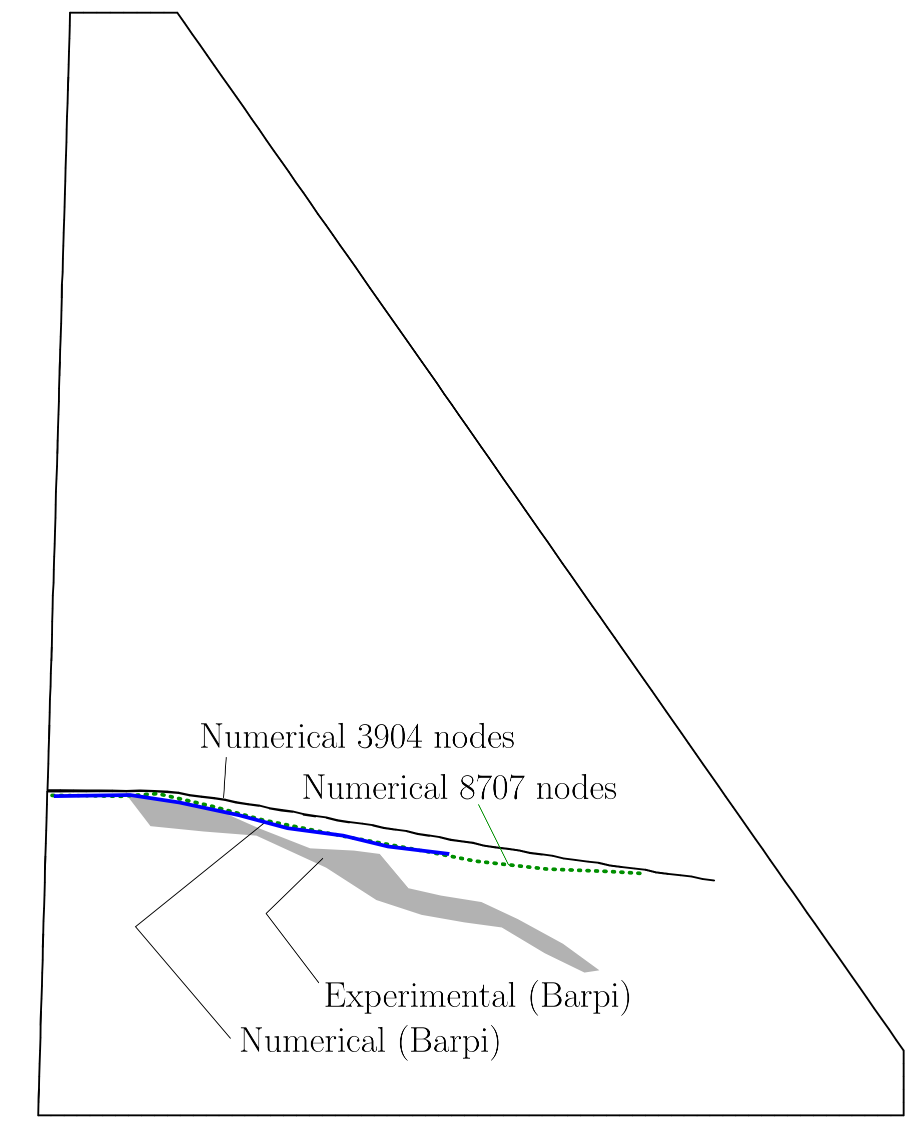

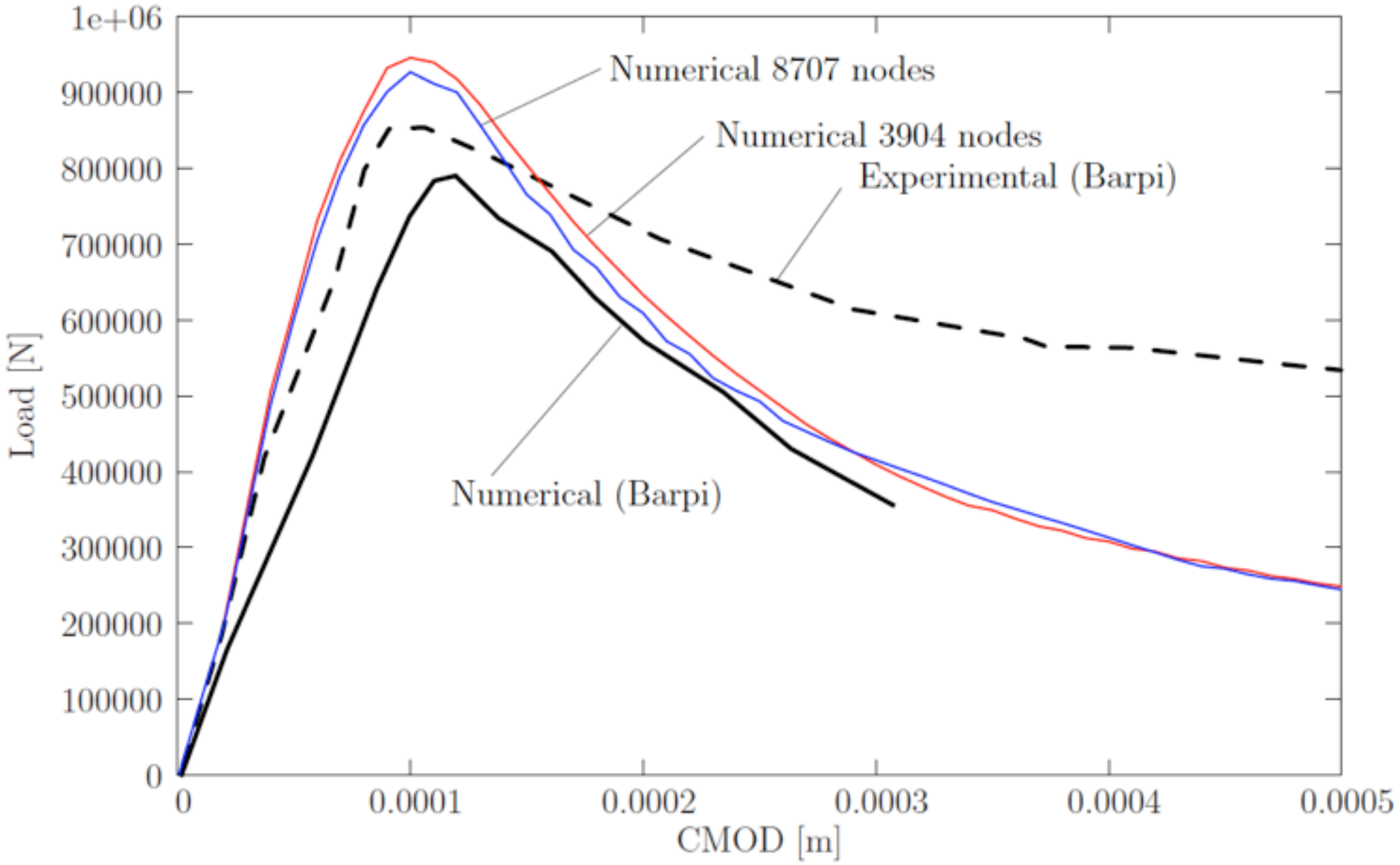

Movie cohesive

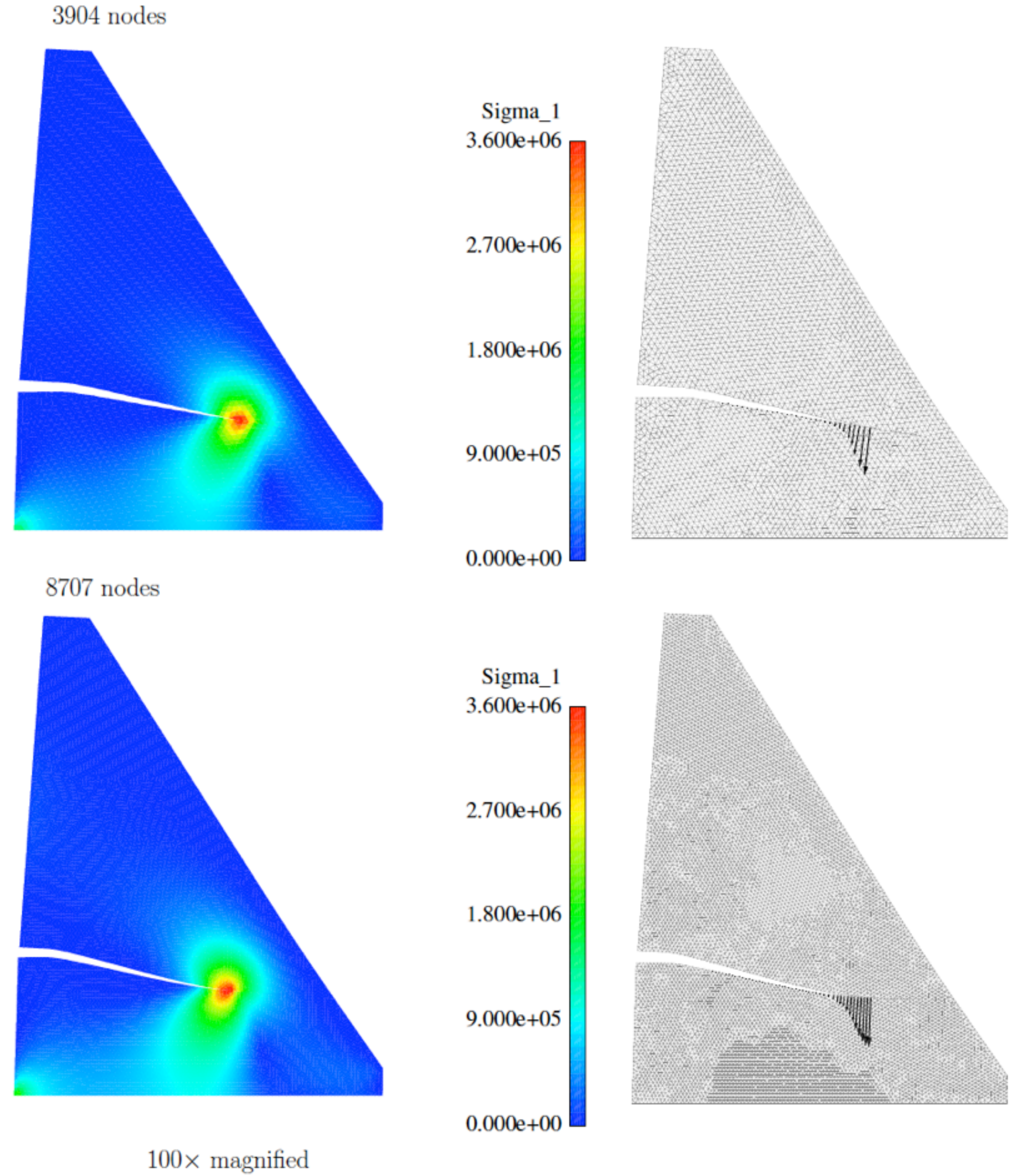

7) Arcan test (Sutton et al. IJSS 2000)

$E = 73.1$ GPa

$\nu = 0.33$

$\sigma_y = 344 + 769.44\bar{\varepsilon}_p$ Mpa for $\bar{\varepsilon}_p \leq 0.18$

$\sigma_y = 483 + 45.122(\bar{\varepsilon}_p - 0.18)$ Mpa for $\bar{\varepsilon}_p > 0.18$

$\bar{\varepsilon}_f = 0.18$

$h = 2.3$ mm

$m = 2$

$f_{\text{crit}} = 0.2$

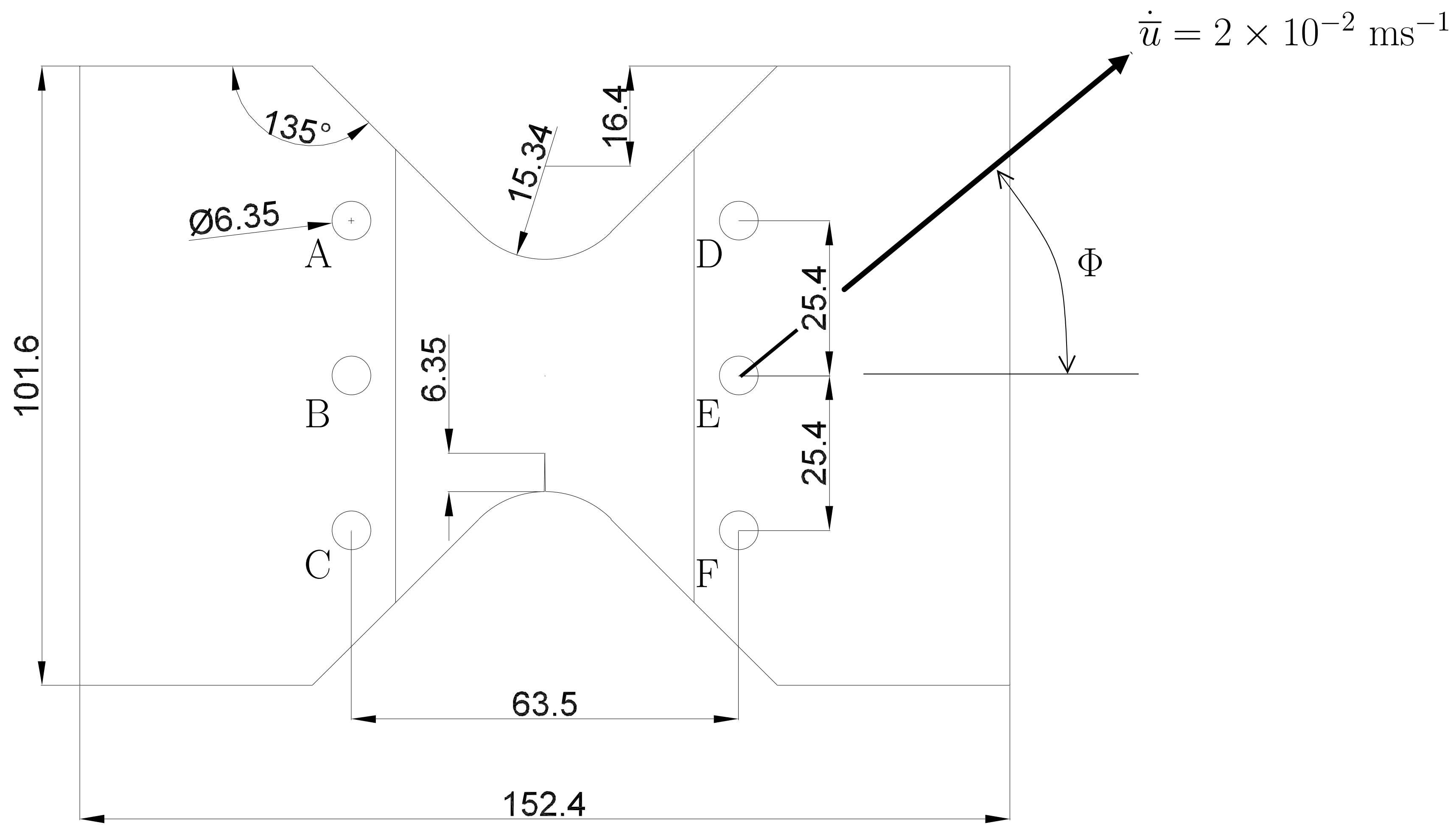

All dimensions in mm

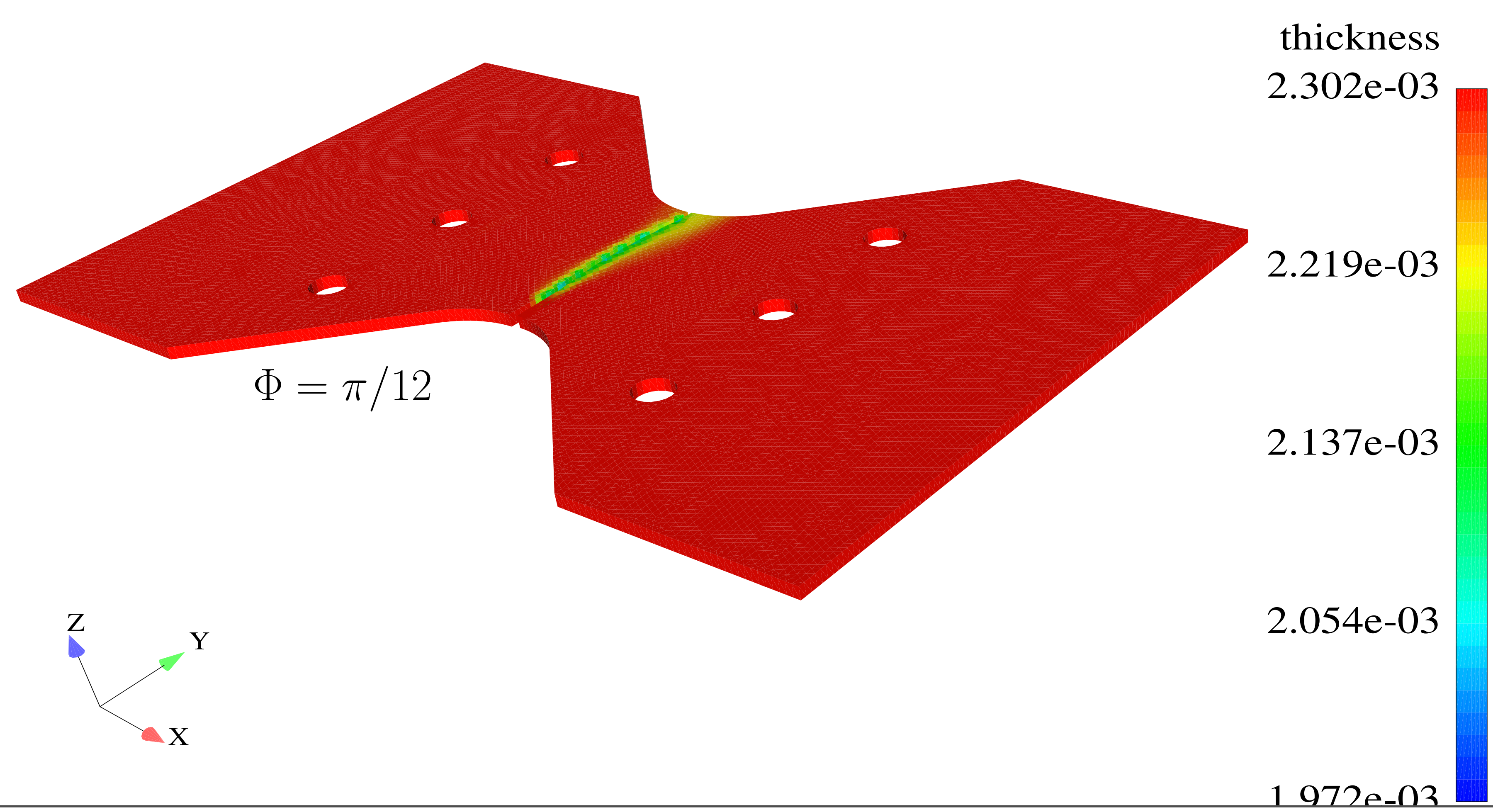

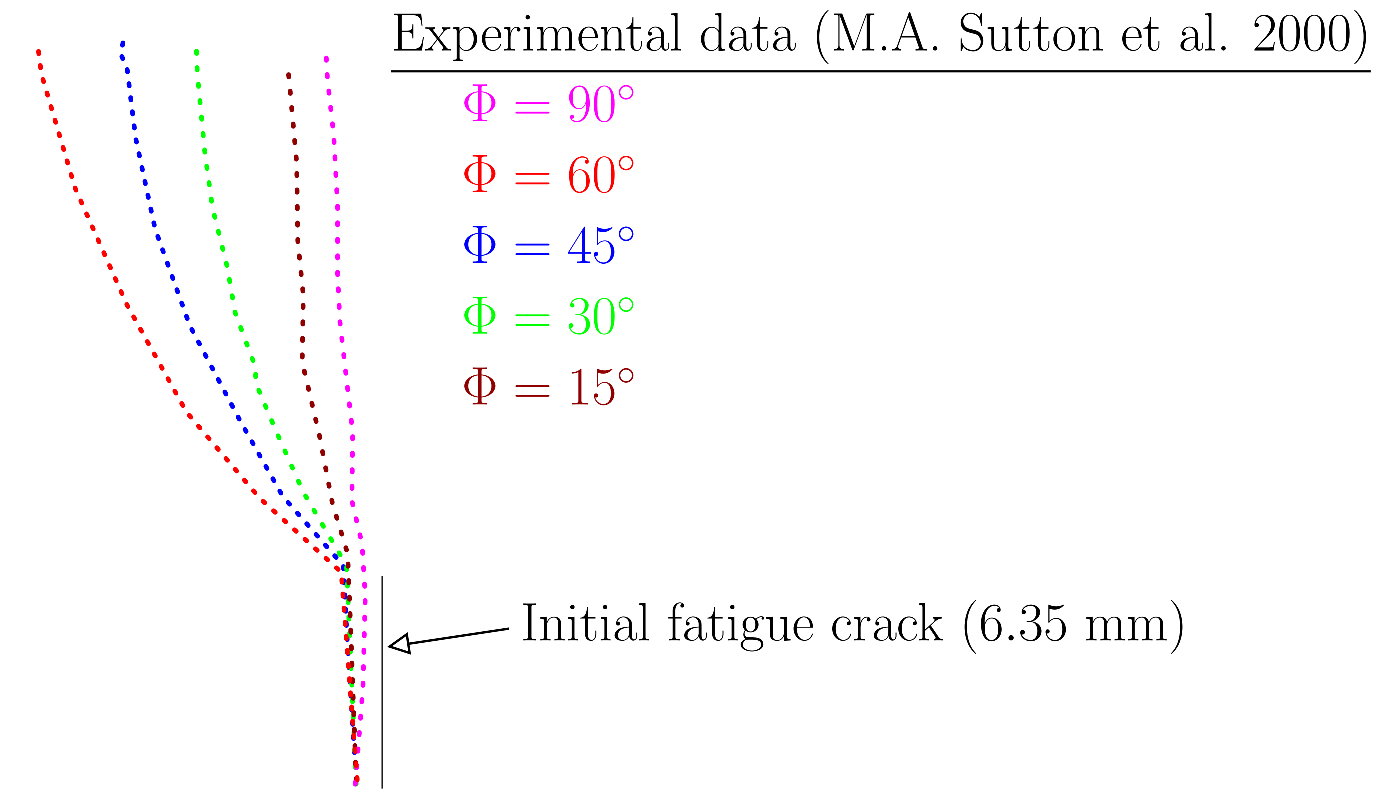

Present simulations

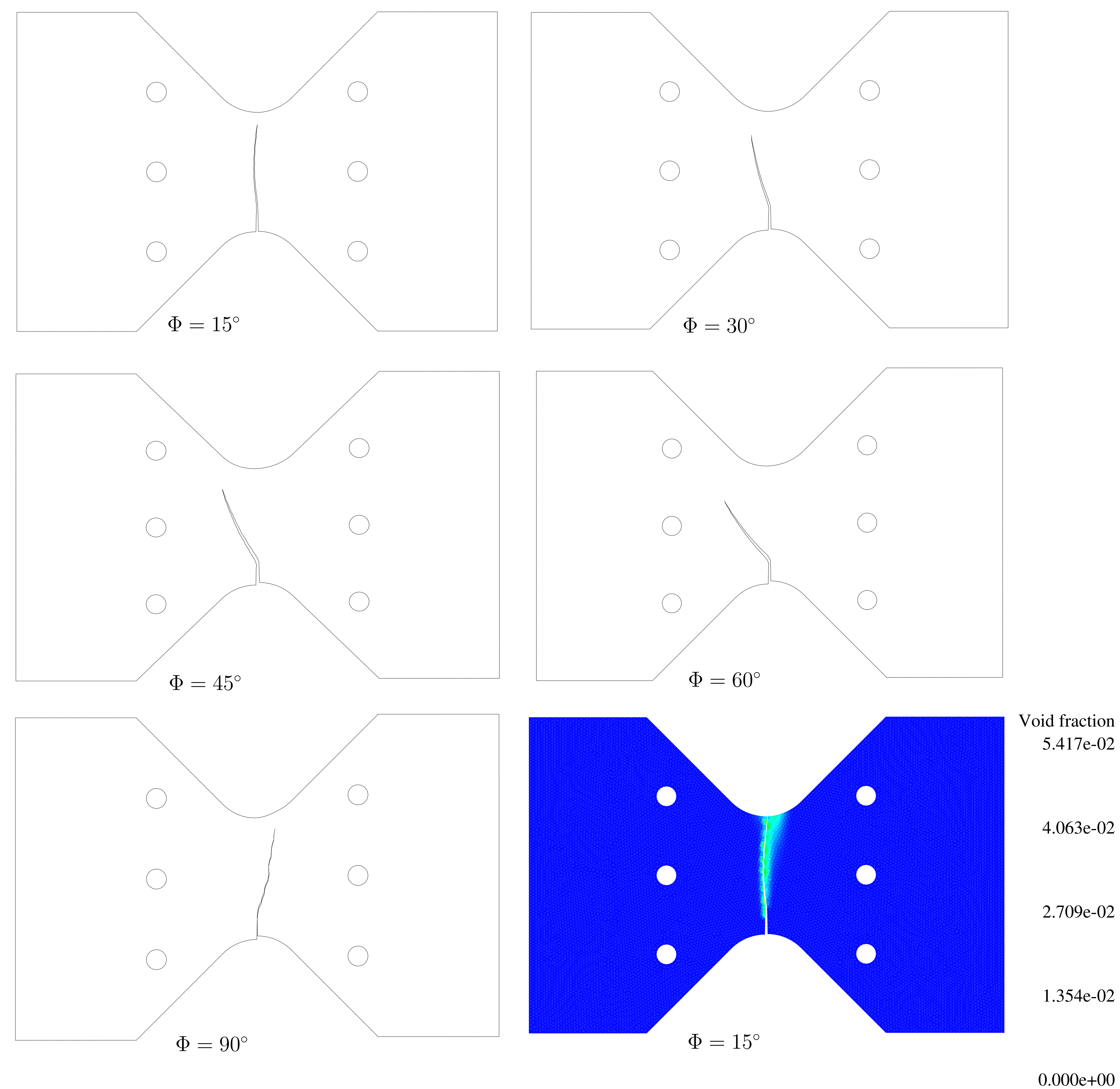

Movie fracture

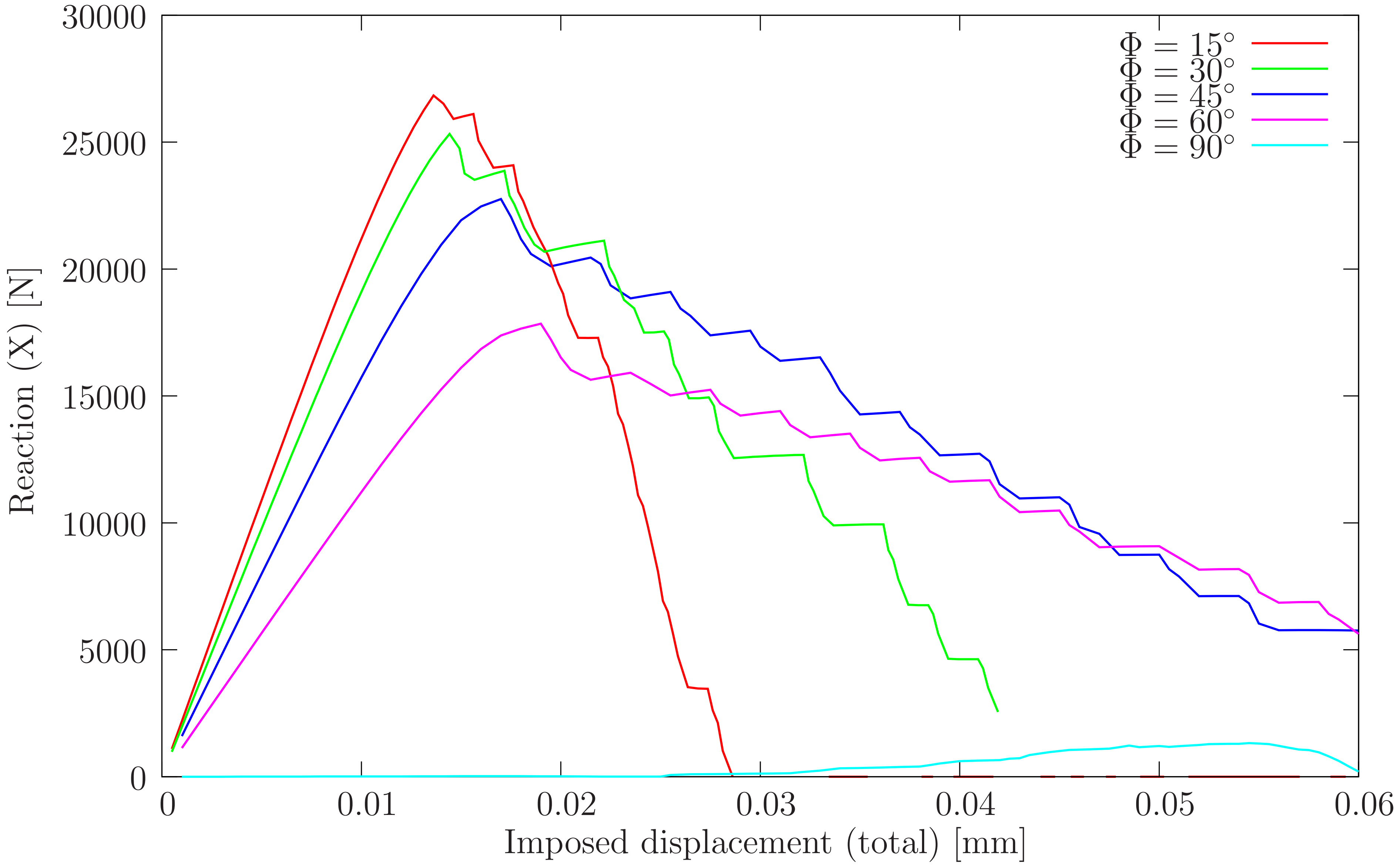

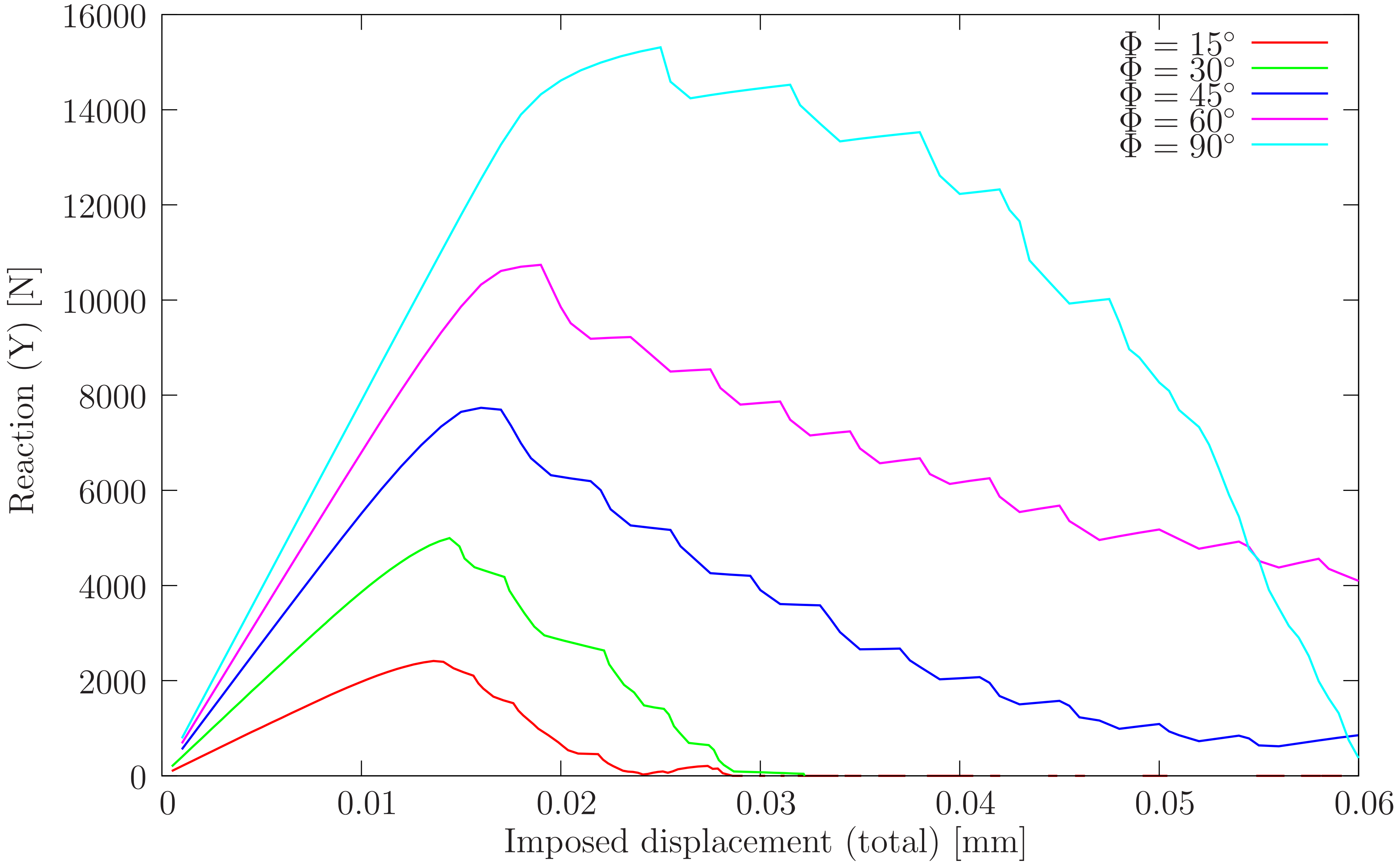

8)Pressure vessel (Kitching and Zarrabi IJPVP 1982)

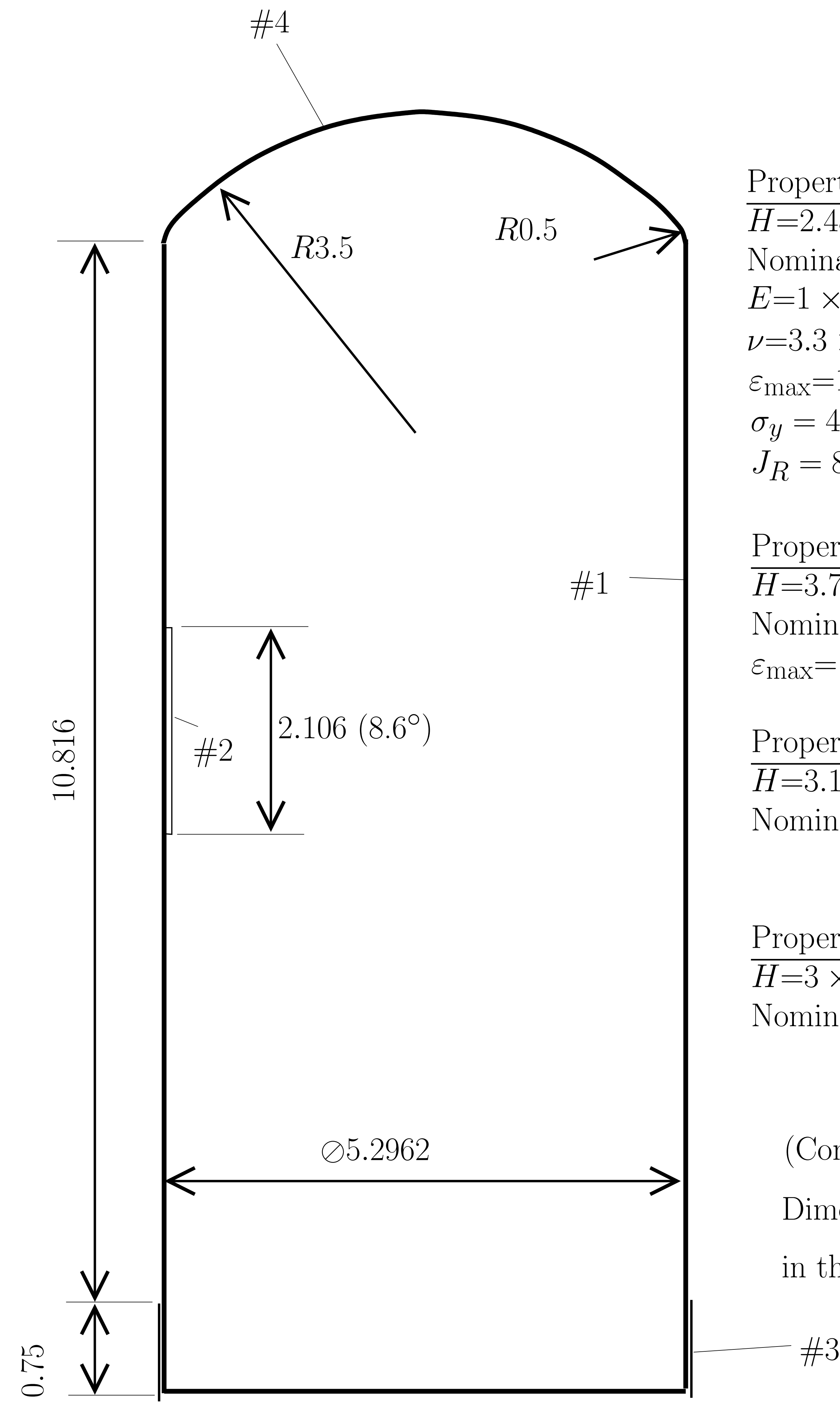

Properties #1:
H=2.48 × 10^{-01}
Nominal normal pressure=1 × 10^{+00}
E=1 × 10^{+07}
ν=3.3 × 10^{-01}
$\varepsilon_{\max}$=1.9 × 10^{-02}
$\sigma_y = 45925.926 + 78851.436\varepsilon_p$
$J_R = 89.3$

Properties #2:
H=3.7 × 10^{-02}
Nominal normal pressure=1 × 10^{+00}
$\varepsilon_{\max}$=1.9 × 10^{-02}

Properties #3:
H=3.15 × 10^{-01}
Nominal normal pressure=1 × 10^{+00}

Properties #4:
H=3 × 10^{-01}
Nominal normal pressure=1 × 10^{+00}

(Consistent units are adopted)

Dimensions correspond to Specimen 12

in the original reference.

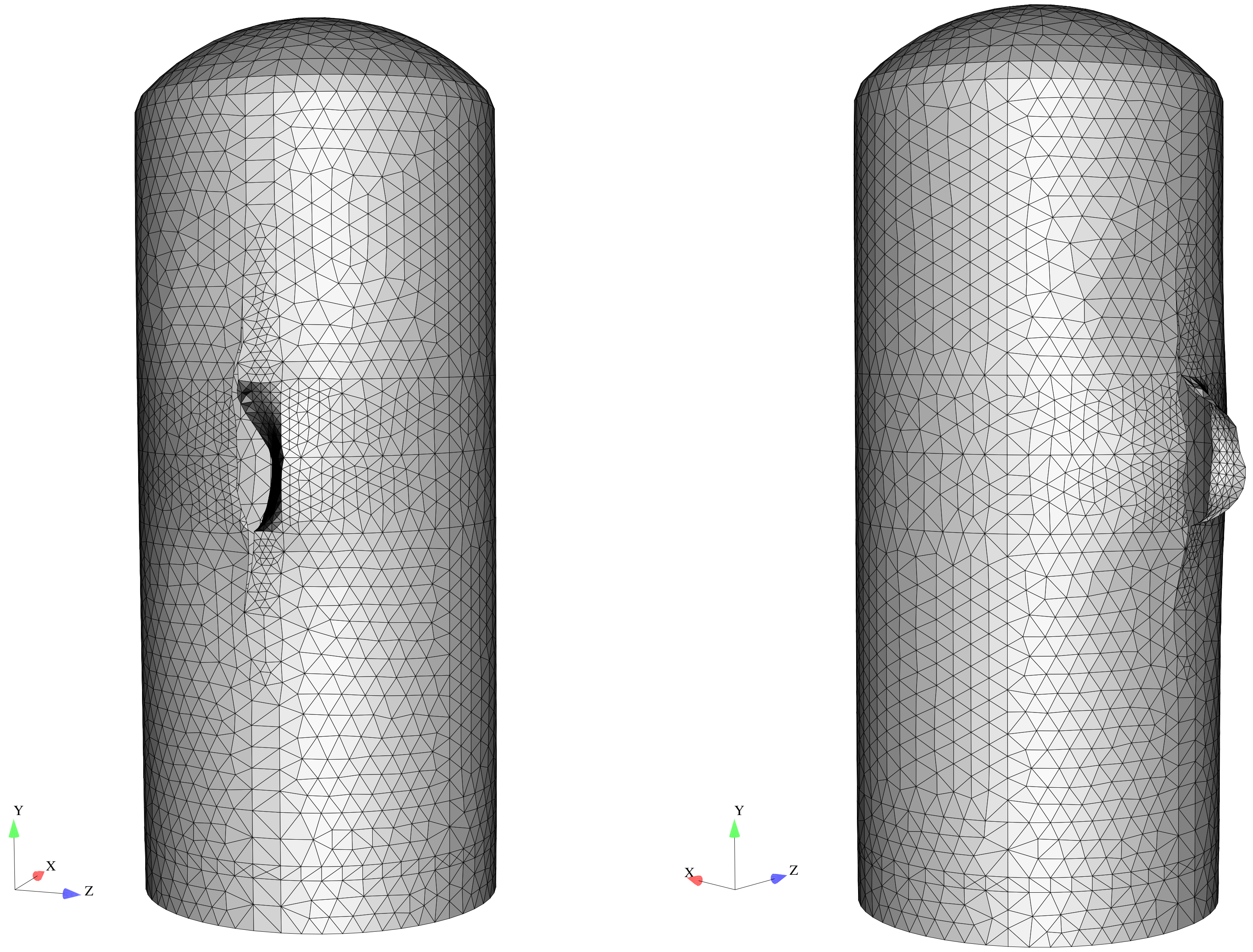

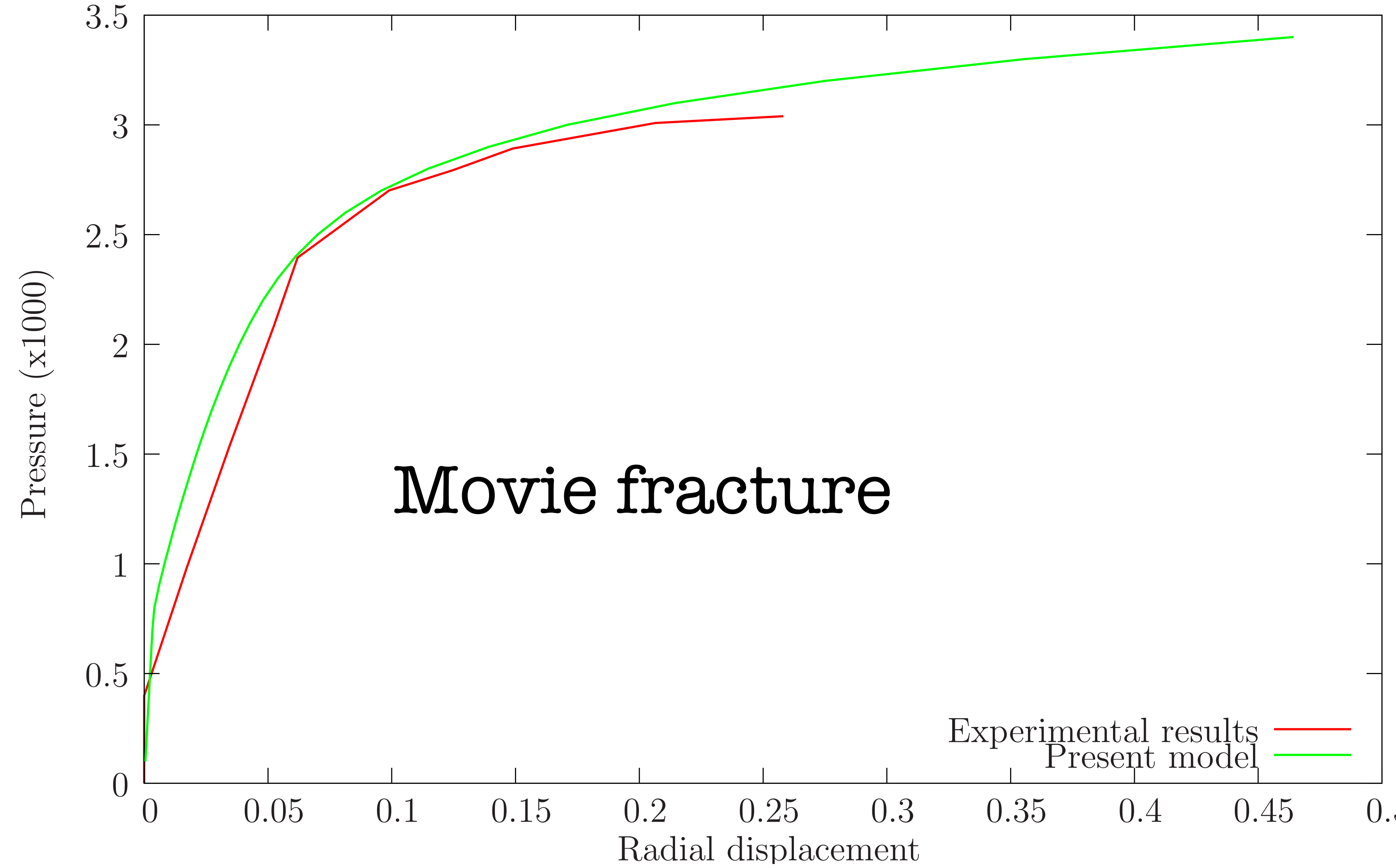

9)Tensioned aluminum plate

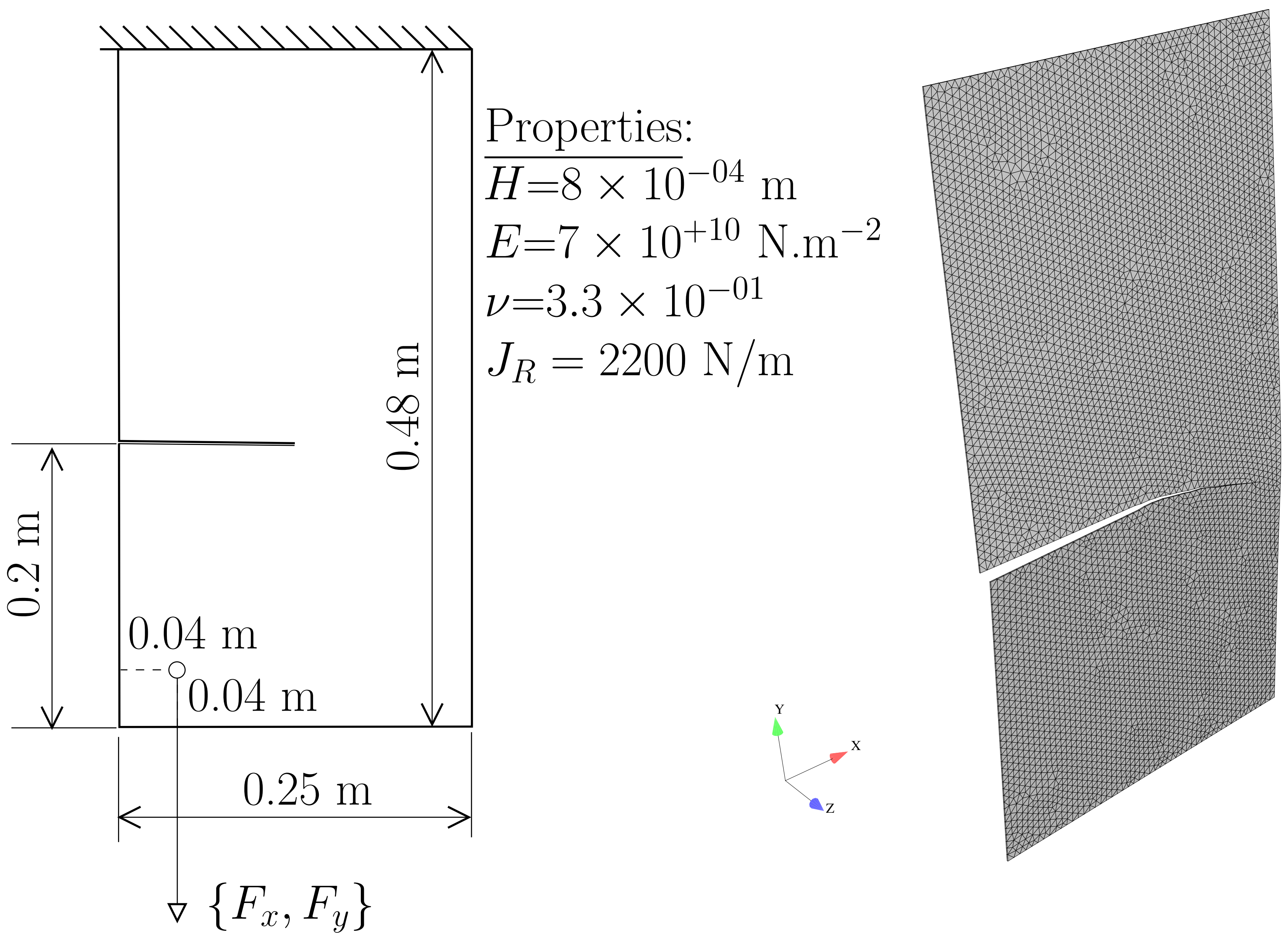

(a) Geometry, properties and crack path representation on the plate.

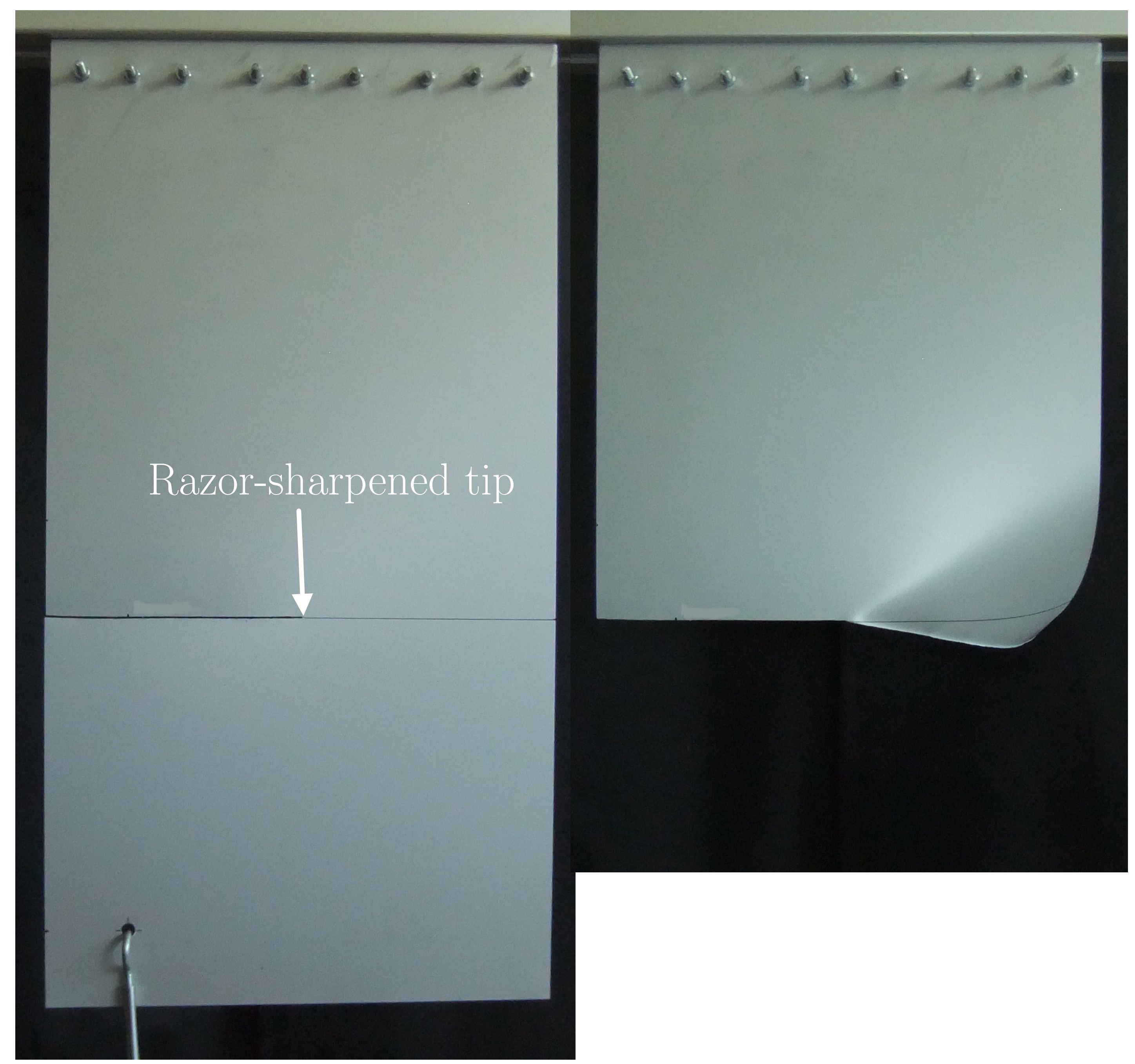

(b) Experimental setup and final result.

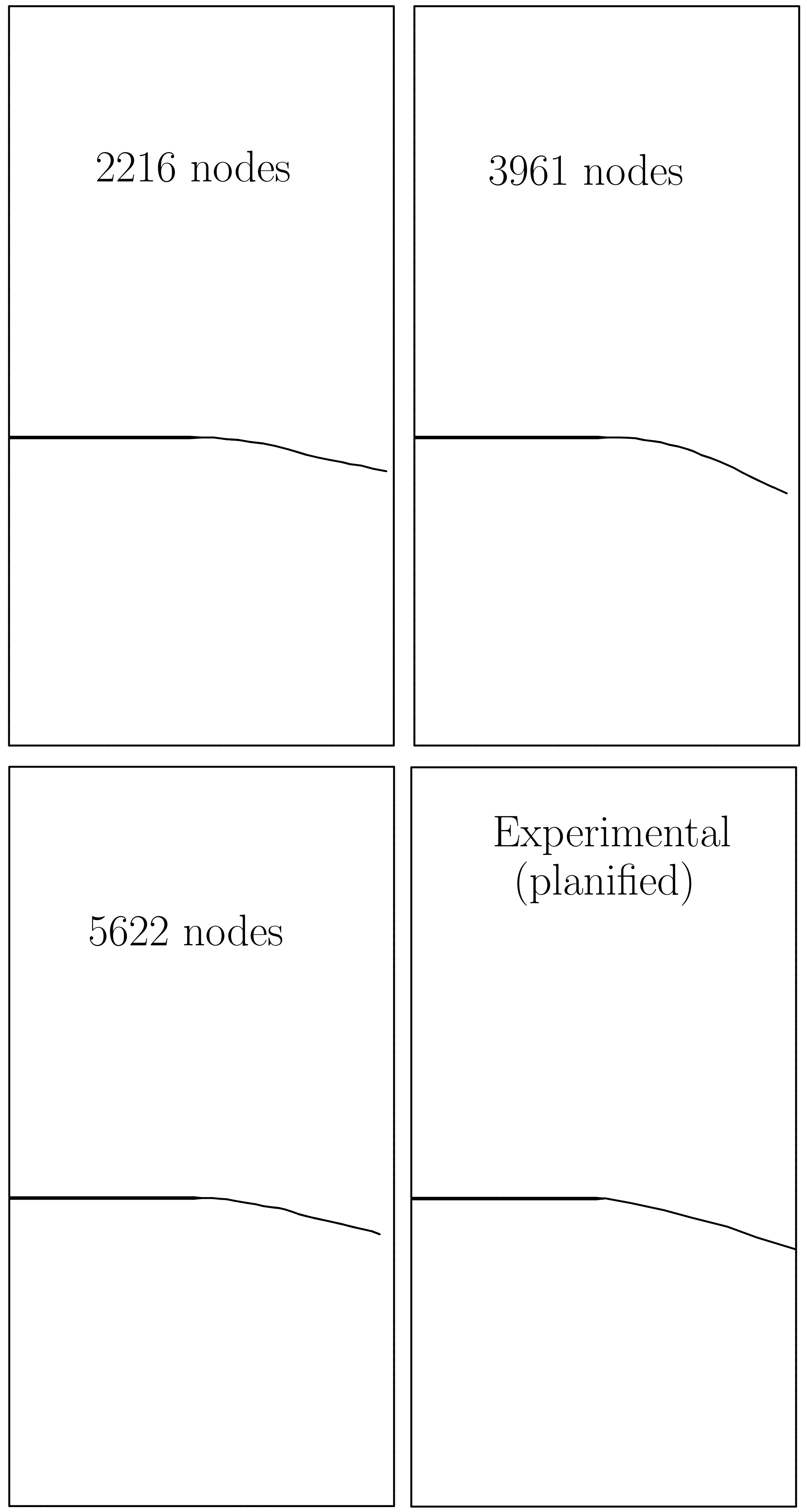

Comparison with experimental results

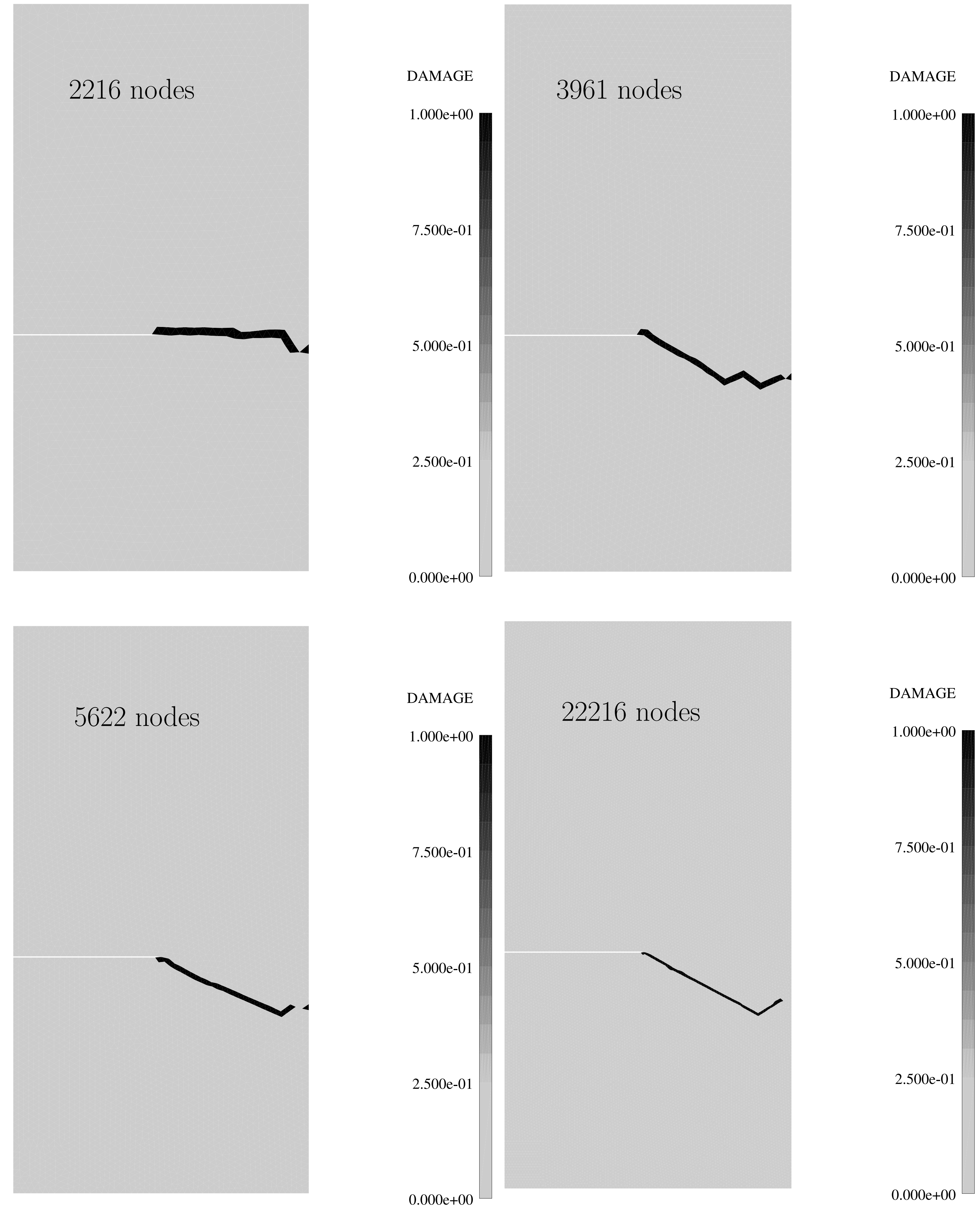

Comparison with the phase field method

2216 nodes/4216 elements

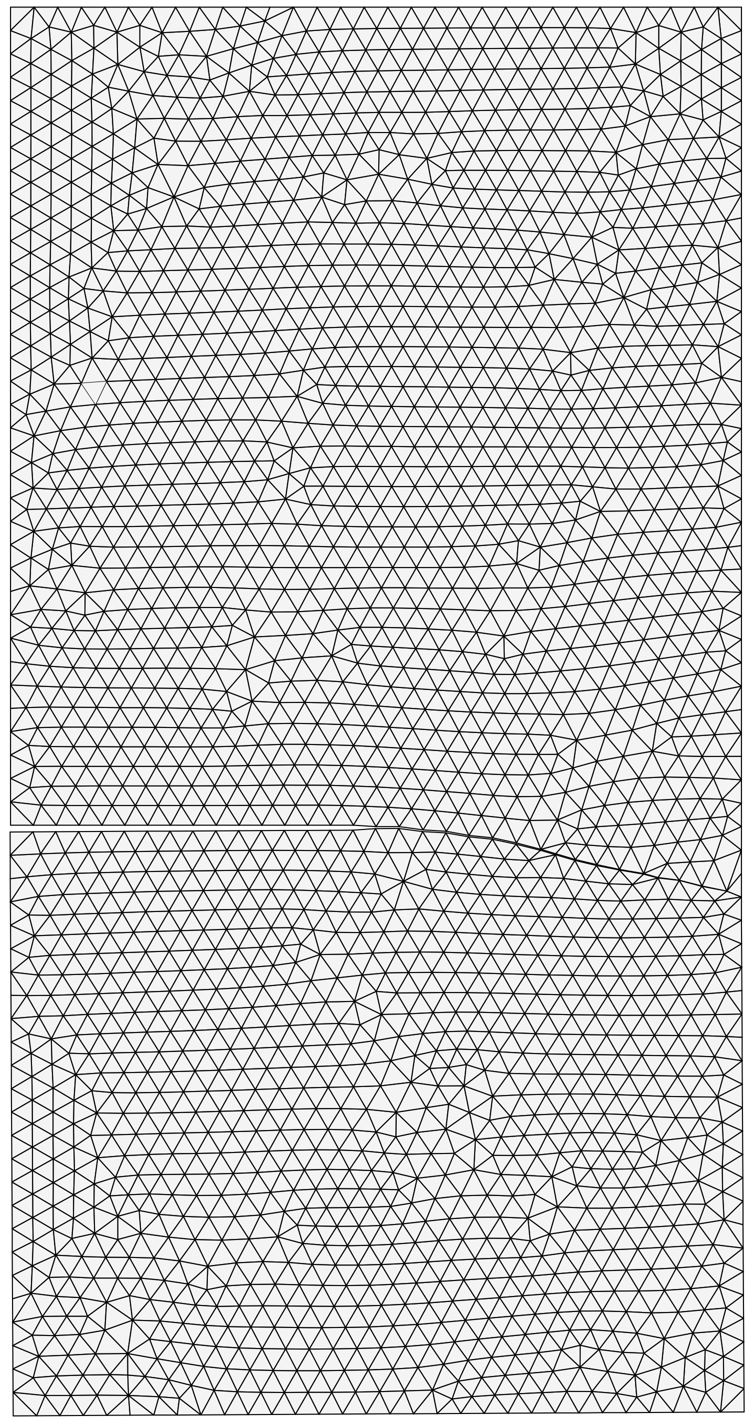

3730 nodes/3585 elements

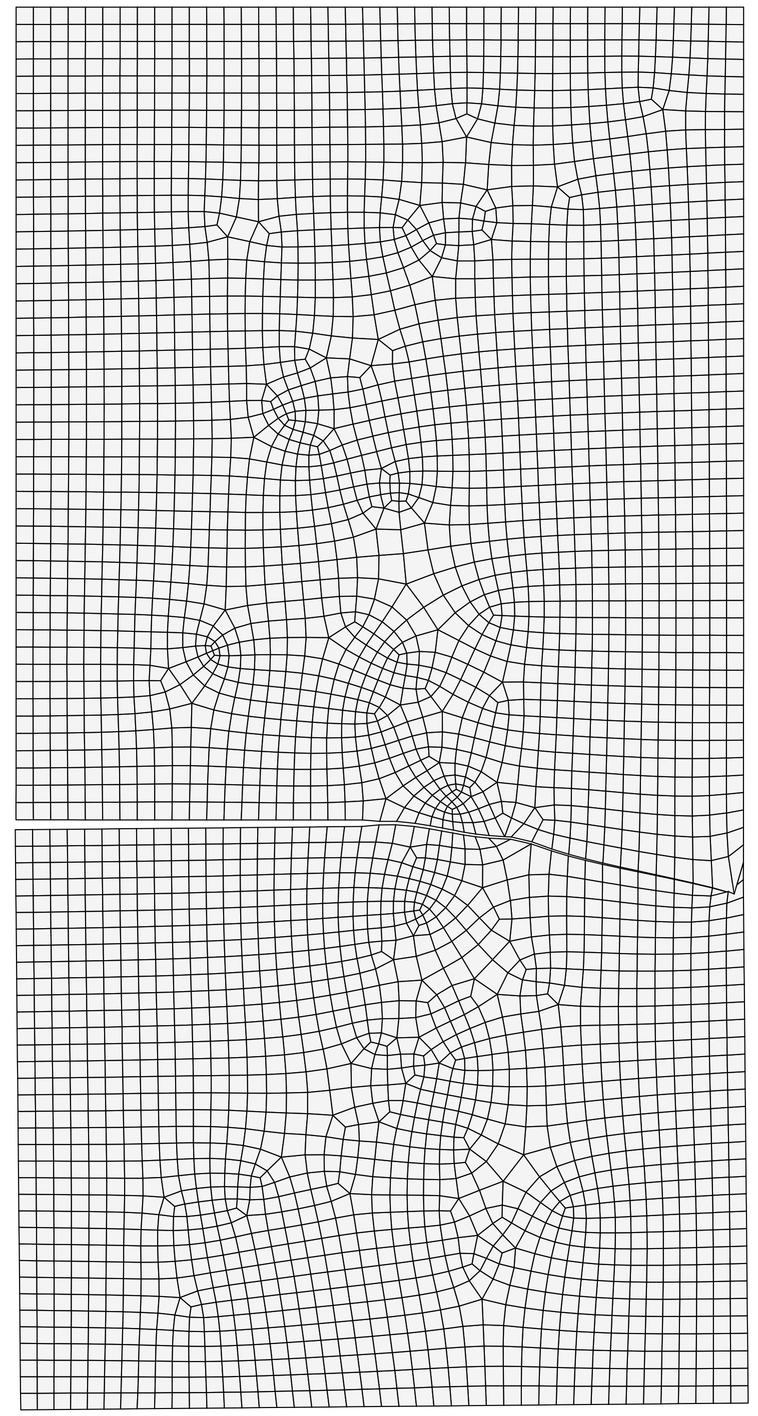

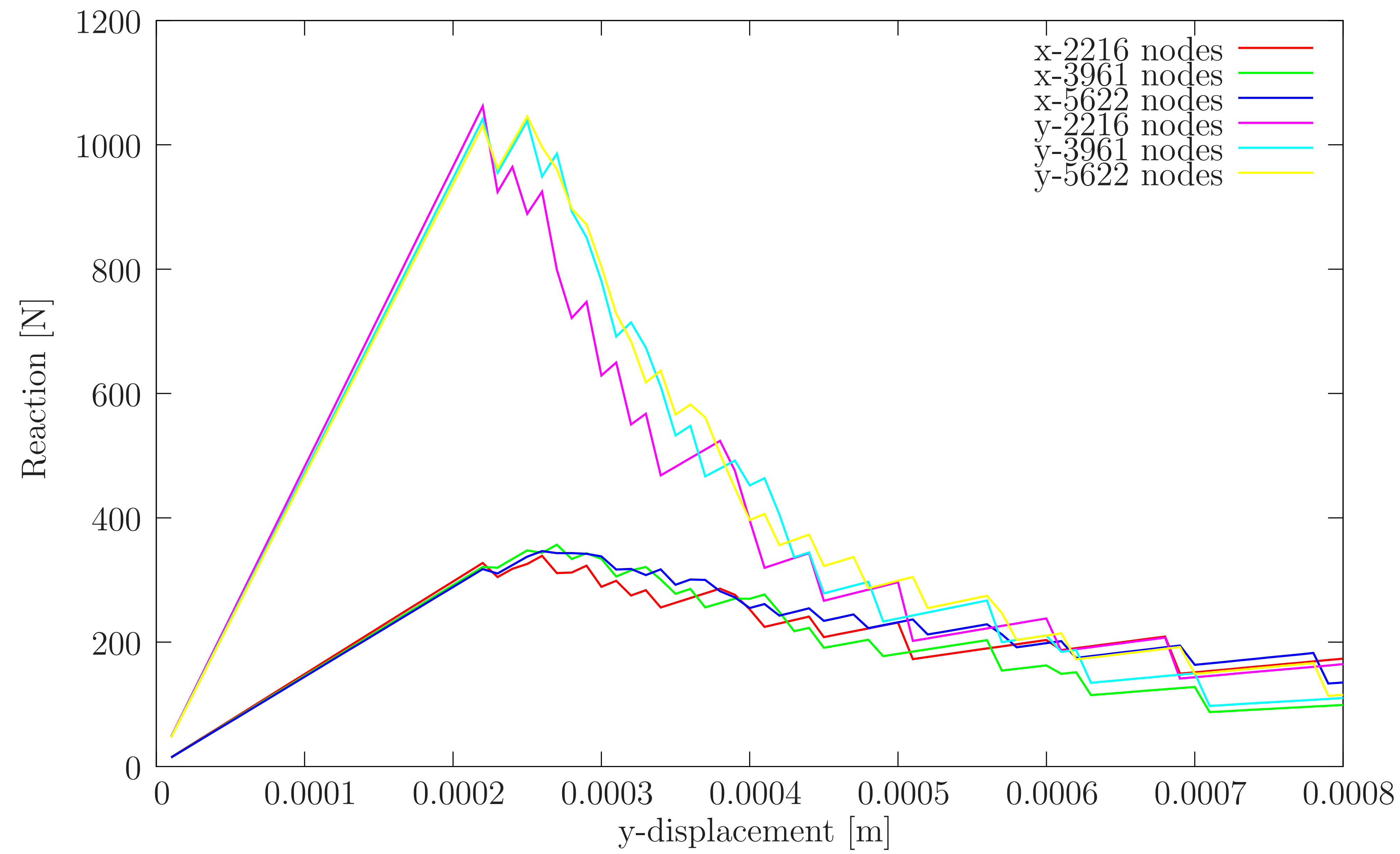

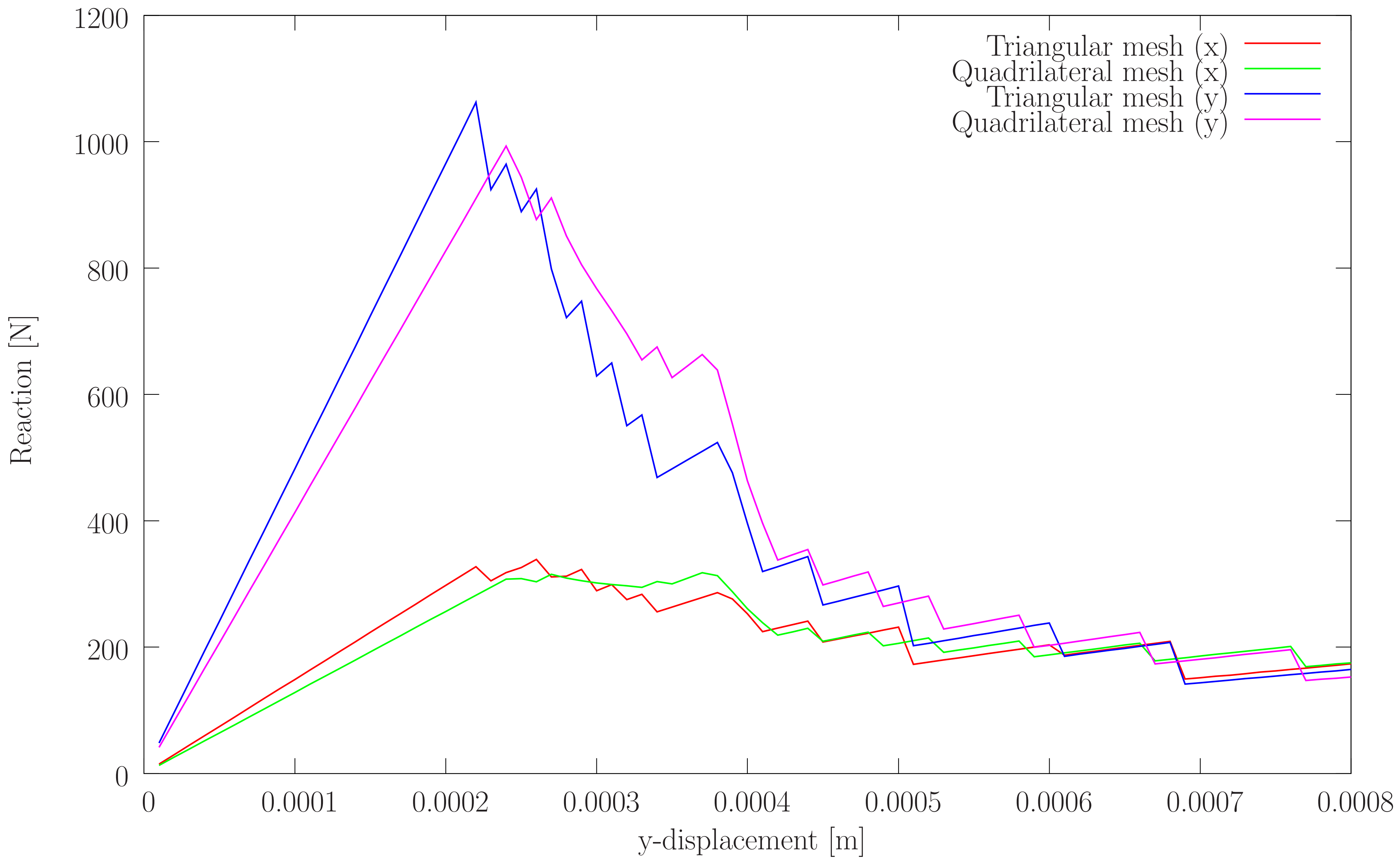

Opportunity for a globally defined constitutive approach:

- Combinations of yield functions, hardening laws, damage and void fraction laws, thermal-coupling
- Ductile damage requires pressure sensitivity (often combinations of Drucker-Prager and Von-Mises)
- Plane strain and stress (with control), shear-deformable shells, full 3D, constrained 3D specified by <u>pre-and-post processing of constitutive subroutines</u>
- Petrov-Galerkin elements ruin symmetry but are better performing and hence correct non-symmetric constitutive laws are now possible
- Use of ACEGEN - allows quick specification of flow vectors and derivatives as well as hyperelastic strain energy density functions
- Availability of OPENMP - not ideal for solvers but adequate for constitutive laws

Multiplicative elasto-plasticity for *elastic* isotropy

$$
\begin{aligned}
\phi_i &\le 0\\
\phi_i\dot\gamma_i &= 0\\
\dot\gamma_i &\ge 0\\
\boldsymbol{F} &= \boldsymbol{F}_e\boldsymbol{F}_p\\
\boldsymbol{d}_p &= \sum_{i=1}^{n_s}\dot\gamma_i\boldsymbol{n}_i\\
\boldsymbol{d} &= \boldsymbol{d}_e+\boldsymbol{d}_p\\
\boldsymbol{\tau} &= 2\frac{\mathrm{d}\psi_b}{\mathrm{d}\boldsymbol{b}_e}\boldsymbol{b}_e = 2\boldsymbol{b}_e\frac{\mathrm{d}\psi_b}{\mathrm{d}\boldsymbol{b}_e}\\
\dot{\boldsymbol{v}} &= -\sum_{i=1}^{n_s}\dot\gamma_i\boldsymbol{\varphi}_i
\end{aligned}
$$

Without specifying the plastic flow

$$
\begin{aligned}
\overset{\star}{\boldsymbol{b}}_{eV} &= -4\sum_{i=1}^{n_s}\dot\gamma_i\boldsymbol{A}_V^{-1}\boldsymbol{n}_{Vi}\\
\dot{\boldsymbol{v}} &= -\sum_{i=1}^{n_s}\dot\gamma_i\boldsymbol{\varphi}_i\\
\boldsymbol{\tau}_V &= 2\left(\frac{\mathrm{d}\psi_b}{\mathrm{d}\boldsymbol{b}_e}\boldsymbol{b}_e\right)_V\\
\mu\dot\gamma_i-\langle\mu\dot\gamma_i+\phi_i\rangle &= 0
\end{aligned}
$$

With our flow rule (not Simo's!)

$$
\dot\psi_b=\frac{\mathrm{d}\psi_b}{\mathrm{d}\boldsymbol{b}_e}:\dot{\boldsymbol{b}}_e=\frac{1}{2}(\boldsymbol{\tau}\boldsymbol{b}_e^{-1}):\dot{\boldsymbol{b}}_e=\frac{1}{2}\boldsymbol{\tau}:(\dot{\boldsymbol{b}}_e\boldsymbol{b}_e^{-1})=\frac{1}{2}(\boldsymbol{b}_e^{-1}\boldsymbol{\tau}):\dot{\boldsymbol{b}}_e=\frac{1}{2}\boldsymbol{\tau}:(\boldsymbol{b}_e^{-1}\dot{\boldsymbol{b}}_e)
$$

$$
\dot{\boldsymbol{b}}_e=\underbrace{\frac{\partial\boldsymbol{b}_e}{\partial\boldsymbol{F}}:\dot{\boldsymbol{F}}}_{\overset{\circ}{\boldsymbol{b}}_e}+\underbrace{\frac{\partial\boldsymbol{b}_e}{\partial\boldsymbol{F}_p}:\dot{\boldsymbol{F}}_p}_{\overset{\star}{\boldsymbol{b}}_e}
$$

Justification

$$
\begin{aligned}
\boldsymbol{d}_\mathrm{p} &= -\frac{1}{4}\overset{\star}{\boldsymbol{b}}_e\boldsymbol{b}_e^{-1}-\frac{1}{4}\boldsymbol{b}_e^{-1}\overset{\star}{\boldsymbol{b}}_e\\
\boldsymbol{d}_e &= \frac{1}{4}\dot{\boldsymbol{b}}_e\boldsymbol{b}_e^{-1}+\frac{1}{4}\boldsymbol{b}_e^{-1}\dot{\boldsymbol{b}}_e
\end{aligned}
$$

Specific models

Table 1: Tested yield criteria

Yield criterion	Number of yield surfaces	Equivalent stresses
von-Mises	1	$\sigma_{\text{eq}_1} = \sqrt{I_1^2 - 3I_2}$
Tresca	6	$\sigma_{\text{eq}_k} = \widetilde{\tau}_i - \widetilde{\tau}_j, \quad i \neq j$
Ductile damage	2	$\sigma_{eq_1} = \frac{\sqrt{I_1^2 - 3I_2 - f c_1 I_1}}{1-f}$ $\sigma_{eq_2} = \frac{\sqrt{I_1^2 - 3I_2}}{1-f}$
Plane Hill criterion ($\boldsymbol{\tau}' = \boldsymbol{T}^T \boldsymbol{\tau} \boldsymbol{T}$)	1	$\sigma_{\text{eq}_1} = \sqrt{f_H(\tau'_{22} - \tau'_{33})^2 + g_H(\tau'_{33} - \tau'_{11})^2 + h_H(\tau'_{11} - \tau'_{22})^2 + 2n_H \tau'^2_{12}}$
$I_1 = \text{tr}\boldsymbol{\tau}, \quad I_2 = \frac{1}{2}\left[(\text{tr}\boldsymbol{\tau})^2 - \text{tr}\boldsymbol{\tau}^2\right], \quad I_3 = \det \boldsymbol{\tau}$ $\boldsymbol{T} = \{\{\cos(\theta), -\sin(\theta)\}, \{\sin(\theta), \cos(\theta)\}\}$		$f_H = \frac{1}{2}(1 - r_{1c} + r_{2c})$ $g_H = \frac{1}{2}(1 + r_{1c} - r_{2c})$ $h_H = \frac{1}{2}(r_{1c} + r_{2c} - 1)$ $n_H = \frac{1}{2} r_{12c}$

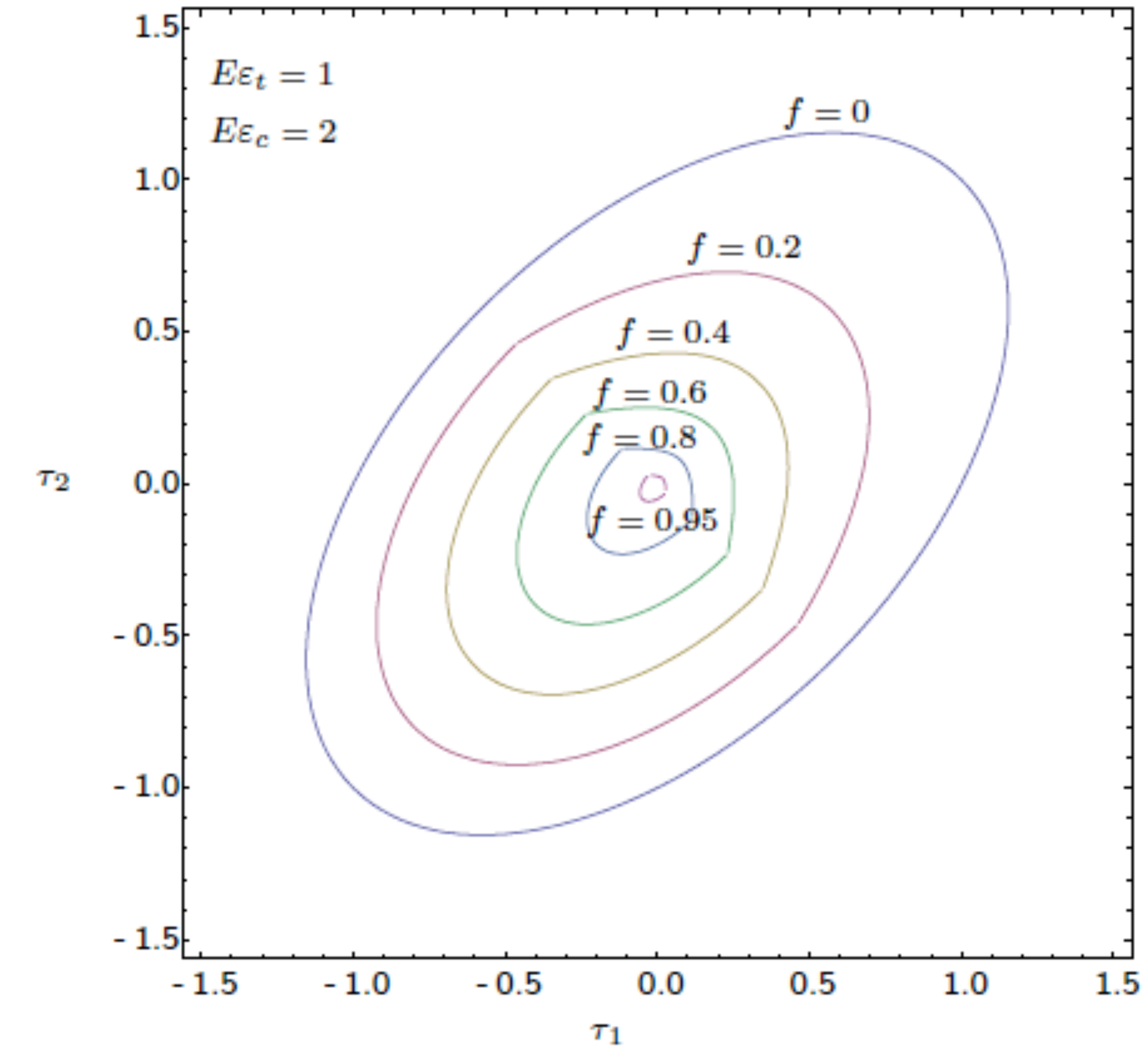

Figure 2: Void fraction f effect on the yield function.

Ductile damage

Table 2: Tested hyperelastic strain energy densities

Hyperelastic law	Kirchhoff Stress
Neo-Hookean (quasi-incompressible)	$\boldsymbol{\tau} = G\left(\det \boldsymbol{b}_e\right)^{-\frac{1}{3}}\left(\boldsymbol{b}_e - \frac{1}{3}\text{tr}\left[\boldsymbol{b}_e\right]\boldsymbol{I}\right) + \kappa\sqrt{\det \boldsymbol{b}_e}\left(\sqrt{\det \boldsymbol{b}_e} - 1\right)\boldsymbol{I}$
Metal plasticity	$\boldsymbol{\tau} = \frac{\mathrm{d}\boldsymbol{\tau}}{\mathrm{d}\boldsymbol{b}_e}\Big\rvert_{\boldsymbol{b}_e = \boldsymbol{I}}\left(\boldsymbol{b}_e - \boldsymbol{I}\right)$

Graph of $\Delta\gamma - S(\Delta\gamma + \phi) = 0$

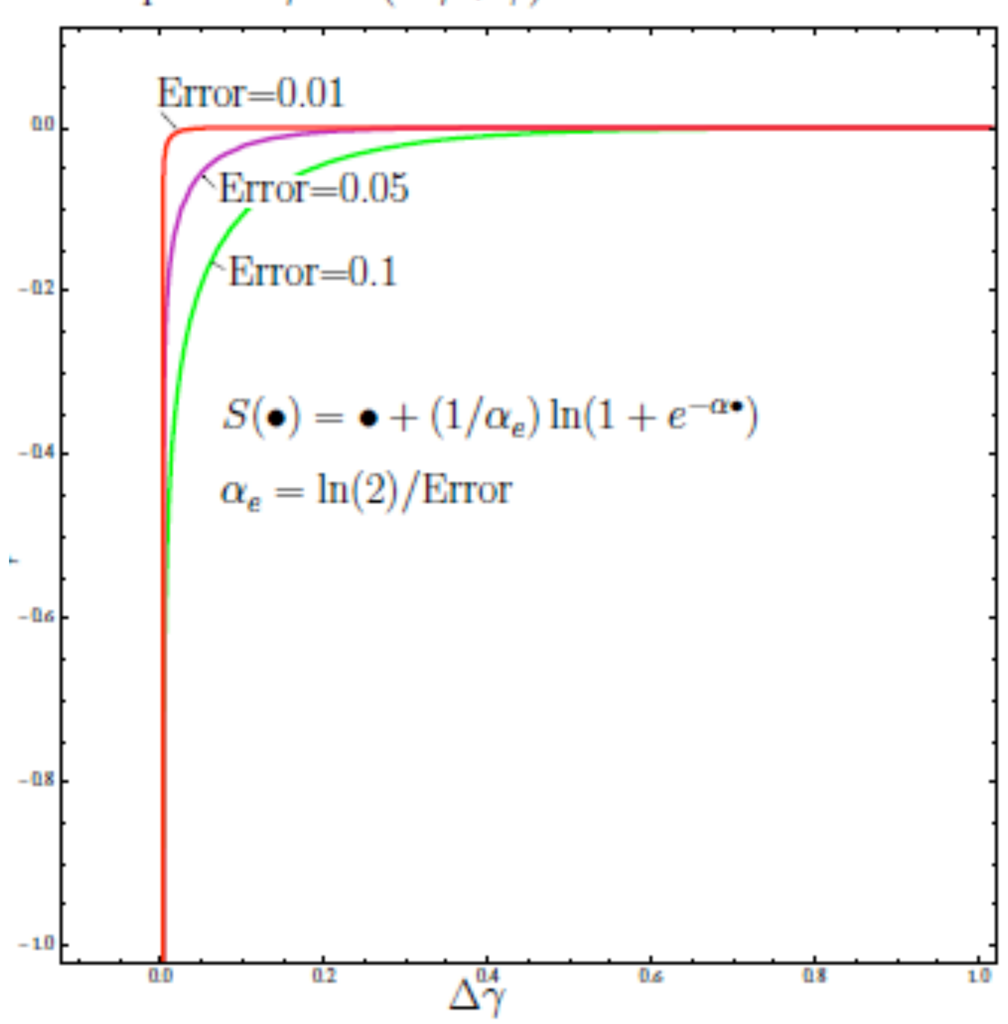

Complementarity alteration

$$\phi^{\star}(\Delta\gamma, \boldsymbol{b}_{n+1}, \boldsymbol{v}_{n+1}) = \mu^{\star}\Delta\gamma - \langle \mu^{\star}\Delta\gamma + \phi \rangle = 0$$

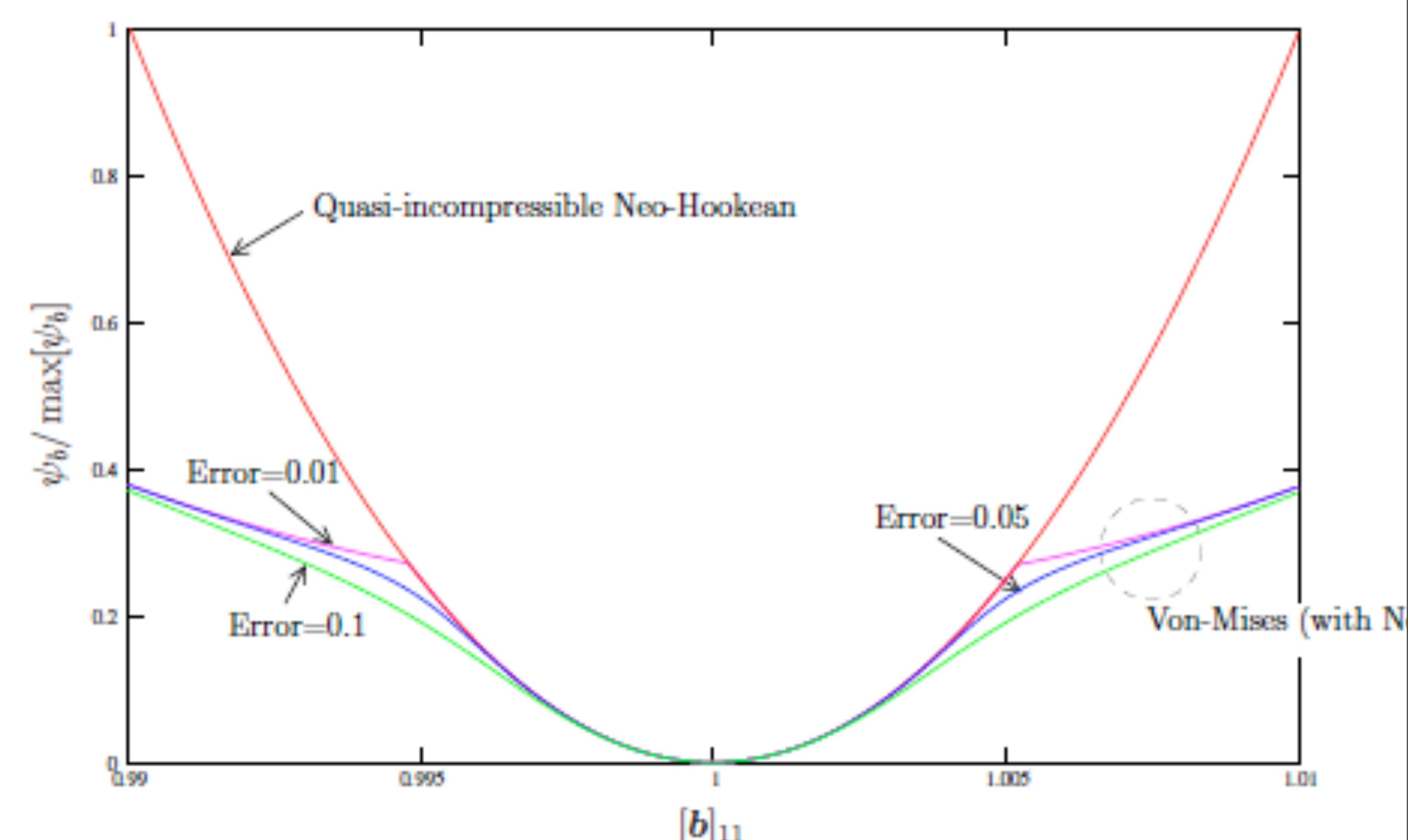

Strain energy density

Constitutive system and linearization

Constitutive Jacobian

$$\boldsymbol{J} = \frac{\partial \boldsymbol{e}}{\partial \boldsymbol{\chi}} = \begin{bmatrix} -\delta_{ij} - 4\,[\boldsymbol{M}]_{ikj}\,[\Delta\gamma]_k & -4\,[\boldsymbol{m}]_{ij} & -4\,[\boldsymbol{N}]_{ikj}\,[\Delta\gamma]_k \\ [\nabla\phi^\star]^b_{ij} & [\nabla\phi^\star]^\gamma_{ij} & [\nabla\phi^\star]^v_{ij} \\ [\nabla\varphi]^b_{ikj}\,[\Delta\gamma]_k & [\varphi]_{ij} + [\nabla\varphi]^\gamma_{ikj}\,[\Delta\gamma]_k & -\delta_{ij} + [\nabla\varphi]^v_{ikj}\,[\Delta\gamma]_k \end{bmatrix}$$

Trial Jacobian

$$\boldsymbol{L} = \frac{\partial \boldsymbol{e}}{\partial \boldsymbol{b}_{eo}} = \begin{bmatrix} -4\,[\boldsymbol{M}]_{ikj}\,[\Delta\gamma]_k \\ [\nabla\phi^\star]^b_{ij} \\ [\nabla\varphi]^b_{ikj}\,[\Delta\gamma]_k \end{bmatrix}$$

Trial Jacobian

$$\boldsymbol{\chi} = \{\boldsymbol{b}_{e_{n+1}}, \Delta\gamma, \boldsymbol{v}_{n+1}\}^T$$

Particular model:

specialization

Linearization

$$\frac{\mathrm{d}\boldsymbol{\tau}_{n+1}}{\mathrm{d}\boldsymbol{F}_{n+1}} = \frac{\partial \boldsymbol{\tau}_{n+1}}{\partial \boldsymbol{b}_{eo}} \left(\boldsymbol{I} - \boldsymbol{T}_{eo}\right) \frac{\partial \boldsymbol{b}_{eo}}{\partial \boldsymbol{F}_{n+1}}$$

$$\frac{\partial\,[\boldsymbol{b}_{eo}]_{ij}}{\partial\,[\boldsymbol{F}_{n+1}]_{mn}} = [\boldsymbol{I}]_{im}\,[\boldsymbol{F}_{n+1}]_{jl}\,\left[\tilde{\boldsymbol{b}}\right]_{nl} + [\boldsymbol{F}_{n+1}]_{ik}\,[\boldsymbol{I}_{n+1}]_{jm}\,\left[\tilde{\boldsymbol{b}}\right]_{kn}$$

$$\boldsymbol{T}_{eo} = \boldsymbol{T}_{\boldsymbol{b}}\boldsymbol{J}^{-1}\boldsymbol{L}$$

$$\tilde{\boldsymbol{b}} = \boldsymbol{F}_n^{-1}\boldsymbol{b}_n\boldsymbol{F}_n^{-T}$$

$$\boldsymbol{m} = \boldsymbol{A}_n^{-1}\boldsymbol{n}$$

$$[\boldsymbol{M}]_{ijk} = \frac{\partial\,[\boldsymbol{m}]_{ij}}{\partial\,[\boldsymbol{b}_e]_k} = \frac{\partial\,[\boldsymbol{m}]_{ij}}{\partial\,[\boldsymbol{\tau}]_l}\frac{\partial\,[\boldsymbol{\tau}]_l}{\partial\,[\boldsymbol{b}_e]_k} = [\boldsymbol{A}_n^{-1}]_{in}\frac{\partial\,[\boldsymbol{n}]_{nj}}{\partial\,[\boldsymbol{\tau}]_l}\frac{\partial\,[\boldsymbol{\tau}]_l}{\partial\,[\boldsymbol{b}_e]_k}$$

$$[\boldsymbol{N}]_{ijk} = \frac{\partial\,[\boldsymbol{m}]_{ij}}{\partial\,[\boldsymbol{v}_{n+1}]_k}$$

$$[\nabla\phi^\star]^b_{ij} = \frac{\partial\,[\phi^\star]_i}{\partial\,[\boldsymbol{\tau}]_k}\frac{\partial\,[\boldsymbol{\tau}]_k}{\partial\,[\boldsymbol{b}_e]_j}$$

$$[\nabla\phi^\star]^\gamma_{ij} = \frac{\partial\,[\phi^\star]_i}{\partial\,[\gamma]_j}$$

$$[\nabla\phi^\star]^v_{ij} = \frac{\partial\,[\phi^\star]_i}{\partial\,[\boldsymbol{v}]_j}$$

$$[\nabla\varphi]^b_{ijk} = \frac{\partial\,[\varphi]_{ij}}{\partial\,[\boldsymbol{b}_e]_k}$$

$$[\nabla\varphi]^\gamma_{ijk} = \frac{\partial\,[\varphi]_{ij}}{\partial\,[\gamma]_k}$$

$$[\nabla\varphi]^v_{ijk} = \frac{\partial\,[\varphi]_{ij}}{\partial\,[\boldsymbol{v}]_k}$$

Definitions

Iso-error maps

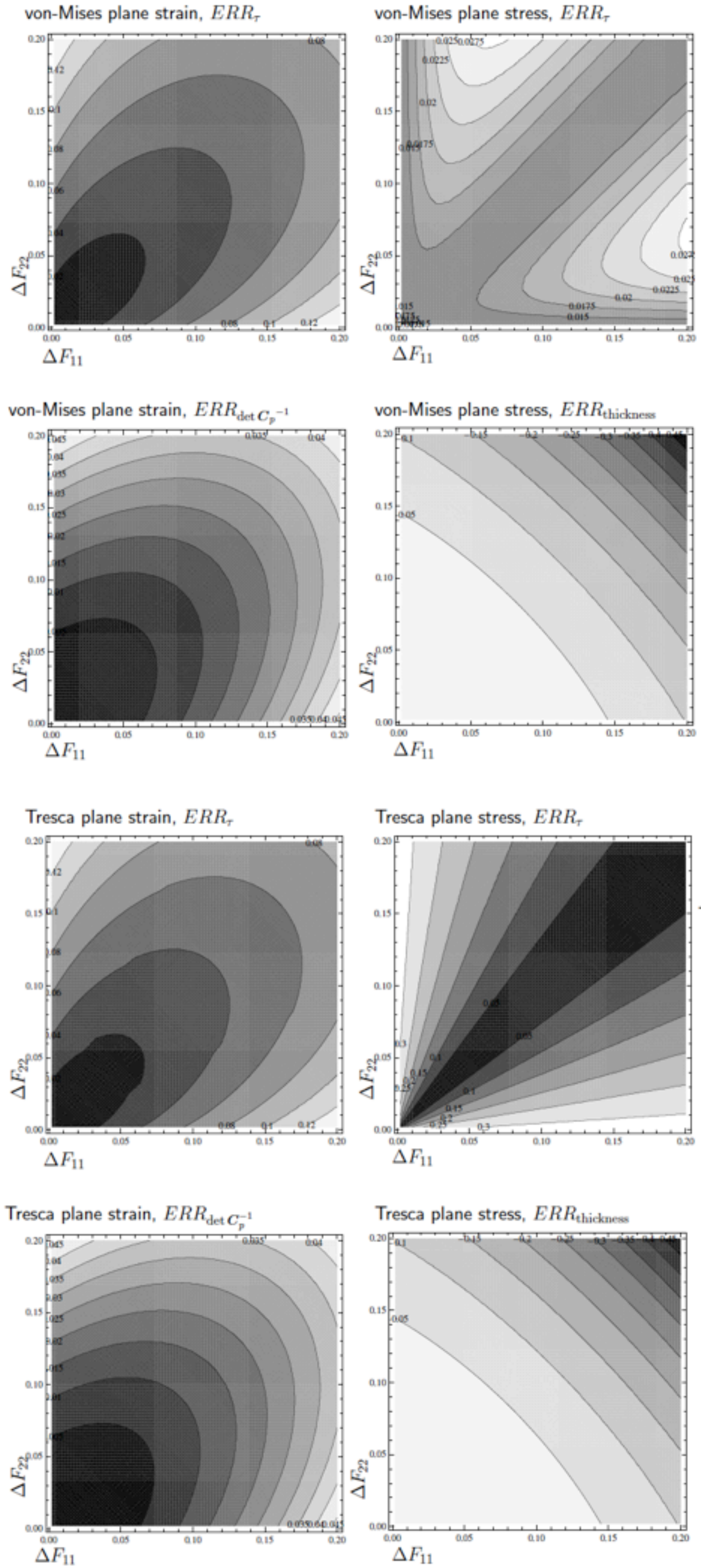

Material properties

$E = 200$ GPa
$\nu = 0.3$
$\sigma_1 = 200$ MPa
$\sigma_2 = 200$ MPa
$\sigma_y = 200$ MPa

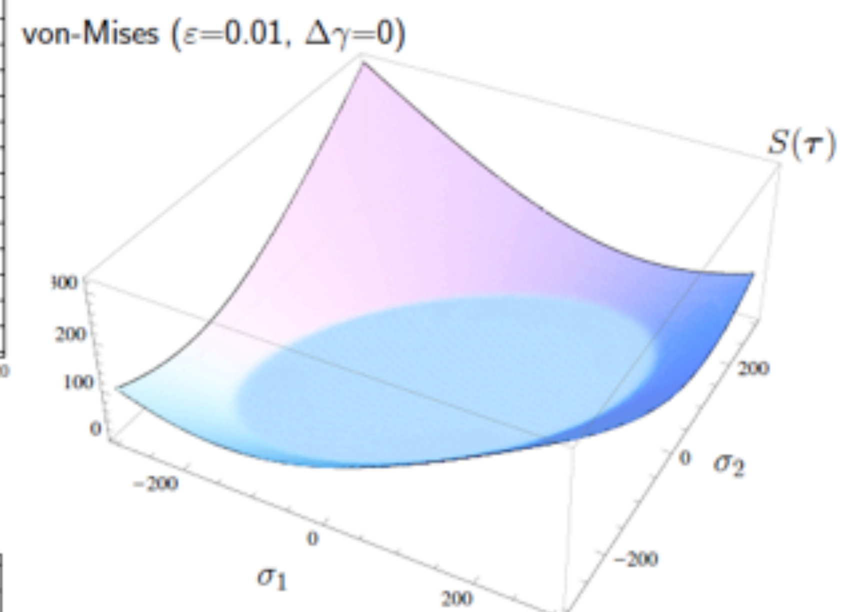

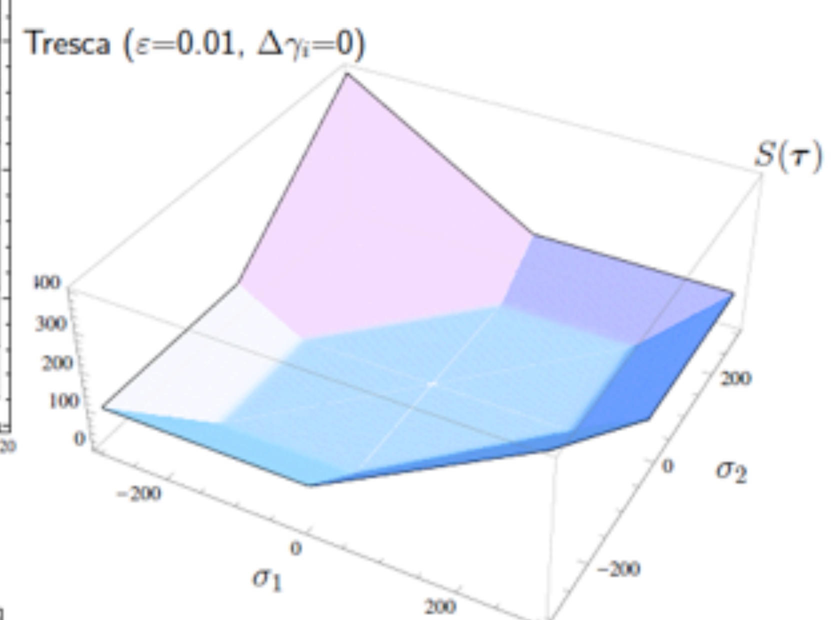

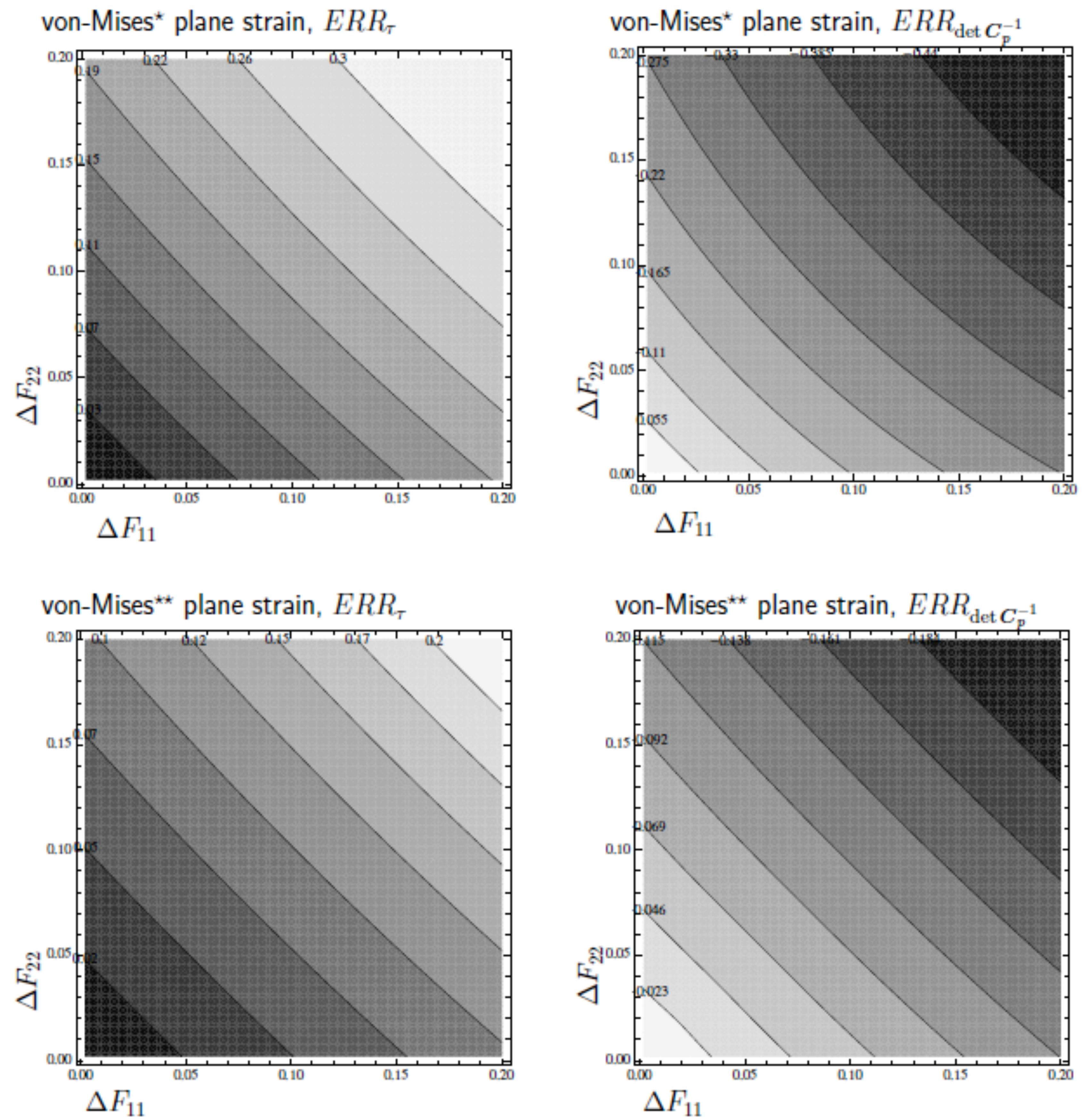

Figure 3: Iso-error maps of two classical finite-strain plasticity models: Simo 1988 [56, 57] ($\star$) and Simo 1992 [58] ($\star\star$) models.

10) Localization Areias and Van Goethem

$H = 0.02$ m
$E = 200$ GPa
$\nu = 0.3$
$\sigma_y = 500 + 10\dot{\varepsilon}_p$ Mpa
$\sigma_y^{(w)} = 400 + 10\dot{\varepsilon}_p$ Mpa
$\varepsilon_{1\,\max} = 0.25$
$l_c = 0.002$ m

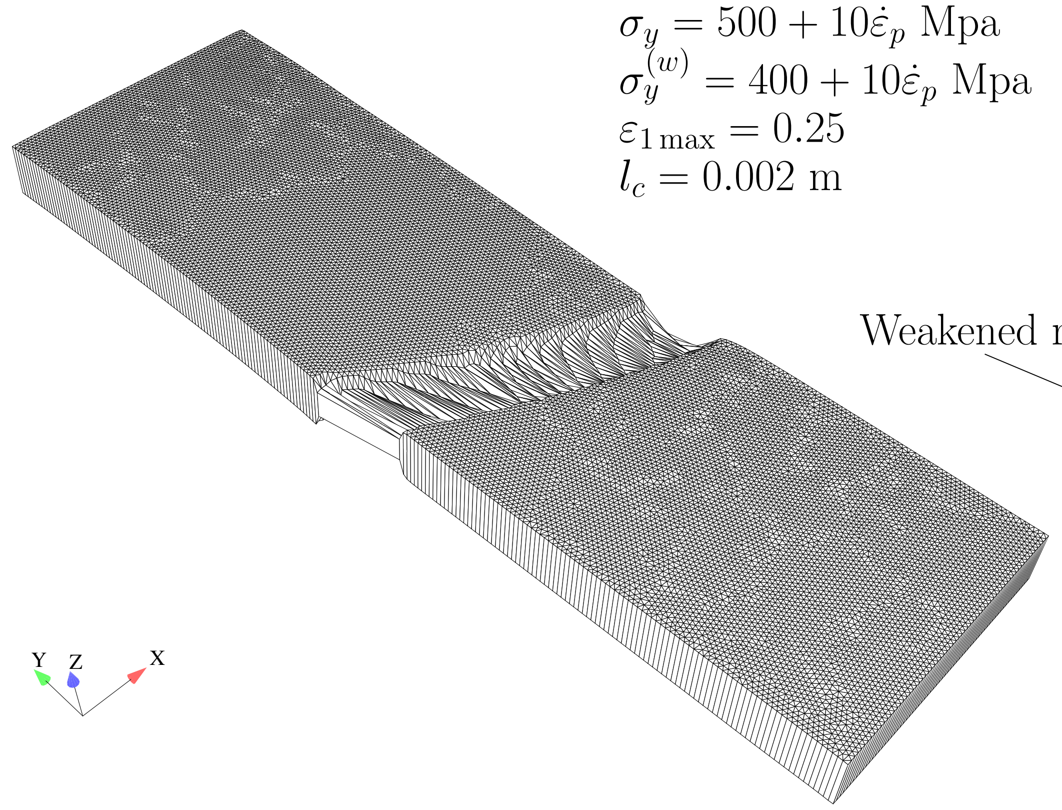

(Extrusion for $\theta = \pi/4$)

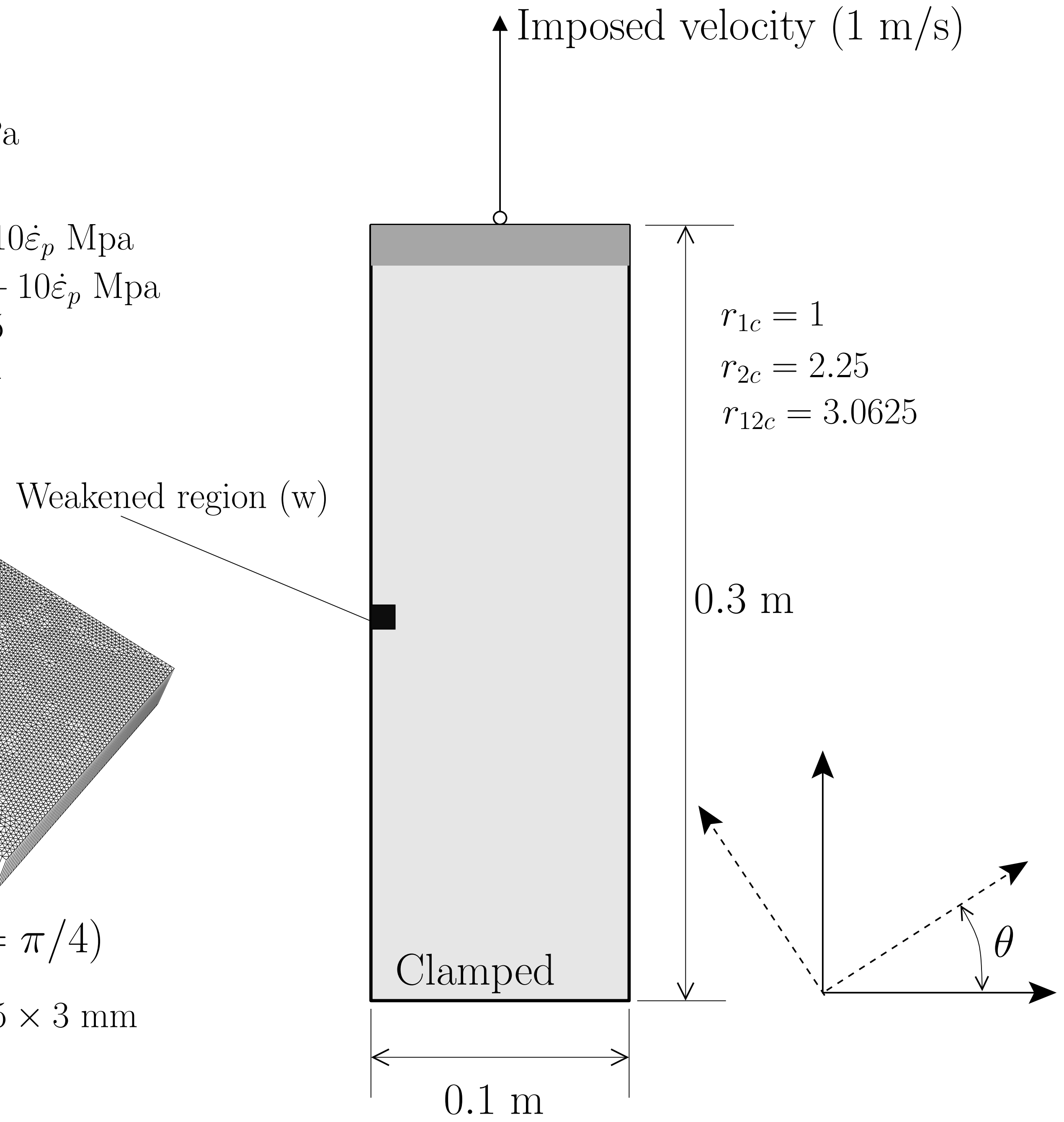

Dimensions of the weakened zone: 5×3 mm
Coarse mesh: 7525 elements
Fine mesh: 30404 elements

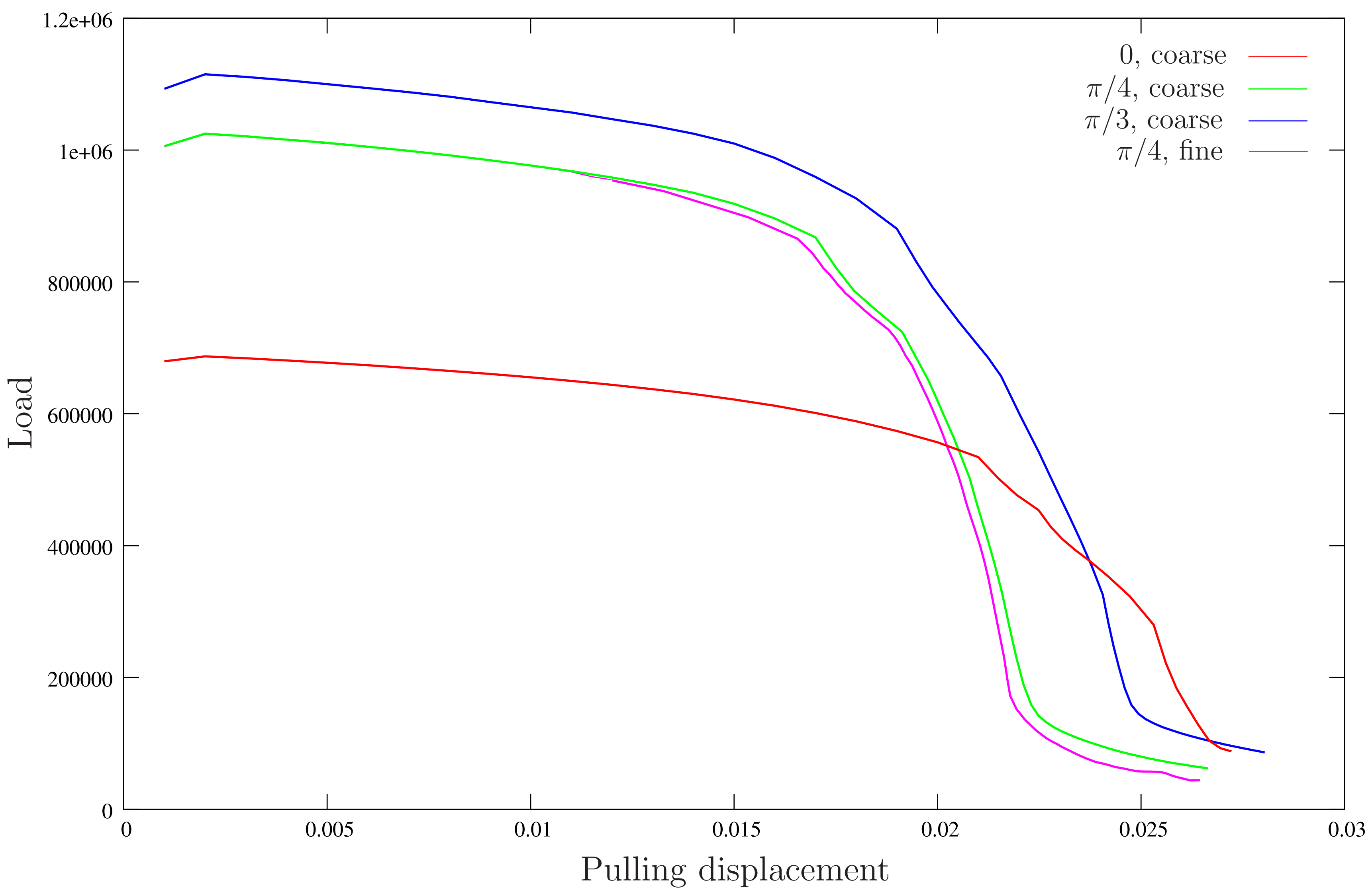

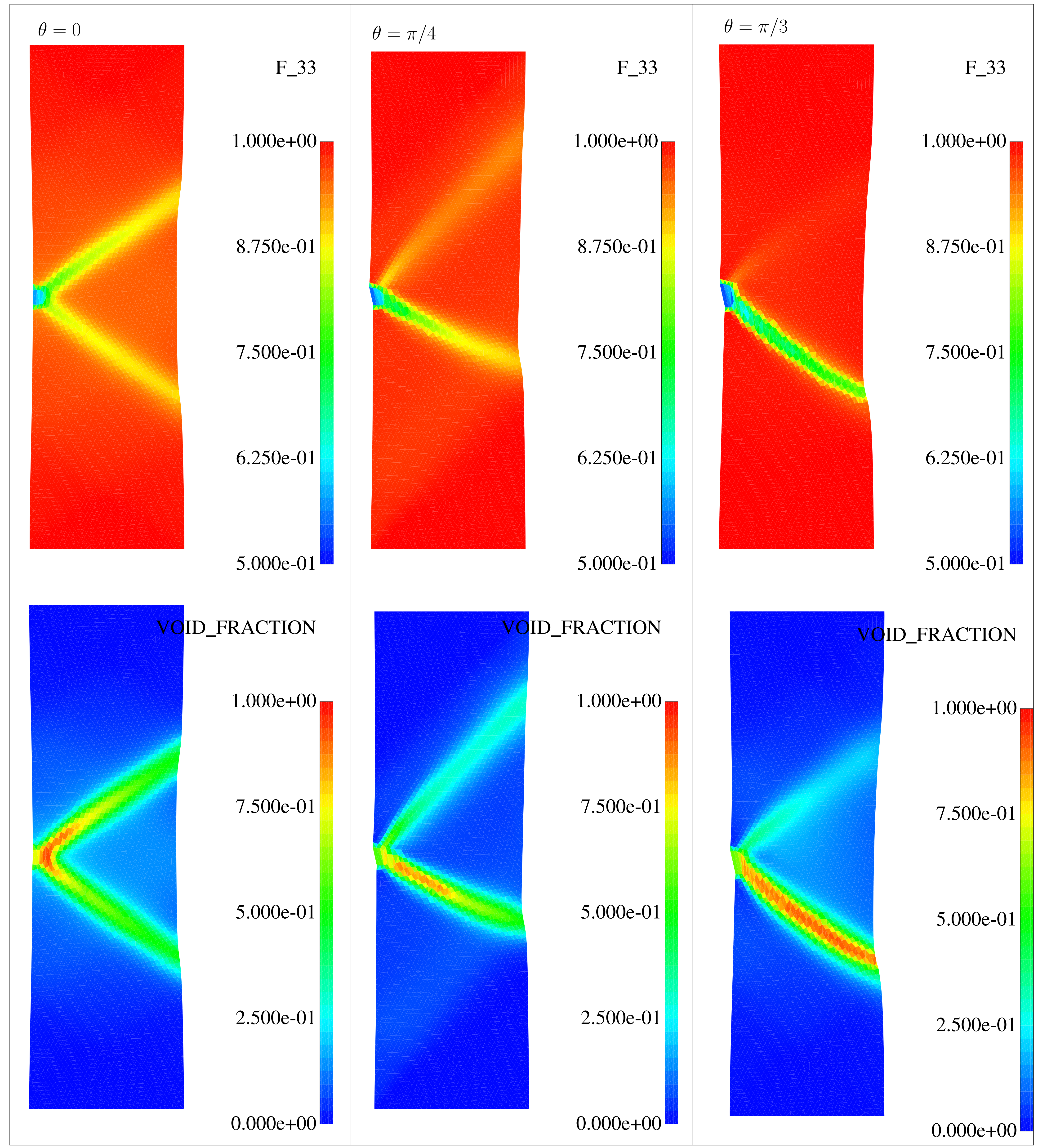

Movie localization

11) Muscat-Fenech & Atkins plate

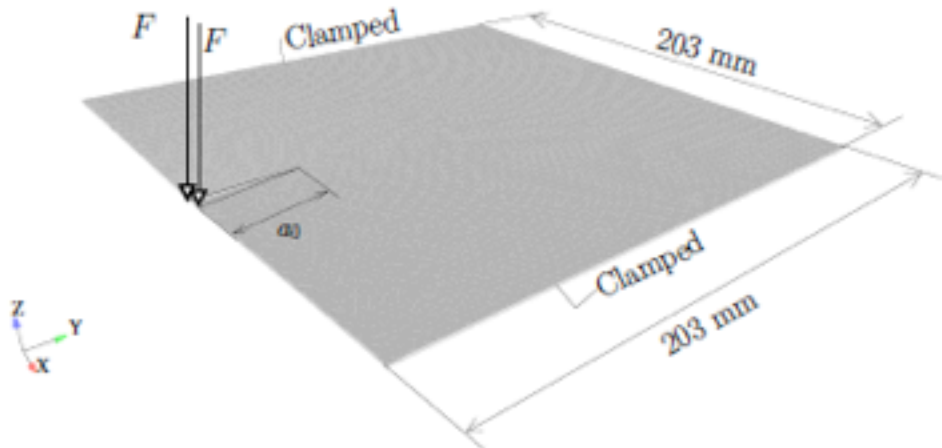

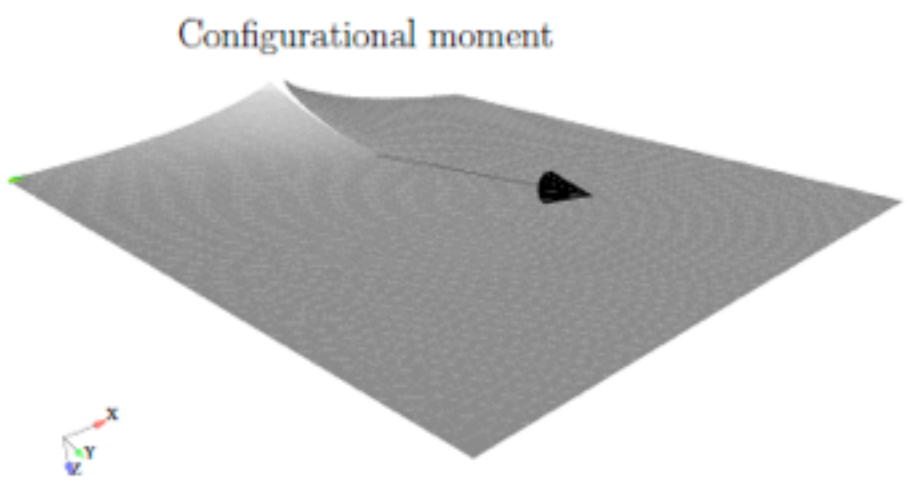

Properties:

H=8 × 10^{-01} mm

ε_e=1.45714 × 10^{-03}

E=2.1 × 10^{+05} N.m^{-2}

ν=3 × 10^{-01}

$\sigma_y = 574(0.010372 + \varepsilon_p)^{0.26}$ MPa

$J_R = 255$ J/mm

$a_0 \in \{40, 60\}$ mm

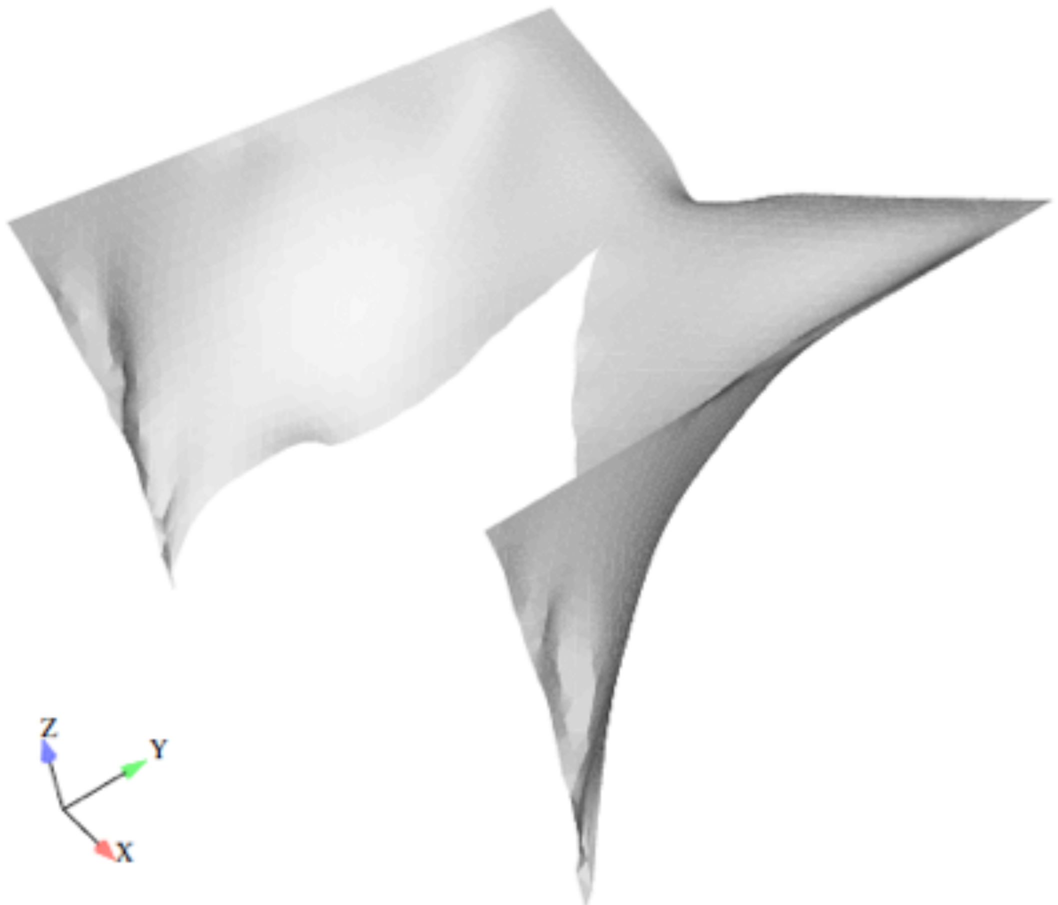

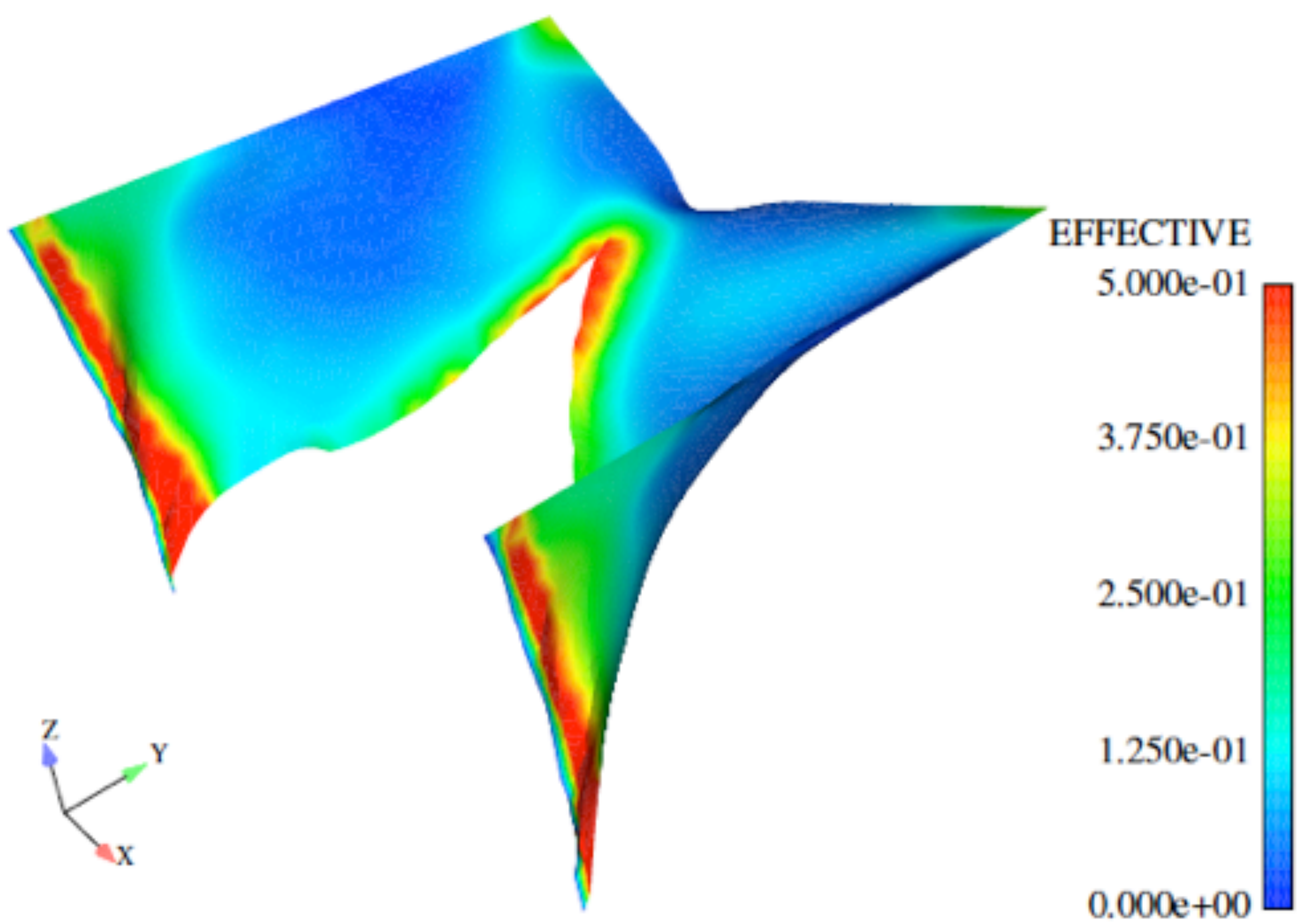

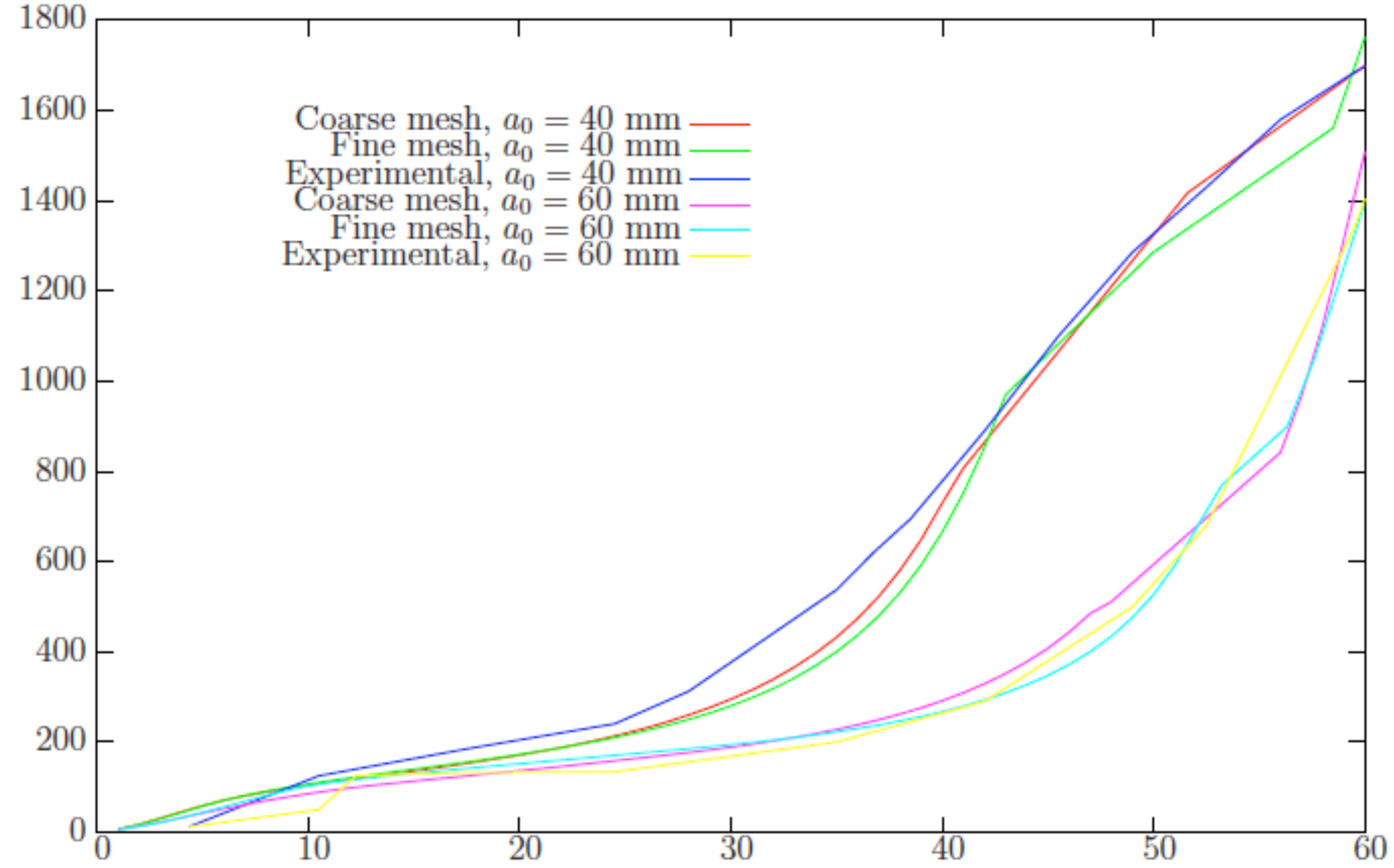

Pressure-displacement results

Movies

12) Tear-strapped cylinder

Properties #1:
H=1.02 × 10^{+00} mm
Nominal normal pressure=1 × 10^{+00} N.mm^{-2}
$CTOA_c$=5°
E=7.1422 × 10^{+04} N.mm^{-2}
ν=3 × 10^{-01}

Properties #2:
H=8.04 × 10^{+00} mm
Nominal normal pressure=1 × 10^{+00} N.mm^{-2}
$CTOA_c$=5°

Properties #3:
H=3.962 × 10^{+00} mm
Nominal normal pressure=1 × 10^{+00} N.m^{-2}
$CTOA_c$=5°

Meshes: 1858 nodes, 3636 elements
6318 nodes, 12480 elements

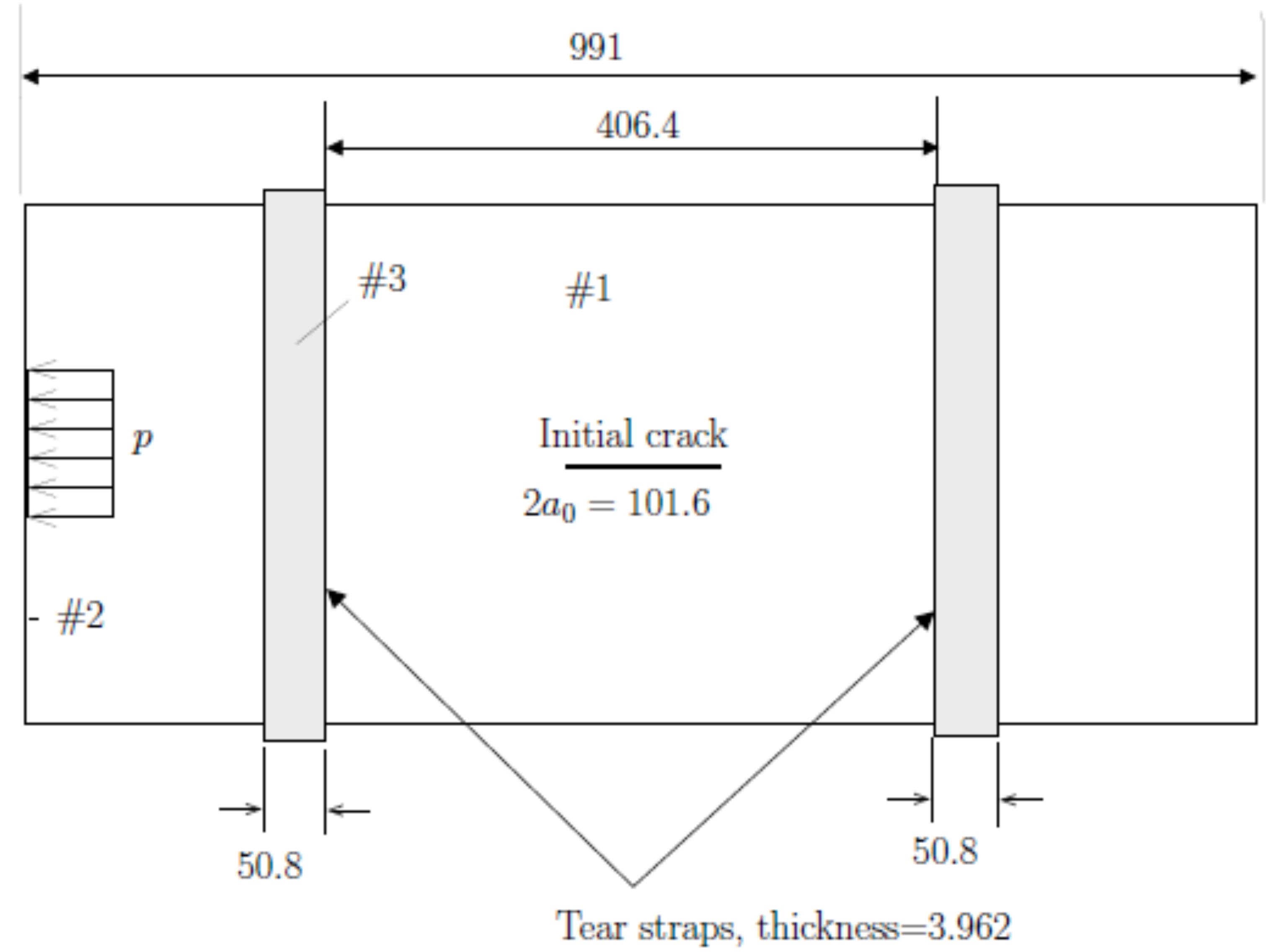

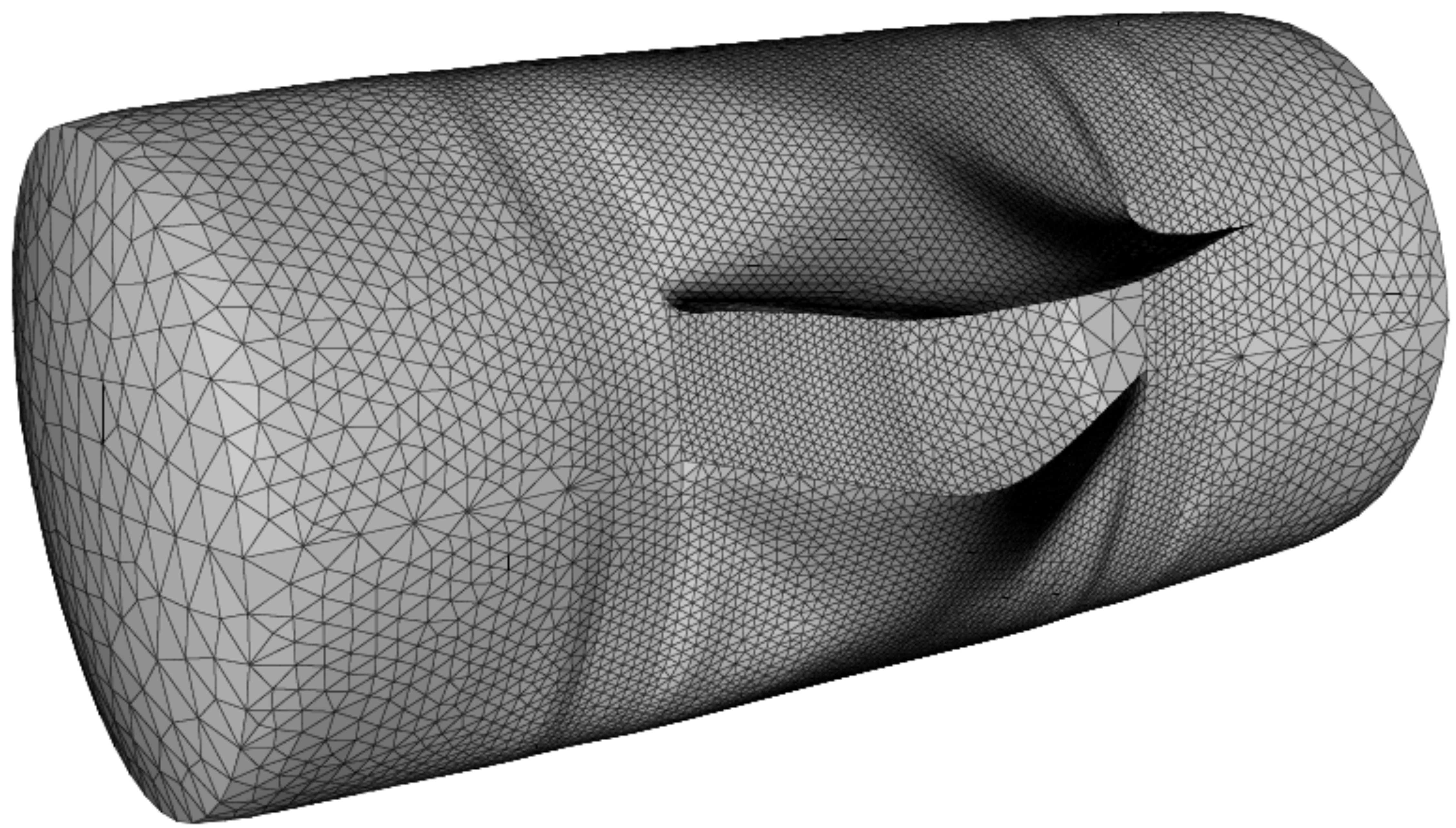

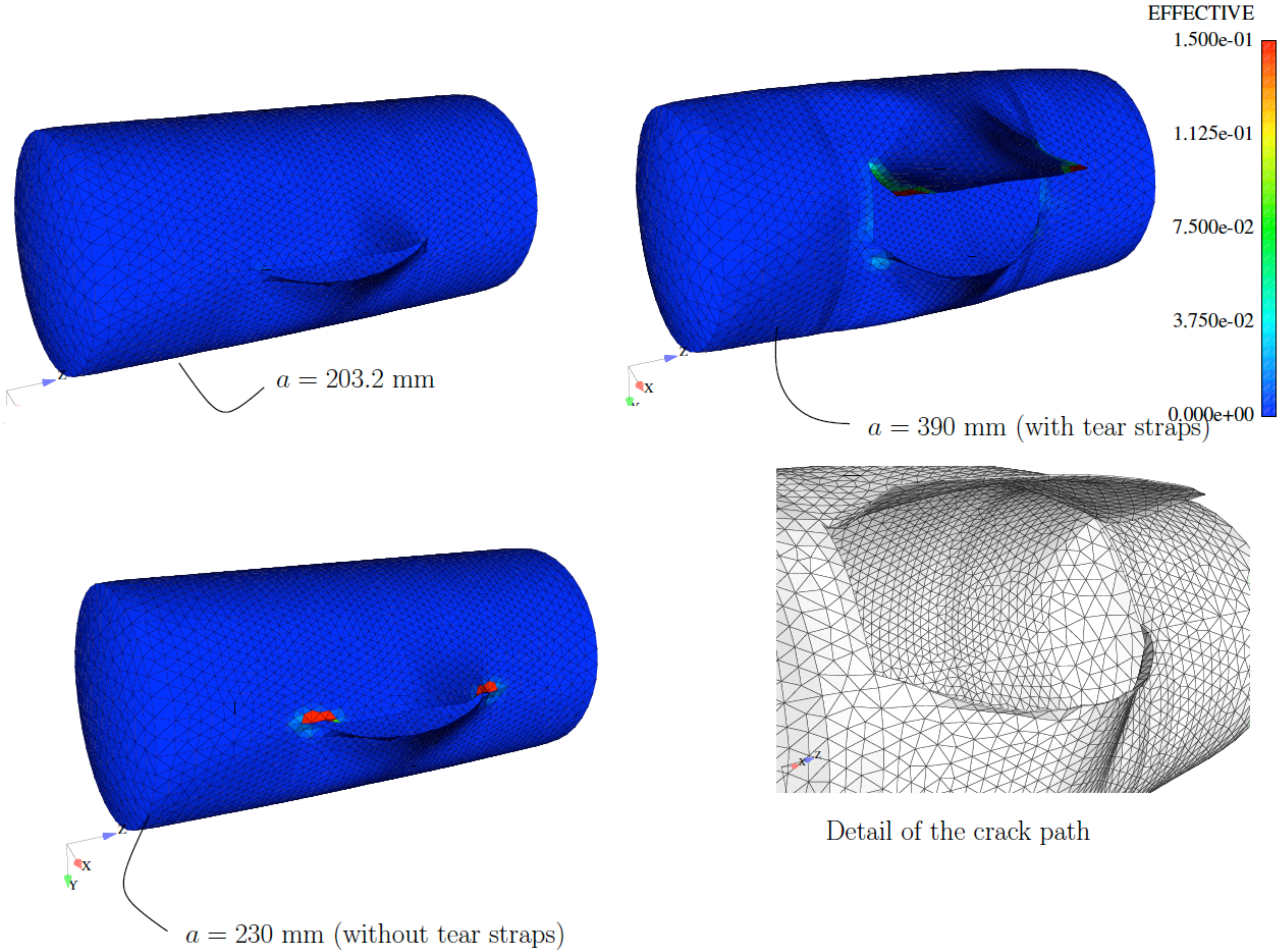
EFFECTIVE
1.500e-01
1.125e-01
7.500e-02
3.750e-02
0.000e+00
a = 203.2 mm
a = 390 mm (with tear straps)
a = 230 mm (without tear straps)
Detail of the crack path

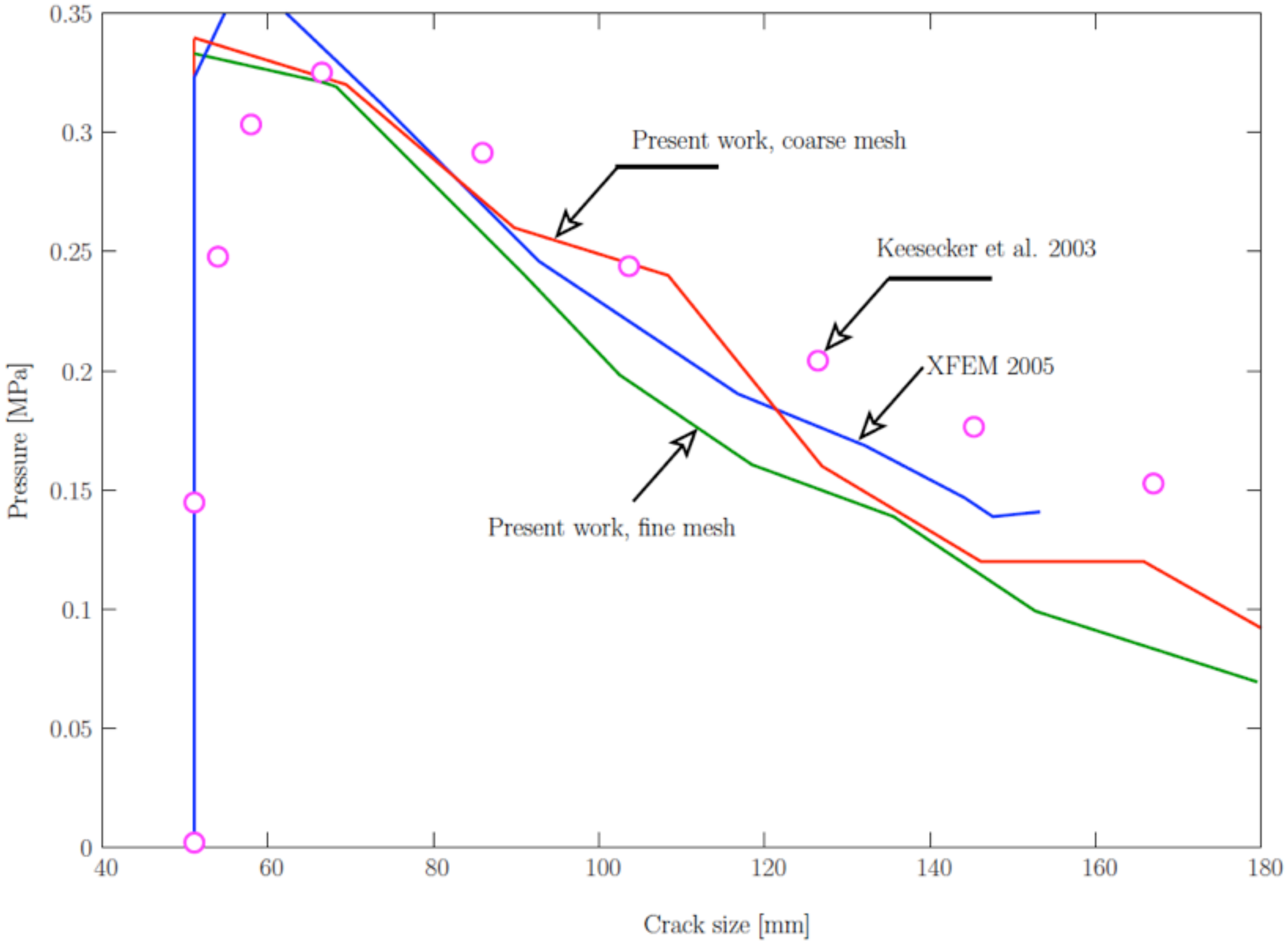

“Adequate” results

Movies

Conclusions

- Fracture of ductile shells achieved by edge rotation, multiple-surface plasticity and appropriate element technology
- Solution algorithm and techniques described in detail
- Benchmarks and newly proposed problems solved with success
- *Still some convergence problems in a given number of examples (not shown!)*
- *Still some crack path issues like cracks turning to clamped boundaries in plates*
- *Still some unsolved problems (crack bifurcation, interaction initiation/propagation)*

Thank you very much for your attention

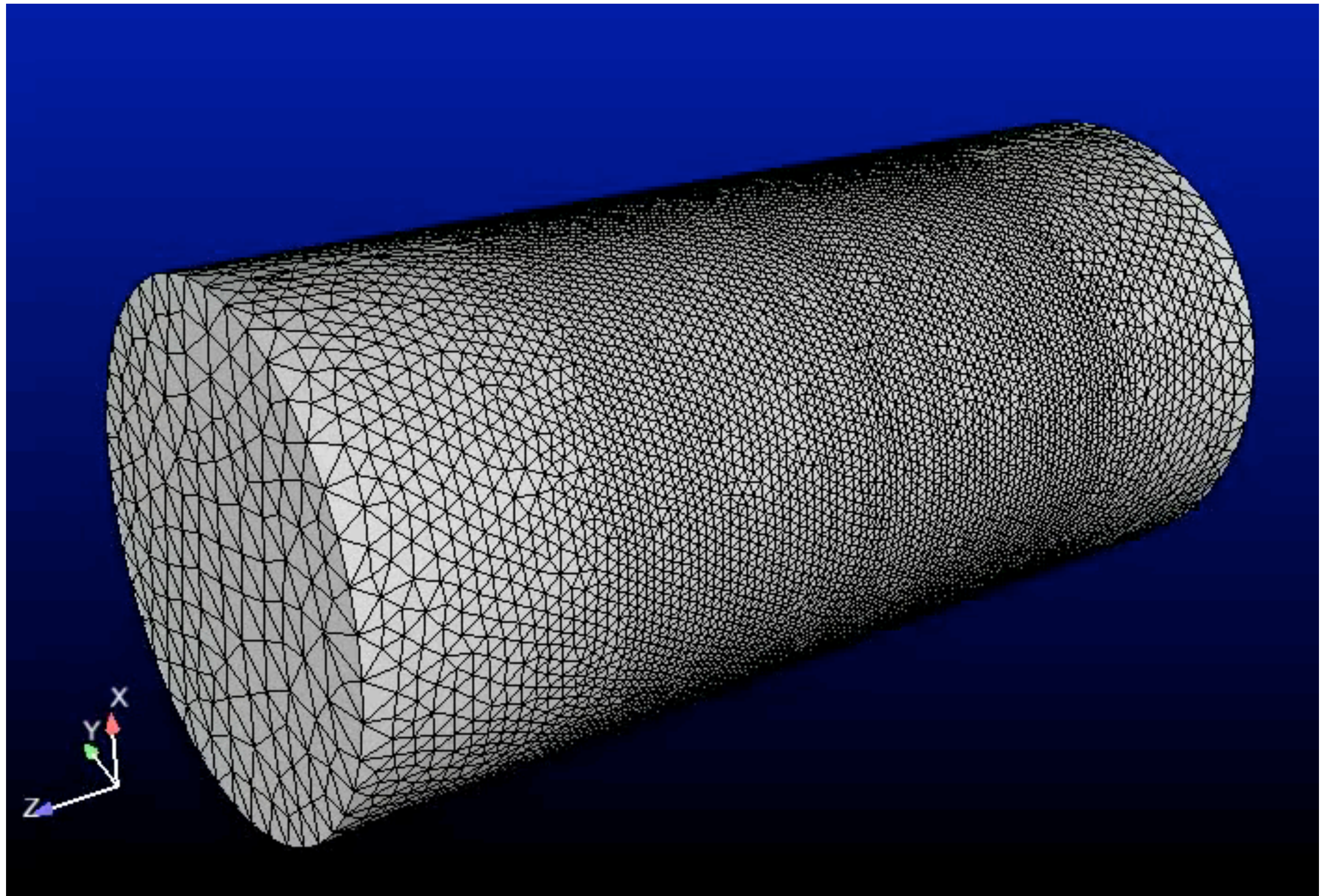
X
Y
Z

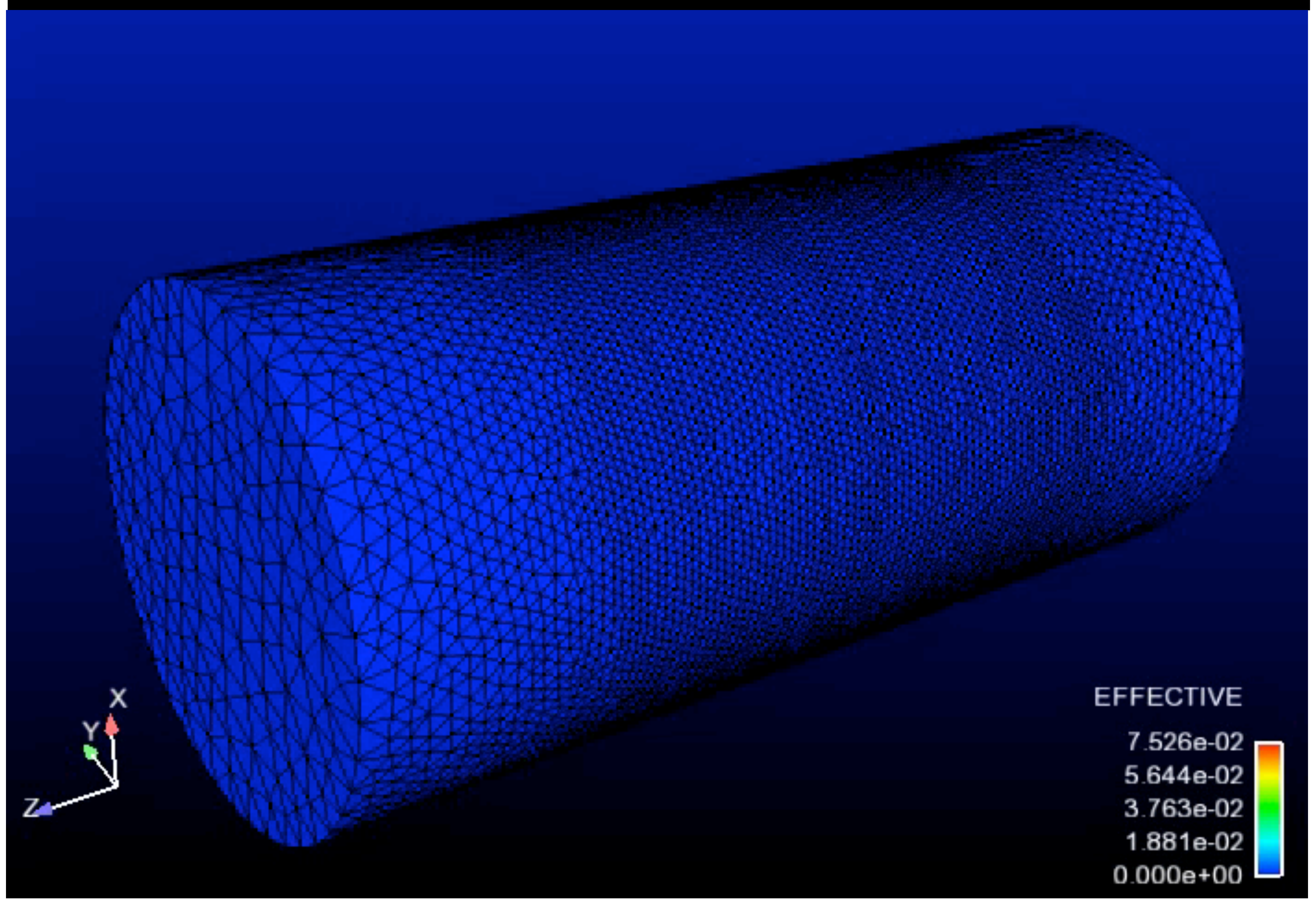
X
Y
Z
EFFECTIVE
7.526e-02
5.644e-02
3.763e-02
1.881e-02
0.000e+00

Return

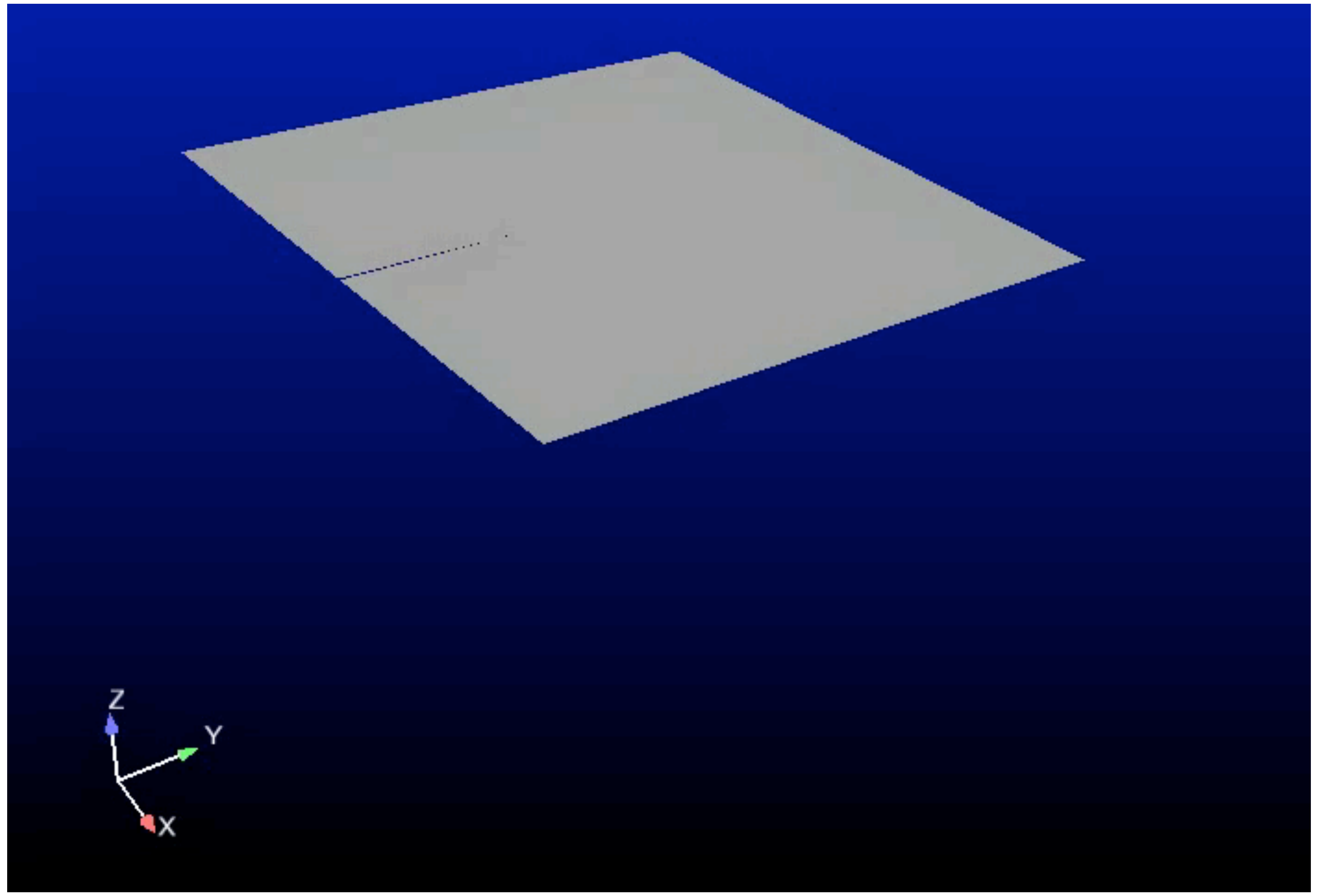

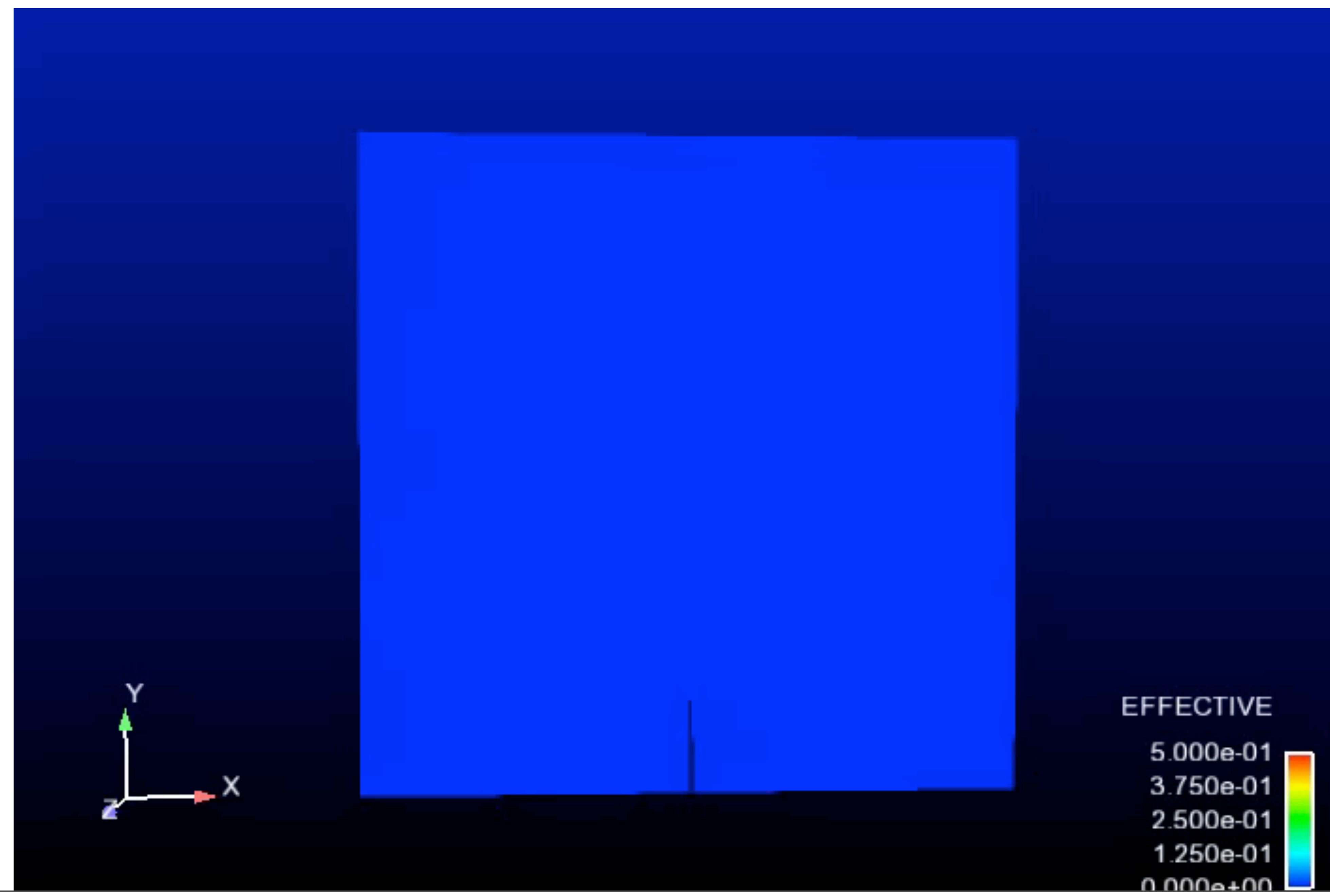

Return

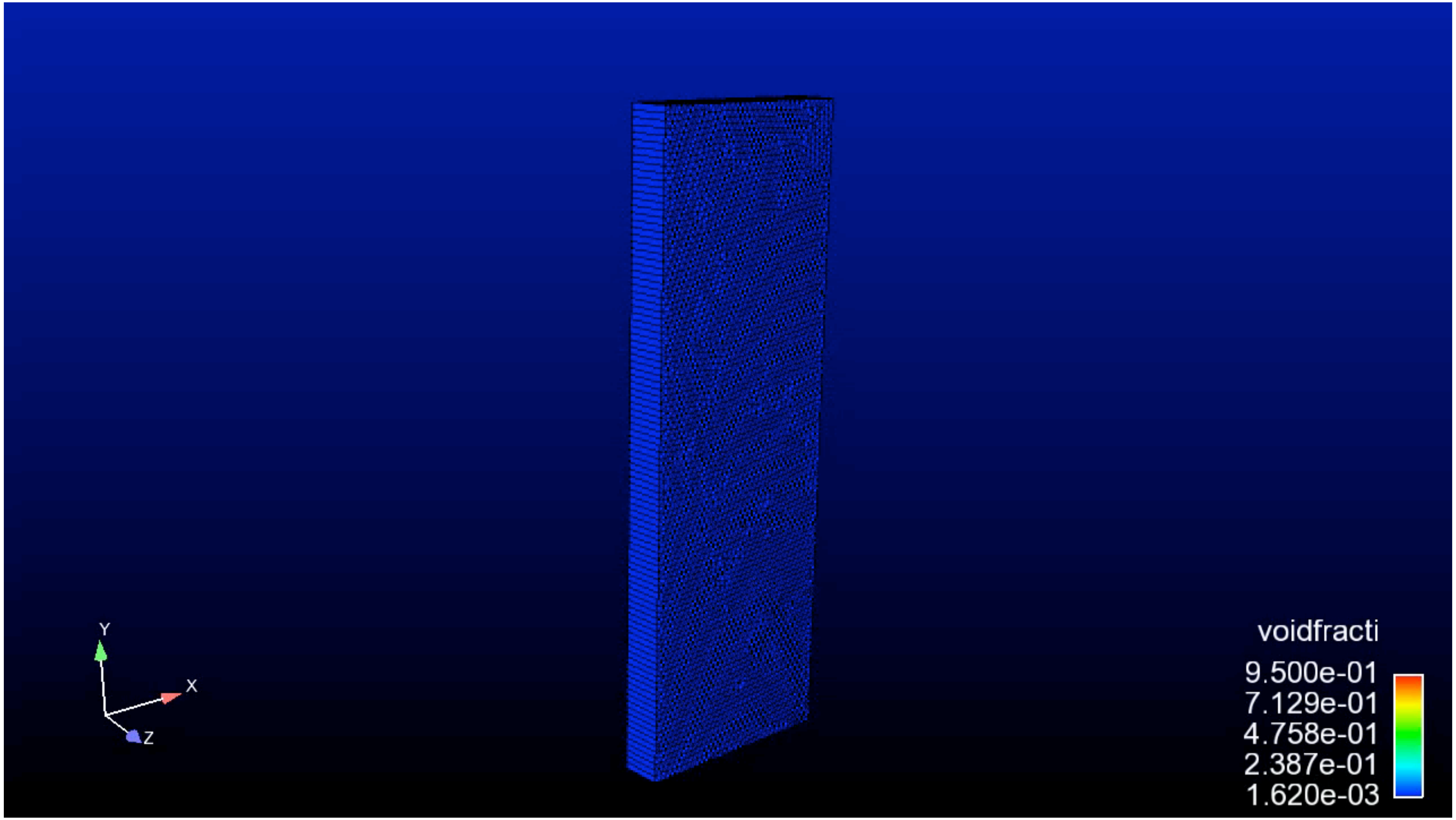

Return

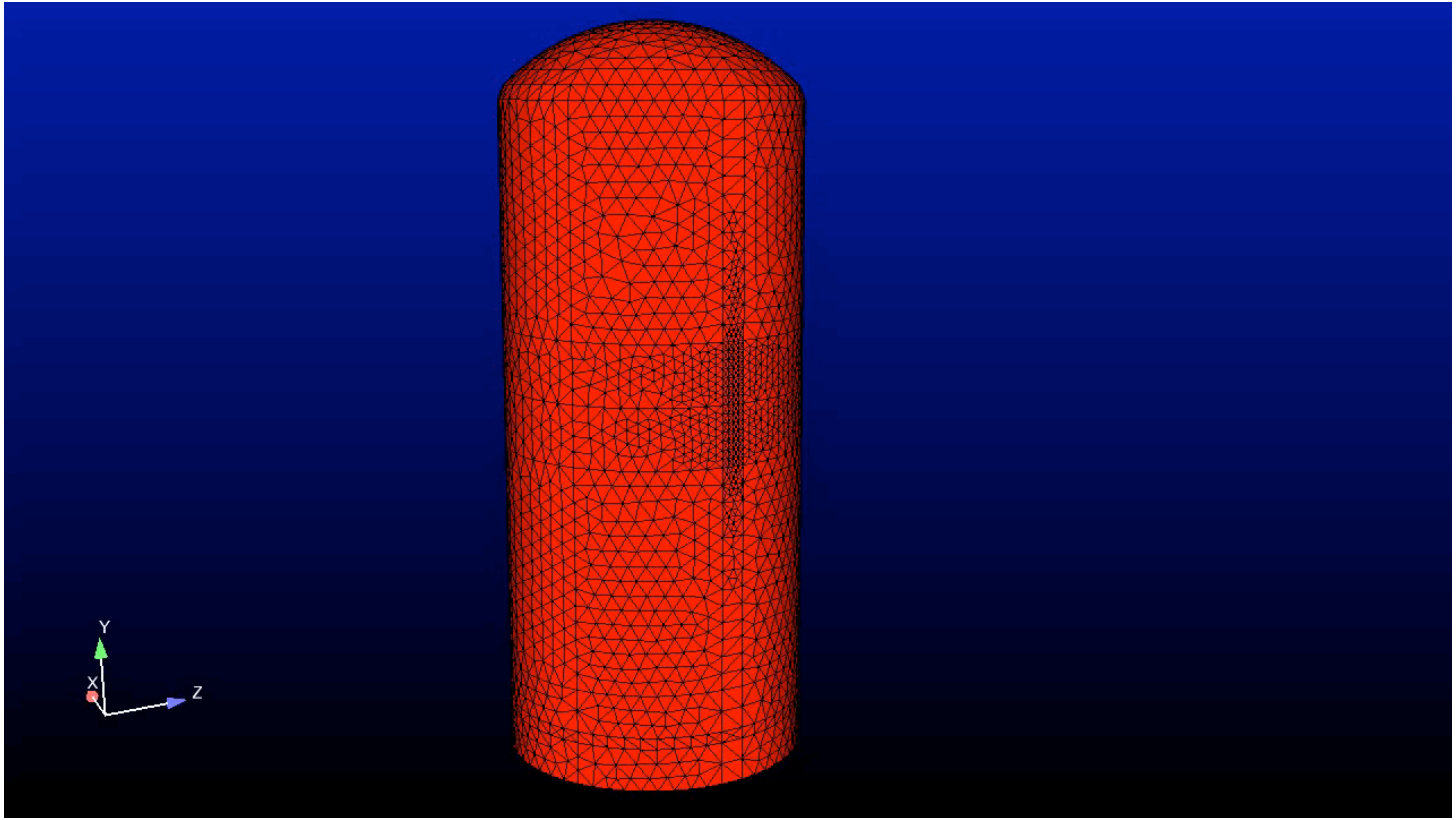

Return

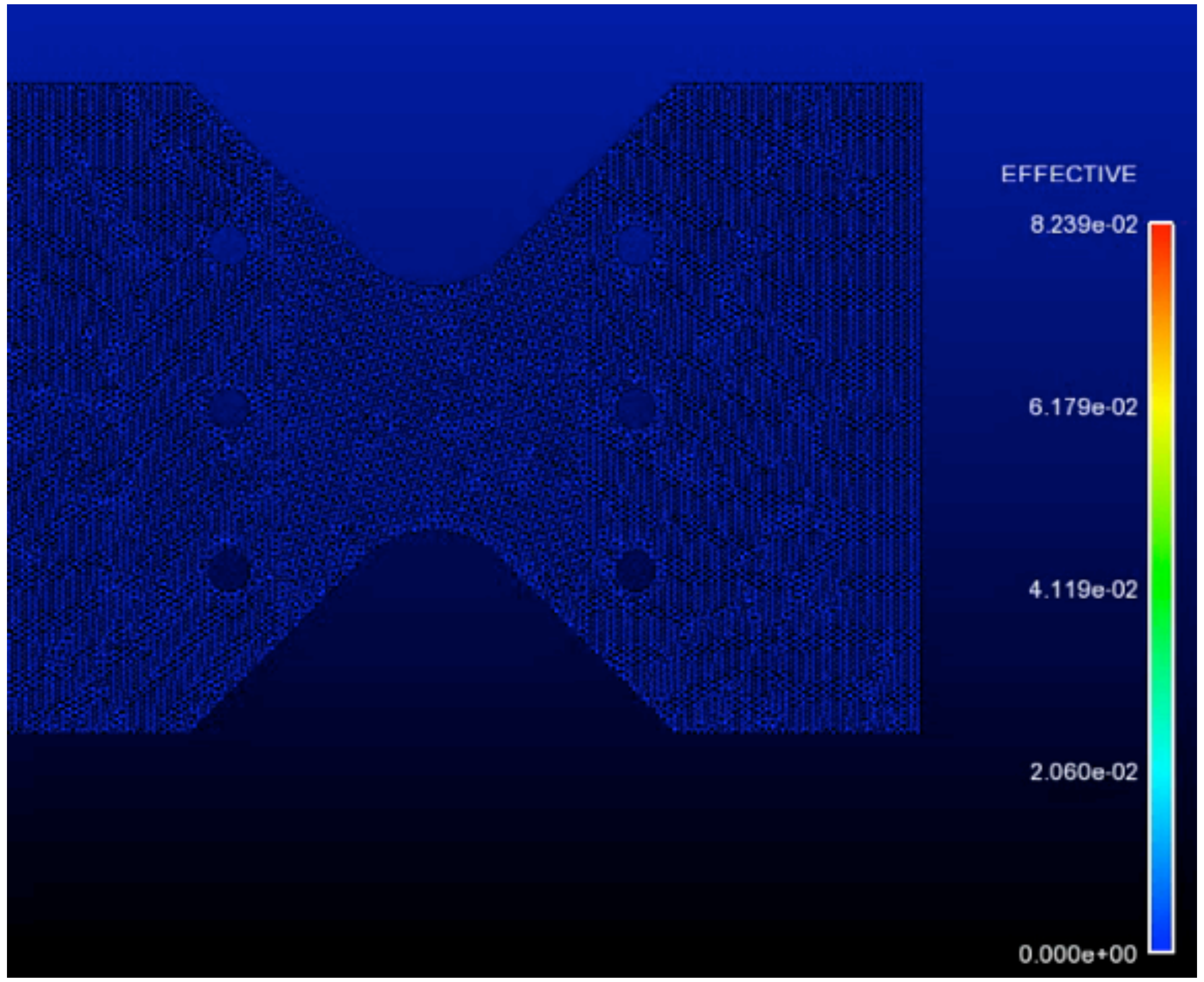
EFFECTIVE
8.239e-02
6.179e-02
4.119e-02
2.060e-02
0.000e+00

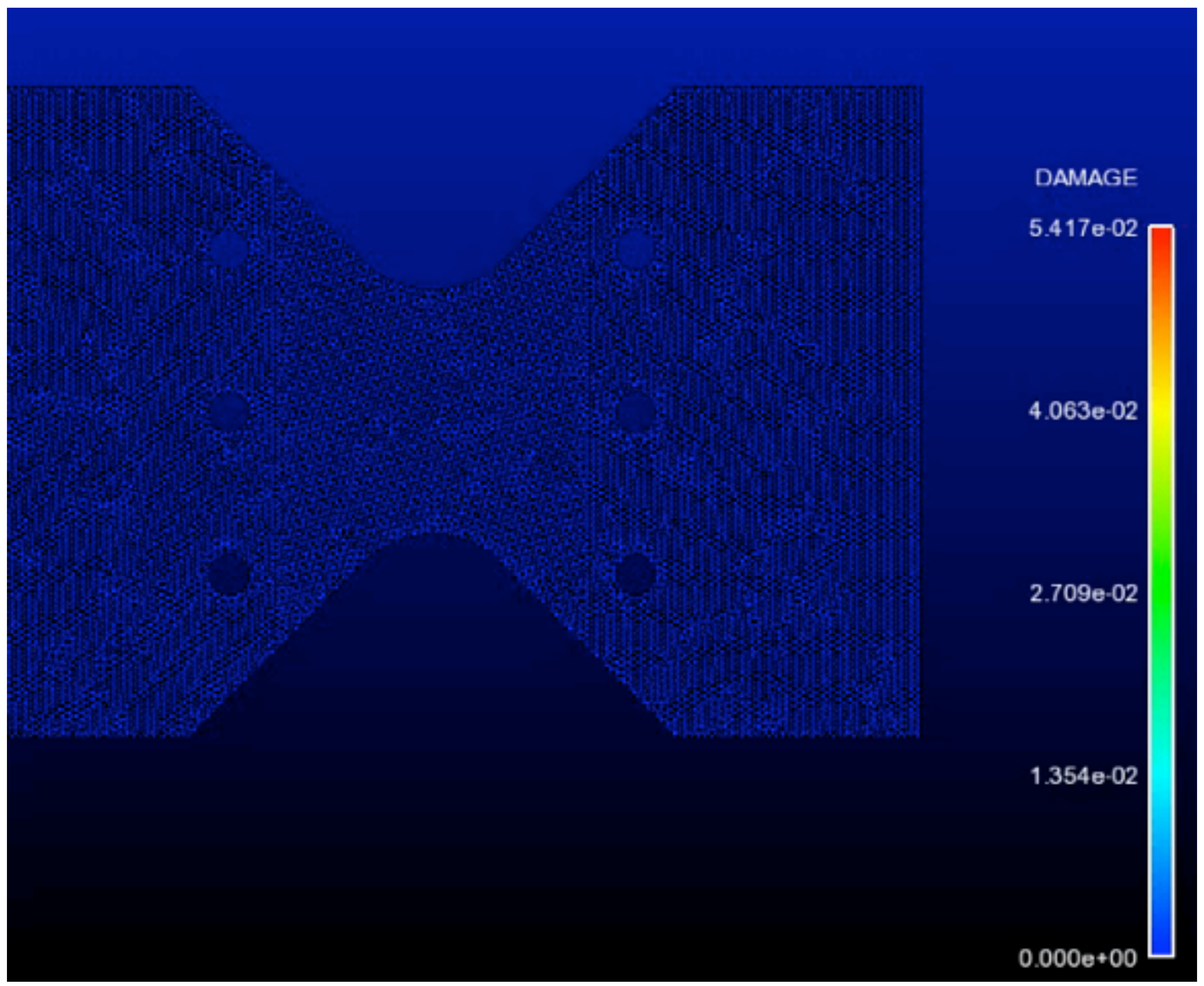
DAMAGE
5.417e-02
4.063e-02
2.709e-02
1.354e-02
0.000e+00

Return

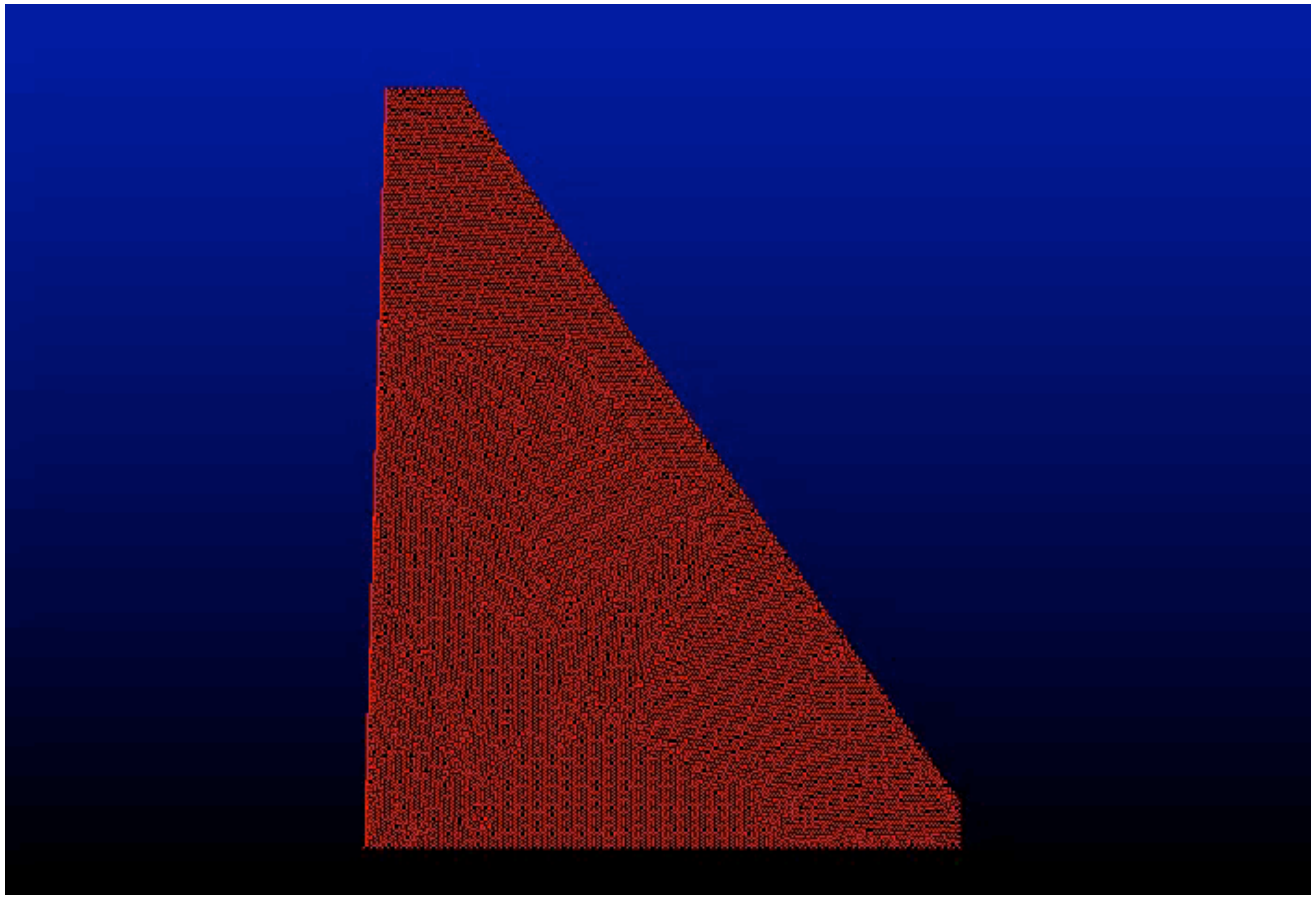

Return

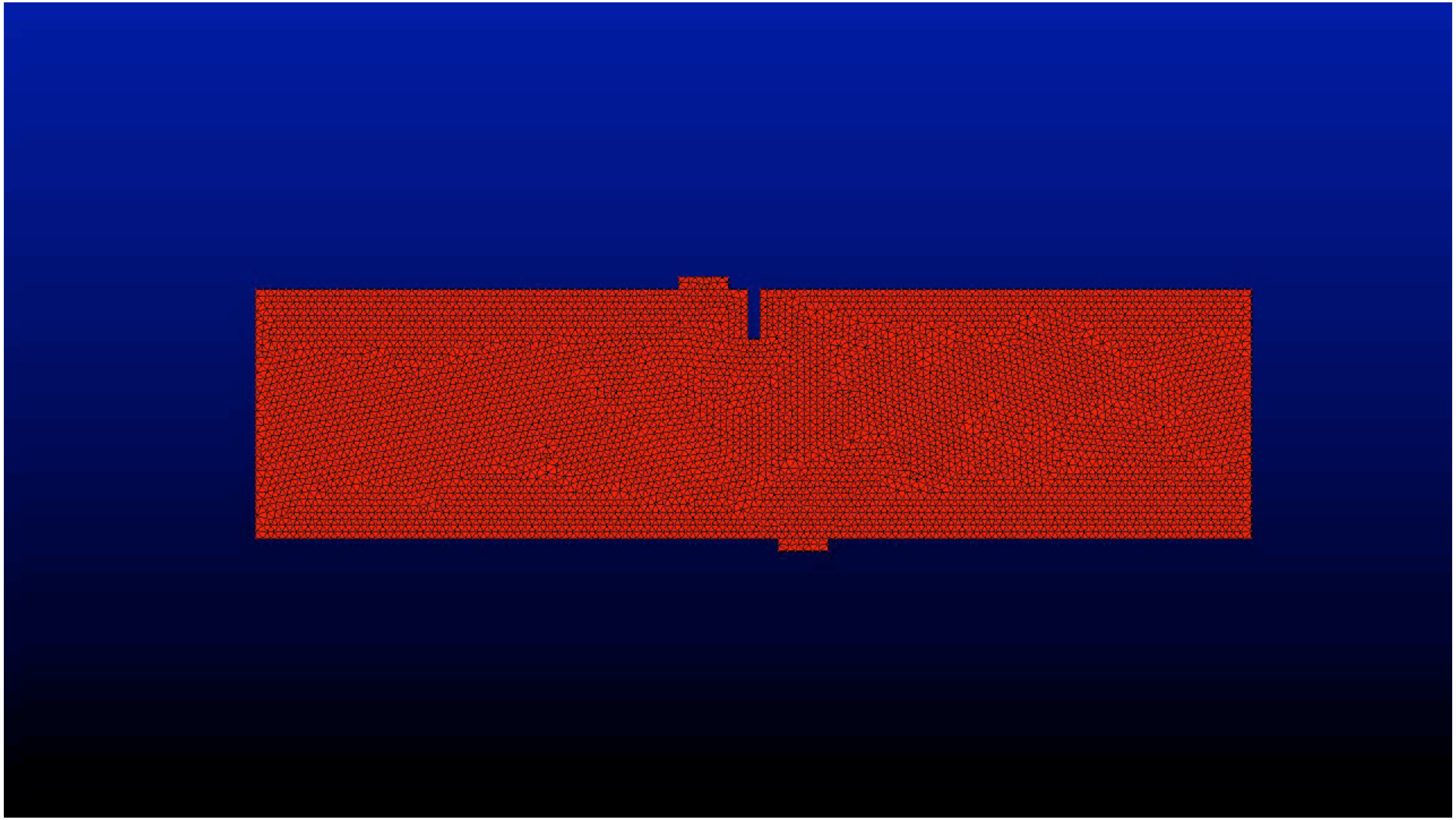

Return

Case I

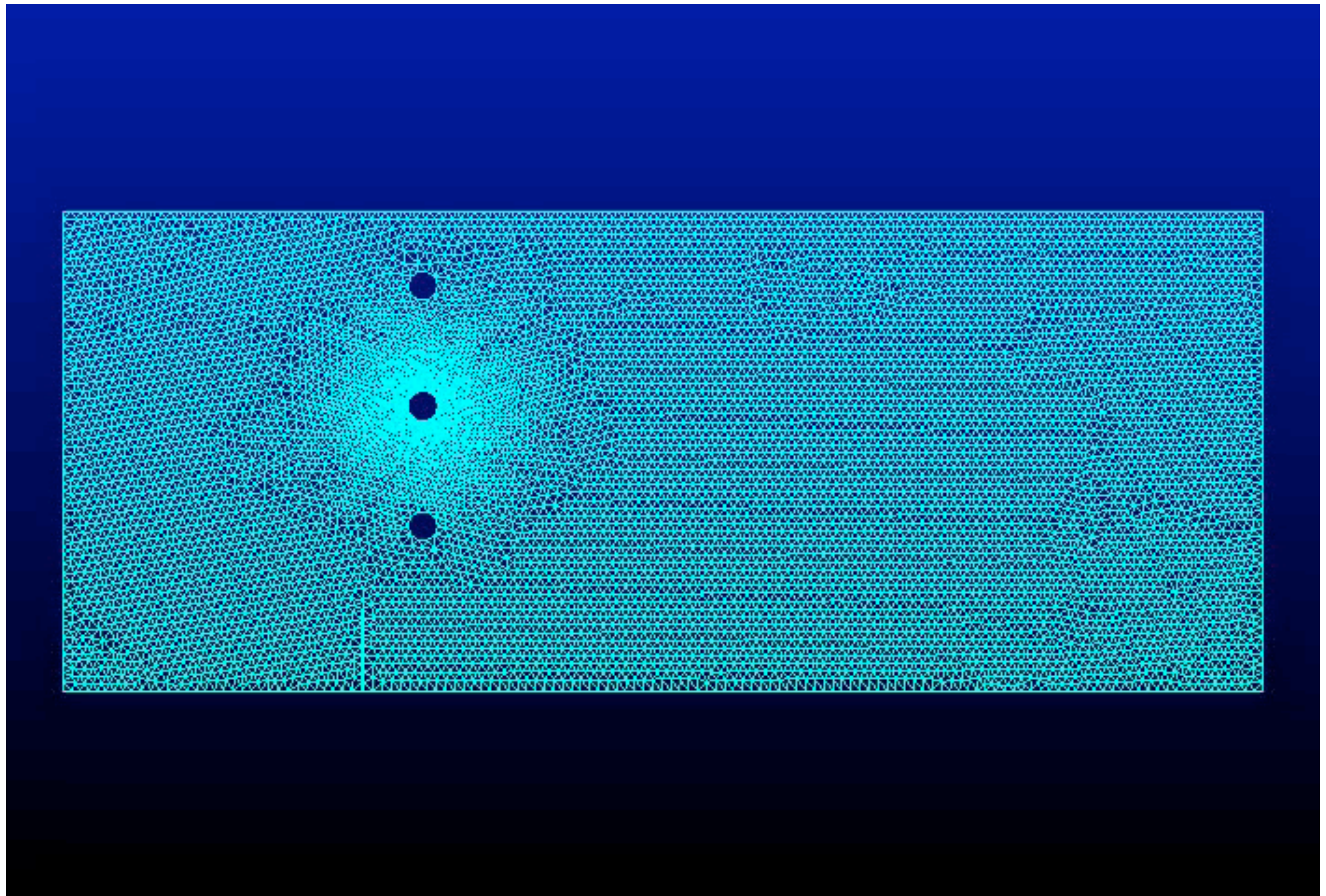

Return

Case II